1959

Tests of a composite aluminum and concrete highway bridge, September 1959

H. Mindlin

S. J. Errera

SYNOPSIS

Embodying the principles of thin-walled cellular design, a prototype composite aluminum and concrete highway bridge was designed to carry AASHO H15-44 loading and fabricated by the Fairchild Engine and Airplane Corporation.

The completed five-cell, 50-foot long, two-lane test span was erected at a site on the Lehigh University campus and underwent a test program designed to evaluate the following:

(1) behavior under static load

(2) ability to withstand an anticipated lifetime of load repetitions

(3) ultimate strength of the structure.

This paper presents a detailed account of the completed test program, the results obtained therefrom, and a comparison of those results with the behavior predicted by the design.

The structure withstood over 1,250,000 cycles of load producing from 100% to 150% of design live plus impact bending moment, and 200,000 cycles of 125% of design live plus impact bending moment applied eccentrically, without any evidence of distress. There was close correlation between theoretical and experimental results under static load.

Final failure of the structure occured at a load producing a moment more than eight times the design plus impact bending moment, and a corresponding shear more than four times the design plus impact shear.

TESTS OF A COMPOSITE

ALUMINUM AND CONCRETE HIGHWAY BRIDGE

by

Harold Mindlin and Samuel J. Errera

This report has been prepared for submission to the Fairchild Aluminum Bridge Technical Committee for comment and approval and is not released for publication.

This investigation has been carried out under the joint sponsorship of the following:

Fairchild Airplane and Engine Corporation
Bureau of Public Roads
Aluminum Company of America
Kaiser Aluminum Company
Reynolds Metals Company
Olin Mathieson Chemical Corporation

Fritz Engineering Laboratory
Department of Civil Engineering
Lehigh University
Bethlehem, Pennsylvania

September 25, 1959

Approved:

William J. Eney
Director

Fritz Laboratory Report No. 275.1

TABLE OF CONTENTS

TABLE OF CONTENTS (Continued)

TABLE OF CONTENTS (Continued)

TABLE OF CONTENTS (Continued)

TABLES AND FIGURES

TABLES AND FIGURES (Continued)

TABLES AND FIGURES (Continued)

TABLES AND FIGURES (Continued)

A. INTRODUCTION

1. Background

Backed with the experience of producing efficient lightweight structures such as aircraft, the Fairchild Kinetics Division of Fairchild Engine and Airplane Corporation investigated the feasibility of designing and fabricating an aluminum alloy highway bridge structure embodying the advantages and efficiency of semi-monocoque airframe construction. As compared to a conventional bridge structure, the following advantages of this construction could be found:

(a) Dead weight stresses would be reduced.

(b) Abutments, footings, or end supports could be of lighter construction.

(c) Transportation costs from the point of fabrication to the erection site would be less.

(d) Erection costs would be less.

(e) Maintenance costs after erection would be reduced.

The result of the Fairchild investigation was a prototype composite aluminum and concrete two-lane fifty-foot span designated the "Fairchild Aluminum Bridge." The basic structural components of this span were a tension flange composed of bottom plating and extrusions; compression flange composed of top plating, extrusions, and concrete deck; and shear webs composed of six diagonal plates.

Designed with the assistance of the Bureau of Public Roads, in accordance with the American Association of State Highway Officials

Specifications[1] and the American Society of Civil Engineers Specifications[2] for the alloy used, the test bridge was fabricated at the Fairchild Plant in Hagerstown, Maryland, and erected on the Lehigh University Campus test site in Bethlehem, Pennsylvania.

2. Purposes and Scope

To fully evaluate the structural performance and adequacy of the structure under service conditions, the bridge was instrumented to record deflections and strains due to applied loads and then subjected to static and dynamic load conditions simulating an above-normal life span.

The primary purposes of this test program were as follows:

(a) Observe deflection behavior and obtain a stress or strain distribution due to applied loads to enable comparison between predicted and actual behavior.

(b) Determine capability of the structure to withstand cyclic loadings in excess of magnitude and number of repetitions anticipated in a normal life span.

(c) Determine the ultimate static strength of the structure.

A full description of the bridge, tests, and test results are herein presented.

3. Test Program - General

The test structure was subjected to 13 static tests and a dynamic test program summarized as follows:

(a) 250,000 cycles at design live load plus impact moment, M_{LL}

(b) 250,000 cycles at 125% M_{LL}

(c) 753,000 cycles at 150% M_{LL}

(d) 200,000 cycles at 125% M_{LL} with load applied eccentrically for a torsional moment equal to 6,220,000 in-lb.

B. DESCRIPTION OF TESTS

1. Bridge

a. Fabrication and Erection of Aluminum Structure

The aluminum substructure was fabricated at the Hagerstown, Maryland plant of the Fairchild Engine and Airplane Corporation. One of the final steps prior to shipment was the mating of the component parts on special jigs to insure a proper fit at the erection site (Figure 1). Five basic subassemblies, consisting of three triangular beams and two bottom plates, were then transported by truck from Hagerstown to the final assembly area and test site on the Lehigh University Campus (Figure 2).

The erection sequence was completed in two days as follows:

(1) Mating of two triangles and one bottom plate to form the first unit placed on the end supports (Figure 3).

(2) Placing of the second bottom plate.

(3) Placing of the third triangular beam.

(4) Completion of the field bolting.

Steps (1) to (3) were completed the first day and step (4) was completed the following day.

The completed structure assembled 11,360 lbs. of 6061-T6 aluminum alloy extrusion and plating into a five cell, semi-monocoque bridge.

With the later addition of a lightweight concrete deck, the composite aluminum and concrete structure placed a 24-foot wide roadway over a 50-foot clear span (Figure 4).

b. Description of Aluminum Structure

Tension flange material was composed of two 0.125-inch plates, three channel extrusions (at the bottom apex of the triangular beams), and four extruded bulbed T-sections (Figure 5). Six shear webs, forming the 45-degree inclined sides of the five cells, were made of 0.081-inch plate. All shear webs and bottom plates had bulb angle transverse stiffeners to prevent buckling due to shear loads.

At the top of each shear web was an extrusion common to both the web and 0.081-inch top plate which completed the triangular sections (Figure 5). At the upper juncture of the center and outer beams these extrusions were designed to interlock, thus joining the three beams into one integral unit. The outer edges of the two outside beams were 1 1/2-inches below the high point of the center beam, providing a transverse camber in the roadway.

Attached to the top 0.081-inch plate, running transversly to the longitudinal bridge axis, and spanning between extrusions was the corrugated aluminum decking which later served as the bottom form for the concrete deck (Figure 6).

Shear ties were attached to the top longitudinal extrusions (Figure 7) to insure composite beam action and prevent uplift of the concrete slab. Approximately two feet from each end of the bridge, attached to the top sheeting and extending up into the concrete deck, was placed a channel section called a thermal beam (Figure 6) designed to react the stresses induced by a temperature change causing unequal expansion of the aluminum and concrete.

At the ends of the three triangular beams, attached to the webs, were frames composed of two channel sections and a 0.125-inch doubler plate which transmitted the applied loads to the footings (Figure 6). Light intermediate frames (spaced five feet center to center) divided the webs into panels of equal length.

Assembly of the extrusion and plate material into three triangular beams and two bottom sheets was done in the fabrication plant using cold-driven rivets. Field erection was completed with the use of standard nuts and bolts and commercial-type lockbolts.

The entire structure was placed on oil-impregnated bronze bearing pads. The blocks at the west end of the span were restrained from horizontal movement but permitted rotation due to bending. The blocks at the east end of the span were free to slide horizontally and also permitted bending rotation. After completion of Tests 1 through 8a, it was necessary to replace each bronze pad at the free end with a nest of seven 3/4-inch rollers due to the failure of the bronze pad to move horizontally.

c. Description of Concrete Deck

The concrete used for the deck embodied a slag aggregate (commercially known as Waylite) whose light weight helped to minimize the stresses in the aluminum due to dead weight of the structure. The deck extended 5-7/8 inches above the top of the 2-1/2-inch deep corrugations. All steel reinforcing bars were placed above the corrugations and separated from the aluminum by insulation. (Figure 7 shows the steel in place before the insulation was inserted). A nine-inch cantilever extended over the edge of the outer triangular beams to complete the full 24-foot width of roadway (Figure 7b).

The need for any external support of the formwork during the pouring of the concrete deck was eliminated by bolting the wooden side forms directly to the top outer edges of the aluminum beams (Figure 7b).

2. Test Program (Table 1)

To achieve the purposes outlined in the introduction, the test program was designed to check the structure statically before and after each series of dynamic load applications. Thus, any damage or change in strain distribution within the structure could be detected.

The completed series of 18 static and dynamic tests applied to the structure is summarized in Table 1. In addition to these tests, three impact loadings were applied to the span to determine the natural frequency of the structure.

A traffic study and analysis[3] made from Bureau of Public Roads surveys predicts 365,000 cycles of design plus impact loadings in the 50-year

life of a Class I span. Allowing for possible errors in prediction, it was determined that 1,500,000 cycles of repetitive loading should be applied to the test span, including allowances for 25% and 50% overload conditions.

The static testing procedure allowed observation of changes within the span due to temperature variation during the period of each static test. Also, continuous deflection measurements were recorded from September 8 to November 6, 1958, under no-load conditions. Strain observations under no external loading of the span were made on November 6.

3. Test Procedures

a. Static Tests (except destruction Tests 17 and 18)

To eliminate the effects of temperature, three readings were made to determine the effects of one load increment:

(1). Readings of all gages with no load on span

(2). Readings of all gages with span loaded

(3). Final readings with span again completely unloaded.

Averaging of the loading and unloading increments eliminated (or minimized) temperature effects on the gages. To check the accuracy of the method, one test (6N) was run during the night, a period of small temperature changes, and repeated (6D) over a normal daytime variation of 10 to 15 degrees. (See Appendix B for analysis of the data from these two tests).

b. Destruction Tests 17 and 18

Because the method of loading the span was altered (dead weight was placed directly on the deck) for these final tests, it was impractical to completely unload the span after each load increment. The loading sequence, therefore, was as outlined in Table 2.

c. Dynamic Tests

All dynamic loads had to be compensated for the inertia effects of the span. To insure that the proper magnitude of load was being applied to the span during repetitive loading, the maximum deflection under dynamic load was kept equal to the deflection obtained for the desired load when applied statically. The minimum load was kept at approximately 10% of the maximum applied load.

d. Natural Frequency

By dropping a weight on the deck of the span and automatically recording the instantaneous deflections, it was possible to determine the frequency of response for the structure.

e. Temperature

This portion of the test program was limited to observation of the behavior of the span due to variations of the ambient air temperature.

4. Method of Load Application

a. Loading Beams (Figures 4 and 8)

The hydraulic jacks used to apply load to the structure were in

bearing against transverse loading beams which applied the loads concentrically in each 12-foot traffic lane. Each beam acted against the deck through two 13" x 26" steel bearing pads, 6-feet center to center, designed to simulate the rear axle tire spacing of an H15-44 truck (Figure 8).

For the eccentric static and dynamic load tests, a jack was placed 3 feet on each side of one traffic lane centerline to produce one-lane loading (Figure 8).

b. Test Equipment

Following is a brief description of the Amsler hydraulic equipment used for the testing of the span:

(1) Hydraulic Jacks

For all except the last three static tests, two hydraulic jacks with a capacity of 55,000 pounds each were used to apply loads to the span. Maximum dynamic stroke for these jacks is 0.88 in. For the last three static tests, two hydraulic jacks with a capacity of 200,000 pounds each were used. All jacks have a maximum static stroke of five inches.

Connected with a suitable oil delivery unit, the jacks produce load hydraulically through a precision-machined lapped ram (or packless piston). Due to the very low friction losses, oil pressure at the jack is used as an accurate measure of the load. Spherical seating at both ends of the jack assure proper load bearing.

(2) Pulsators

For cyclic load tests each jack was connected hydraulically to a pulsator. The two required pulsators were connected in parallel to insure equality of magnitude and synchronization of load application. Basically these units consist of a pump which produces a constant load in a pressure cylinder and a piston in this cylinder having an adjustable stroke (through a mechanical linkage) to produce a sinusoidal variation of the pressure in the cylinder and subsequently in the jacks. Maximum and minimum pressures were measured directly at the piston of one jack and read at gages mounted on the pulsator. Dynamic loading was applied at the rate of 250 cycles per minute.

(3) Pendulum Dynamometer

The final series of three static tests was completed with the use of the 200,000 pound capacity jacks connected to a pendulum dynamometer. The dynamometer basically contains a hydraulic pumping unit and a separate load measuring system.

Oil is pumped from the dynamometer through one small-diameter pipeline to a distributor where two lines then branch to the two jacks. Hydraulic pressure in the distributor also acts on a measuring piston (in the dynamometer) which activates the pendulum. The swing of the pendulum is proportional to the distributor pressure which in turn is a measure of the load in the jacks. The jack load is read directly on a large dial on the front of the dynamometer.

c. Loading Frames (Figure 4)

The hydraulic jacks were suspended from cross beams bolted to the tops of two frames. The two frames were placed three feet on each side of the transverse centerline of the bridge permitting load application directly at the centerline.

The reaction system consisted of the dead weight of the frame, frame footings, and steel slabs on the frame and footings.

d. Dead Weight (Figure 9)

For the last series of static tests (17 and 18) the magnitude of load required for failure exceeded the capacity of the test equipment, necessitating the use of dead weight placed on the deck of the bridge. Steel slabs with an approximate 6" x 36" cross section and varied lengths were piled on the deck symmetrically to the transverse centerline. The weight of these slabs varied from 2-1/2 to 4 tons each.

5. Instrumentation

To fully evaluate the behavior of the structure under an applied normal force at the centerline, the instrumentation was designed to define the strains (1) at the centerline due to the application of this normal force and induced bending; (2) at the quarter point due to bending and shear; and (3) at the end frames or reaction points. Deflections of the structure were recorded by taking measurements at the centerline and quarter point. Instrumentation used for the observation of the magnitude of the strains due to temperature changes is also included in this section. Because of

symmetry of the test structure and applied load, most measurements were made on the east half of the bridge only.

a. Static Testing

(1) Strain Measurements

All aluminum strain measurements were made with resistance type SR-4 electrical strain gages bonded to the metal surface (Figure 10). A strainometer, also an electrical resistance type gage, was used to measure internal concrete strains. On the concrete deck, surface strains were measured with a mechanical Whittemore gage over a 10-inch gage length. Strain gages were placed at various stations as described below.

At Station 25 bending strains were determined by placing one gage on each of the seven main longitudinal members A through G. To determine the action of the transverse centerline frame in the distribution of load within the structure, two gages were placed on each of the frame members in the three triangular beams. Centerline gaging is shown in Figure 11.

At Station 22 a strainometer was placed at mid-height between the top and bottom steel reinforcing to determine the magnitude of the internal concrete strains. At Station 23 on the longitudinal centerline and 4 and 8 feet on each side of this centerline, Whittemore strain gage readings were taken to determine the concrete surface strains. These gages were offset from the transverse centerline to minimize the local effects at the point of load application. Figure 12 shows the location of the strain gages for the deck.

At Station 12 + 6 bending strains were again determined by gaging the seven main longitudinal members A through G. At the same station at the center of each of three top plates BC, CD, and DE and at four points on the bottom plates AG and GF were placed 45° rosettes to measure bending and shear strains. Uni-directional gages were placed in line with the bottom sheet rosettes on the top and bottom of each sheet AG and GF to detect transverse bending of the sheets. Rosettes were also placed at the center of panel 10 - 15 to measure shear strains. Internal concrete strains were again measured with a strainometer buried at mid-height of the deck. Quarter point gaging is shown in Figure 13.

At Station 0 two cross sections at the third points of each of the six diagonal members of the end frame were investigated by placing one strain gage on each channel and one strain gage on the doubler. Hence, a transfer of the load from the web into the end frame and then to the end support could be determined.

Preliminary investigation of test data after Test 15 revealed the desirability of discontinuing strain readings in areas which could no longer yield any more valuable information, and complementing selected existing strain gages to further define the behavior of the structure during the final phase of testing. Therefore, the following changes in instrumentation were made:

1. Readings were discontinued on 18 strain gages mounted on the transverse centerline frame because this was a non-critical area.

2. Because the action of the end frame was defined and found to be consistent through earlier static tests, the 12 strain gages on the channels at the upper cross section were also discontinued.

3. Transverse bending of the bottom sheet at the quarter point was found to be negligible, eliminating the need for these four gages.

4. To define more completely the vertical strain distribution due to bending at the quarter point cross section, three additional gages were placed to measure bending strains at points one-sixth, one-third, and three-fourths of the height of each web. From the total of four gages then on each web, a better picture of the vertical strain distribution was obtained.

(2) Deflections

Deflection of the span due to applied load were measured with dial gages under the three main longitudinal members at the centerline (Station 25) and the quarter point (Station 12 + 6). To check the dial deflections and to determine any relative deflection between the deck and tension members, scales were placed on the deck at the centerline, quarter point, and over the end supports. These scales were read against a fixed reference with an engineer's level.

After Test 15 additional dial gages were placed to measure settlement of the end supports under applied load. As a safety measure at the high loads of the final tests, deflections were measured only at the outside longitudinal extrusions. Due to the placing of dead weight on the deck for the final tests the deflection scales being used at the centerline became inaccessible; as were the Whittemore gage points at Station 23.

(3) End Movement

Dial gages were used to measure the horizontal movement of the free end of the bridge relative to the fixed center pedestal of the end support,

and the relative movement between the concrete deck and top longitudinal member C. After Test 15 another dial gage was placed at the opposite end of member C.

b. Dynamic Testing

During all dynamic load tests maximum centerline deflections under the north and south extrusions were measured with slip gages, a mechanical device employing a dial gage to record maximum downward movement (Figure 14). At intervals during one dynamic test in which load was applied eccentrically to the span, a record of centerline deflections and strains in the three bottom longitudinal extrusions was made with a six channel Brush recorder.

c. Natural Frequency

The instantaneous centerline deflection of the span due to a suddenly applied load was automatically recorded on one channel of a Brush recorder. A transducer (pictured on the right of Figure 14) was used to convert deflections into electrical impulses which were recorded on the moving tape of the Brush equipment.

d. Temperature

To get an indication of the temperature distribution within the span, temperature measuring devices were placed on the bridge. Bottom sheet temperature was measured at the centerline of the span with a surface thermometer, recordings being made at each load interval during static testing. Buried in the concrete of the deck at the centerline and each quarter point along the longitudinal bridge axis were three electrical temperature gages. A seven day automatic recorder maintained a continuous record of the ambient air temperature at the bridge site.

Initial observations indicated the need for additional temperature gages within the cells of the span. Five electrical resistance type gages were bonded to the aluminum on the top sheet, interior webs, and bottom sheet.

For one sixty day period deflections were measured at the centerline and quarter point due to temperature changes only. This temperature study was carried one step further by placing seven electrical temperature-compensated strain gages on the span opposite existing gages and comparing responses to temperature variations.

C. THEORETICAL ANALYSIS

The following is a brief summary of the theoretical analysis used by Fairchild Engine and Airplane Corporation.(4)

1. Section Properties

a. Basic Assumptions

The following assumptions and considerations were used to determine the effective areas of the cross section for the span without the slab:

(1) Bending stresses are carried by the top and bottom plating and longitudinal extrusions. The cross section was divided into elements having a 22 1/2 inch horizontal projection whose contributions were summed to determine the section properties. (See Figure 15).

(2) Upper plating was restrained against buckling at approximately 4-inch intervals by the deck corrugations and was, therefore, considered fully active in compression.

(3) Because of the high ratio of flange to web areas, only 0.50 square inches of each web was considered effective in resisting bending.

In determining the areas of the cross section of the composite aluminum and concrete bridge, the following additional considerations were used:

(1) Modular ratio of aluminum to concrete was taken as 3 for all calculations.

(2) Effective slab thickness was assumed to be 5 1/2-inches, the clear depth of concrete from the deck surface to the top of the 2-1/2 inch corrugations.

(3) Governed by AASHO Specifications, the effective concrete slab width on each side of the top longitudinal extrusions was taken as 6 times the effective slab thickness.

(4) The influence of the steel reinforcing bars was neglected.

b. Calculation of Section Properties

(1) Equivalent slab areas

Based on previously outlined assumptions and conditions, the total effective slab width was

$$6 \times 5\ 1/2" = 33 \text{ in.}$$

on each side of two center extrusions C and D and one side of outer extrusions B and E for a total width (including the 9-inch cantilever at the outer edge of the deck) of

$$6 \times 33" + 2 \times 9" = 216 \text{ in.}$$

Therefore, the total effective slab area

$$A_{eff} = 216" \times 5\ 1/2" = 1188 \text{ in}^2.$$

The equivalent aluminum area (modular ratio = 3)

$$A_e = \frac{1188}{3} = 396 \text{ in}^2.$$

This gives an equivalent aluminum plate thickness for the concrete deck across the top of the span

$$t_e = \frac{396 \text{ in}^2}{270\text{" width}} = 1.47 \text{ in.}$$

Adding to this the 0.081-inch top plate, the deck was taken as 1.55 inches thick at a centroidal height of 5 1/4 inches above the upper aluminum extrusions.

(2) Geometric Properties

The preliminary calculations of the section properties are presented in Tables 3 and 4 and Figure 15. Following are the final calculations:

Without Slab - Section subjected to bending about horizontal X-axis only.

$$A_{total} = 86.99 \text{ in}^2$$

$$\bar{z} = \frac{A\,z}{A_{total}} = \frac{1897.88}{86.99} = 21.82 \text{ in.}$$

$$I_x = \Sigma A\,z^2 - A_{total}\,\bar{z}^2 = 85{,}400 - 86.99(21.82)^2 = 44{,}000 \text{ in}^4$$

With Slab

$$A_{total} = 483.1 \text{ in}^2$$

$$\bar{z} = \frac{2202^{3.5}}{483.1} = 45.59 \text{ in}$$

$$I_x = \Sigma A\,z^2 - A_{total}\,\bar{z}^2 = 1{,}106{,}700 - 483.1\,(45.59)^2 = 102{,}664$$

$$I_z = \Sigma A\,\bar{x}^2 = 2{,}898{,}200 \text{ in}^4$$

2. Bending Analysis - AASHO Loading

a. Dead Load

Dead Load deflection and stresses were caused by the weight of the

span was estimated as follows:

span and the wet concrete immediately after pouring. The dead weight for a complete 50 foot span was estimated as follows:

Aluminum Structure	9,000 lbs.
Roadway Slab	74,250
Curb and Sidewalk	26,973
Railing	1,803
Total	112,026 lbs.

This weight divided by a bridge length of 51.15 ft. produced a figure of 2200 lb/ft or 183 lb/in which was used for calculations. The loading condition was as follows:

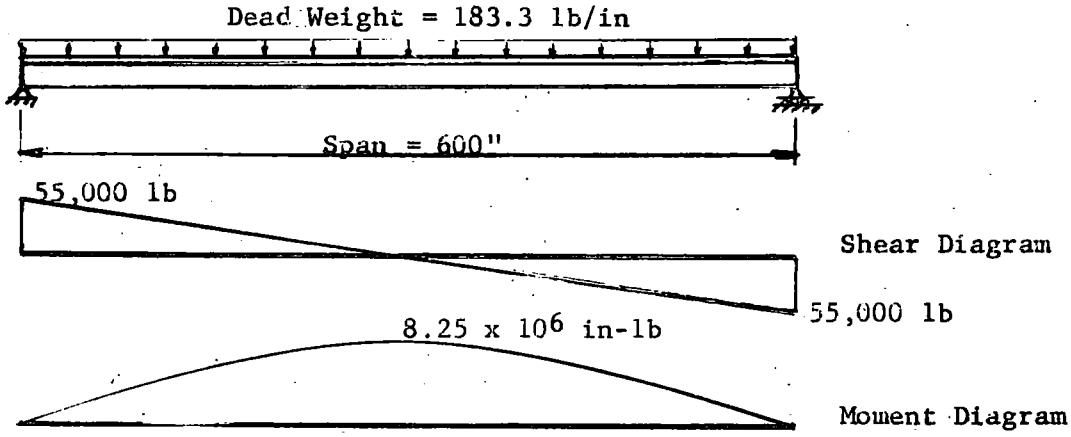

(1) Predicted Deflection (Dead Load)

$$\delta = \frac{5wL^4}{384\ E\ I_x} = \frac{5 \times 183.3 \times (600)^4}{384 \times 10.6 \times 10^6 \times 44{,}000} = 0.664"$$

Where δ = centerline deflection

I_x = moment of inertia of span without roadway slab.

Shear deflections were not calculated for this condition.

(2) Predicted Bending Stresses (Dead Load)

Top aluminum extrusions in compression:

$$f = \frac{M\,c}{I} = \frac{8.25 \times 10^6 \times 23.18}{44{,}000} = 4347 \text{ psi}$$

Bottom aluminum extrusions in tension:

$$f = \frac{M\,c}{I} = \frac{8.25 \times 10^6 \times 21.82}{44{,}000} = 4091 \text{ psi}$$

b. Live Load

Based on an H15-44 AASHO loading, the maximum live load moment occurs when the design vehicle is on the span in the following position:

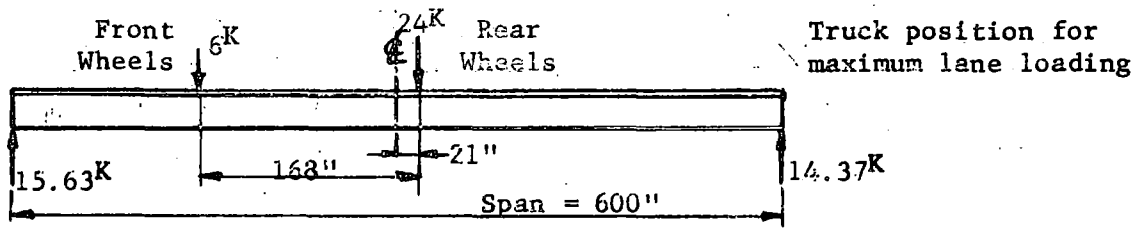

Impact Factor

$$I = \frac{50}{L + 125} = \frac{50}{50 + 125} = 28.57\%$$

where

I = impact factor as percent of live load moment

L = length of span in feet.

Therefore, the totallive load plus impact moment for two lanes

M_{LL} = 14,370 lbs x 279 in x 2 x 1.2857

M_{LL} = 10,313,000 in-lb.

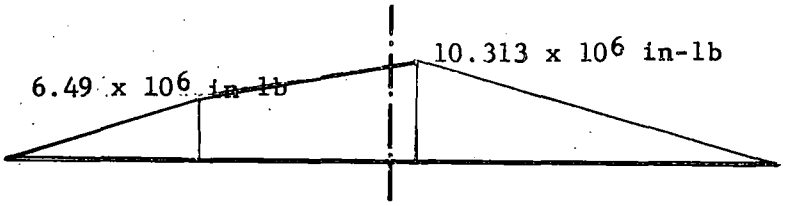

Live Load plus Impact
Moment Diagram at
Design Loads

Maximum shear load, as dictated by the specification, is to be placed directly over the support with the magnitude

$$V_z = 31{,}500 \text{ lbs} \times 1.2857 \text{ impact} \times 2 \text{ lanes} = 81{,}000 \text{ lbs}$$

(1) Predicted Deflections (Live Load)

Specifications require deflection to be computed for a uniformly distributed live load and a concenterated load at the center. Therefore, the deflection due to live load plus impact is:

$$\delta = \left[\frac{5\,w\,L^4}{384\,E\,I_x} + \frac{P\,L^3}{48\,E\,I_x}\right]\left[1 + I\right]$$

Substitution of the following values

$w = 80$ lb per in $\qquad I_x = 102{,}664$ in^4

$L = 600$ in $\qquad P = 27{,}000$ lbs

$E = 10.6 \times 10^6$ psi $\qquad I = 28.57\%$ (Impact factor)

yields

$\delta = 0.3032"$.

(2) Predicted Bending Stresses (Live Load)

Maximum tensile stresses in bottom aluminum extrusions:

$$f = \frac{M\,c}{I} = \frac{10.313 \times 10^6 \times 45.589}{102{,}664} = 4580 \text{ psi}.$$

The top aluminum extrusions are located 0.589 in. from the neutral axis, therefore stresses would be negligible. 59.2 psi

Maximum compressive stresses at top of concrete deck:

$$f = \frac{M\,c}{I} = \frac{10.313 \times 10^6 \times 4.661}{102{,}664} = 468 \text{ psi}$$

3. Unit Shear Analysis

a. Assumptions and Theory

(1) All assumptions associated with the elastic bending of a statically determinate open cross section, such as Hooke's Law and plane cross sections remain plane after bending, apply to this analysis. The equation for normal bending stress and the equation for shear stresses due to bending can be applied. These equations are:

$$\text{Bending stresses } f = \frac{M\,c}{I}$$

$$\text{Shearing stresses } \tau = \frac{V\,Q}{I\,t}$$

The equation for shearing stresses is more conveniently used if the concept of shear flow (q), shear force per unit length, is introduced:

$$q = \tau\,t = \frac{V\,Q}{I}$$

(2) Consider next the closed tube of arbitrary cross section, where the ratio of cross-sectional area of material to the area enclosed by the perimeter is small, subjected to a pure torsional moment as illustrated.

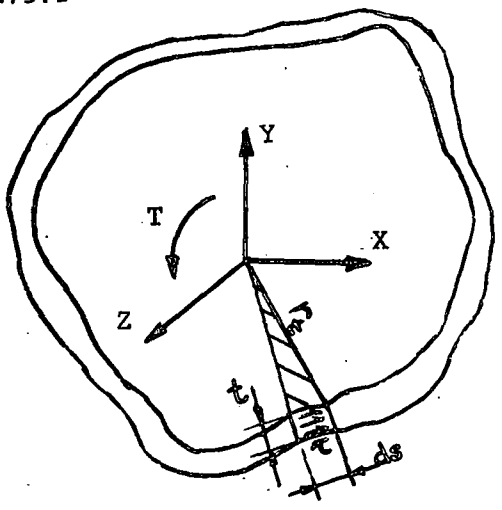

T = externally applied torsional moment

r_t = distance to tangent at a point on the circumference

ds = elemental length of thickness t

τ = shear stress, uniform across thickness t.

To maintain internal equilibrium, the shear flow, q, around the cross section must be constant; and for equilibrium of the cross section:

$$T = \tau t \oint r_t \, ds$$

where $\oint r_t \, ds = 2A_o$ = twice the area enclosed by the section

or $T = t\tau 2A_o$; $\tau = \dfrac{T}{t\, 2A_o}$

To establish the energy relationships for the section, a small element of unit length, dz = 1, is removed. The internal energy, u_i, for this element.

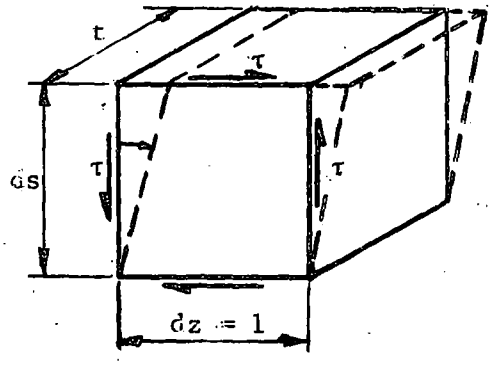

where $u_i = 1/2\, \tau\, \gamma\, dV$

$dV = 1 \times t \times ds.$

Also, $\gamma = \dfrac{\tau}{G}$

where

γ = shear strain

G = shear modulus of elasticity

Subsituting the value for γ in the equation for the internal energy and summing elements around the perimeter, the total internal energy, U_i, becomes:

$$U_i = \frac{1}{2} \oint \frac{\tau^2}{G} \, t \, ds$$

The external energy

$$U_e = 1/2\ T\theta$$

where

θ = angle of twist

Equating the external and internal energy:

$$U_e = U_i$$

$$\frac{1}{2}\ T\theta = \frac{1}{2}\oint \frac{\tau^2}{G}\ t\ ds = \frac{1}{2}\oint \frac{\tau^2 t^2}{G}\ \frac{ds}{t}$$

Substituting

$$\tau t = q \text{ and } T = q2A_o$$

then

$$q2A_o\ \theta = \frac{q^2}{G}\oint \frac{ds}{t}$$

and

$$G\theta = \frac{q}{2A_o}\oint \frac{ds}{t}$$

b. Application to Test Span

Shear analyses of the test span are made for unit shears of 10,000 lbs applied vertically (V_z) and horizontally (V_x), and a torsional moment (T) equal to 1,000,000 in-lb applied at the centerline. The following considerations apply:

(1) The vertical axis of the cross section is an axis of symmetry; therefore, bending is about a principal axis.

(2) Effective bending resistance in the flange is considered to be concentrated at the centroids of the elements as shown in Figure 15. Thus the sheet material between centroids of flange elements is assumed to be subjected to shear stresses only.

The structure is first theoretically cut in such a manner as to make it statically determinate. This permits calculation of statically determinate shear flows due to bending only, from the equation

$$q = \frac{V\,Q}{I},$$

where V is the unit load causing bending about an axis of the cross section perpendicular to its line of action. The following figure shows where the span was cut.

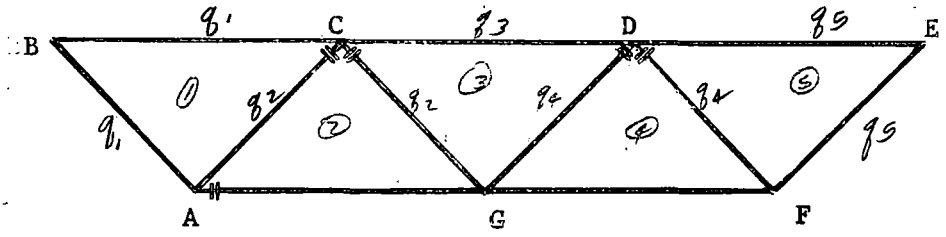

The shear flows within elemental areas are:

$$q = \frac{V}{I} A\,c$$

where A = elemental areas.

These values are calculated in Tables 5, 6, and 7 for the various loading conditions on the bridge with and without the slab.

For each cut made to make the structure statically determinate, a redundant shear flow must be introduced to restore continuity.

Applying the equation developed for the angle of twist of a closed cross section

$$G\,\theta = \frac{q}{2A_o} \oint \frac{ds}{t}$$

to each of the five cells yields the following set of simultaneous equations:

Cell 1: $2 A_1 G \theta_1 = \sum \frac{\ell}{t_1} q_1 - \underset{\text{web AC}}{\frac{\ell}{t}} q_2 + \sum \frac{\ell}{t_1} q$

Cell 2: $2 A_2 G \theta_2 = \sum \frac{\ell}{t_2} q_2 - \underset{\text{web AC}}{\frac{\ell}{t}} q_1 - \underset{\text{web GC}}{\frac{\ell}{t}} q_3 + \sum \frac{\ell}{t_2} q$

Cell 3: $2 A_3 G \theta_3 = \sum \frac{\ell}{t_3} q_3 - \underset{\text{web GC}}{\frac{\ell}{t}} q_2 - \underset{\text{web GD}}{\frac{\ell}{t}} q_4 + \sum \frac{\ell}{t_3} q$

Cell 4: $2 A_4 G \theta_4 = \sum \frac{\ell}{t_4} q_4 - \underset{\text{web GD}}{\frac{\ell}{t}} q_3 - \underset{\text{web DF}}{\frac{\ell}{t}} q_5 + \sum \frac{\ell}{t_4} q$

Cell 5: $2 A_5 G \theta_5 = \sum \frac{\ell}{t_5} q_5 - \underset{\text{web DF}}{\frac{\ell}{t}} q_4 + \sum \frac{\ell}{t_5} q$

Also, the following conditions apply:

(1) For bending about X-axis, no twisting of cells:

$$G\theta_1 = G\theta_2 = G\theta_3 = G\theta_4 = G\theta_5 = 0$$

(2) For an applied torsional moment, no bending:

$$T = 2A_1 (q_1 + q_2 + q_3 + q_4 + q_5)$$

(3) For bending about the vertical (Z) axis

$$T = \sum 2Aq + 2A_1 (q_1 + q_2 + q_3 + q_4 + q_5) = 0$$

The following are unit solutions for five separate loading conditions of the span, with and without the deck slab:

(1). Bridge Without Slab

Unit vertical shear: $V_z = 10{,}000$ lb.

Statically determinate shear flow for cut structure

$$q = \frac{V_z}{I_x} A z$$

Angle of Twist: $G\theta_n = 0$

Tabulated calculations are given in Table 5.

A-B-C-A A-C A-B-C
Cell 1 $2682.46\ q_1 - 785.67\ q_2 + 35{,}500.6 = 0$

C-D-G-C C-G G-D C-D
Cell 3 $2682.46\ q_3 - 785.67\ q_2 - 785.67\ q_4 - 78{,}462 = 0$

D-E-F-D D-F D-E-F
Cell 5 $2682.46\ q_5 - 785.67\ q_4 - 303{,}385 = 0$

D-F-G-D D-G D-F F-G
Cell 4 $2291.34\ q_4 - 785.67\ q_3 - 785.67\ q_5 - 86{,}621.2 = 0$

A-C-G-A A-C C-G G-A
Cell 2 $2291.34\ q_2 - 785.67\ q_1 - 785.67\ q_3 - 15{,}068.2 = 0$

Redundant shear flows are computed to be

$q_1 = -4.699$ lb/in (4.669) $\quad q_4 = 111.988$ lb/in

$q_3 = 70.615$ $\quad q_2 = 29.242$

$q_5 = 145.899$

The resultant shear flows are shown in Figure 16.

2. Bridge Without Slab

Unit torsional moment: $T = 1{,}000{,}000$ in-lb

Statically determinate shear flows: $q = 0$

Angle of twist: $G\theta \neq 0$

$$2 A_1 G \theta_1 = 2628.46\ q_1 - 785.67\ q_2$$

$$2 A_3 G \theta_3 = 2682.46\ q_3 - 785.67\ q_2 - 785.67\ q_4$$

$$2 A_5 G \theta_5 = 2682.46\ q_5 - 785.67\ q_4$$

$$2 A_4 G \theta_4 = 2291.34\ q_4 - 785.67\ q_3 - 785.67\ q_5$$

$$2 A_2 G \theta_2 = 2291.34\ q_2 - 785.67\ q_1 - 785.67\ q_3$$

$$1{,}000{,}000 = 2 A_1 (q_1 + q_2 + q_3 + q_4 + q_5)$$

Redundant shear flows are computed to be:

$q_1 = q_5 = 38.424$ lb/in.

$q_2 = q_4 = 57.413$

$q_3 = 69.242$

The resultant shear flows are given in Figure 16.

(3). Bridge With Slab

Unit vertical shear: $V_z = 10{,}000$ lb.

Statically determinate shear flows for cut structure

$$q = \frac{V_z}{I_x} A z$$

Angle of Twist: $G\theta_n = 0$

Tabulated calculations are given in Table 6.

A-B-C-A A-C A-B-C

$$1723.670\ q_1 - 832.765\ q_2 + 30{,}374.9 = 0$$

$$1723.670\ q_3 - 832.765\ q_2 - 832.765\ q_4 - 3678.5 = 0$$

$$1723.670\ q_5 - 832.765\ q_4 - 143{,}077.5 = 0$$

$$2385.530\ q_4 - 832.765\ q_3 - 832.765\ q_5 - 77{,}590.2 = 0$$

$$2385.530\ q_2 - 832.765\ q_1 - 832.765\ q_3 - 13{,}511.3 = 0$$

Redundant shear flows are computed to be:

$q_1 = -5.022$ lb/in $\qquad q_4 = 100.545$ lb/in

$q_2 = 25.978$ $\qquad q_5 = 131.594$

$q_3 = 63.261$

The resultant shear flows are given in Figure 17.

(4). Bridge With Slab

Unit horizontal shear: $V_x = 10{,}000$ lb.

Statically determinate shear flow for cut section

$$q = \frac{V_x}{I_z} A x$$

Angle of twist: $G\theta_n \neq 0$

Tabulated calculations are given in Table 7.

$$2 A_1 G\theta_1 = 1723.670\ q_1 - 832.765\ q_2 + 3844.5$$

$$2 A_3 G \theta_3 = 1723.670 q_3 - 832.765 q_2 - 832.765 q_4 + 3051.8$$

$$2 A_5 G \theta_5 = 1723.670 q_5 - 832.765 q_4 - 3844.5$$

$$2 A_4 G \theta_4 = 2385.530 q_4 - 832.765 q_3 - 832.765 q_5 - 550.2$$

$$2 A_2 G \theta_2 = 2385.530 q_2 - 832.765 q_1 - 832.765 q_3 - 550.2$$

$$\sum 2 Aq + 2 A_1 (q_1 + q_2 + q_3 + q_4 + q_5) = 0$$

where $\sum 2 Aq = \oint_1 r_t ds$

Redundant shear flows are computed to be:

$q_1 = -6.799$ lb/in $\qquad q_4 = 1.431$ lb/in

$q_2 = 1.431 \qquad q_5 = -6.799$

$q_3 = -5.678$

The resultant shear flows are given in Figure 17.

(5). Bridge With Slab

Unit torsional moment: T = 1,000,000 in-lb.

Statically determinate shear flows: q = 0

Angle of twist: $G \theta_n \neq 0$

$$1723.670 q_1 - 832.765 q_2 = 2 A_1 G \theta_1$$

$$1723.670 q_3 - 832.765 q_2 - 832.765 q_4 = 2 A_3 G \theta_3$$

$$1723.670 q_5 - 832.765 q_4 = 2 A_5 G \theta_5$$

$$2385.530 q_4 - 832.765 q_3 - 832.765 q_5 = 2 A_4 G \theta_4$$

$$2385.530 q_2 - 832.765 q_1 - 832.765 q_3 = 2 A_2 G \theta_2$$

$$1,000,000 = 2 A_1 (q_1 + q_2 + q_3 + q_4 + q_5)$$

Redundant shear flows are computed to be:

q_1 = 36.922 lb/in q_4 = 44.440 lb/in

q_2 = 44.440 q_5 = 36.922

q_3 = 58.392

The resultant shear flows are shown in Figure 17.

c. Predicted Shear Flows for AASHO Loading

The predicted shear flows, based on specification loading, are given in Table 8 and Figure 18. The values, as given, are for the maximum shears which would occur in the end panel extending from Station 0 to Station 5.

The various loading conditions to be investigated are:

(1) Dead Weight (Acting on bridge without slab, Figure 18)

The loading for this condition consists of the dead weight of the aluminum substructure and the wet concrete. The shear actually varies from zero at the centerline to a maximum of 55,000 pounds at the supports (Station 0). The shear flows for this condition are 5.5 times the unit solution for V_z = 10,000 lbs, acting on bridge without slab.

(2) Live Load Plus Impact (Figure 18)

Specifications require that the design shear load be obtained from a uniformly distributed live load plus a concentrated load placed directly over the end support, giving for this span a maximum shear of 81,000 lbs. (which includes the impact factor). However, the concentrated load in this position would be transfered from the deck to the footings through the end frame; but, for this load a small distance from the end of the bridge, this shear

value is approached. The solution is then 8.1 times the unit solution for the composite bridge section (V_z = 10,000 lbs acting on bridge with slab).

According to specification, the live load is assumed acting at a maximum eccentricity of 12 inches, producing a torsional moment

$$T = 63{,}000 \text{ lbs} \times 12 \text{ in} \times 1.2857 \text{ (impact)} = 0.972 \times 10^6 \text{ in-lb.}$$

This solution is 0.972 times the unit solution for a torsional moment equal to 1,000,000 in-lb acting on the bridge with slab.

(3) Live Load Overload (Figure 18)

This condition is the same as for the live plus impact loading on the span except the eccentricity is increased to six feet, causing a torsional moment

$$T = 63{,}000 \text{ lb} \times 72 \text{ in} \times 1.2857 \text{ (impact)} = 5.832 \times 10^6 \text{ in-lb}$$

This solution is 5.832 times the unit solution for T = 1,000,000 in-lb acting on the bridge with slab.

(4) Other Loading Conditions

The following loading conditions were investigated and found to be non-critical; therefore, solutions are not included:

(a) Wind Loading on Bridge

Based on the area of the span as seen in elevation, the wind load causes a horizontal reaction equal to 8282 lbs. This is equivalent to a uniform load acting horizontally and causing bending about a vertical axis of the cross section and a small torsional moment about the longitudinal bridge axis.

(b) Longitudinal Force

This force is taken as five percent of the live load in all lanes carrying traffic in one direction with no impact. The effects of this loading are negligible.

(c) Vehicular Wind Loads

This load is considered to be centered six feet above the roadway acting on two passing vehicles for maximum effect. This causes bending about a vertical axis of the bridge cross section and a torsional moment.

d. Predicted Shear Stresses

To find the magnitude of shear stresses at a point, the shear flows must be divided by the thickness of the section at that point. Predicted shear stresses for the webs and bottom sheets appear in Figure 19.

4. End Frame Analysis

To find the magnitude of the loads in the end frame, it was first necessary to determine the resultant shear flows from the cross section. The horizontal shears are then balanced within the frame and the vertical shears are transfered from the structure to the bearing blocks. For the shear calculations, the elemental loads are equal to the shear flows for a given loading times the length of segment over which the shear flow is acting. The forces in the top sheet and bottom frame members are assumed reacted equally in all six webs.

With loads known and balanced, each diagonal segment of the end frame was then analyzed as a column with an end fixity equal to 0.75. The column cross

sections are taken as shown in Figure 6. The horizontal members did not take any plating into account as effective material.

The theoretical loading condition is shown in Figure 20. The "p" load at the top of the column is due to the shear loading in the top horizontal members. The linearly varying load, α lbs. per in. is due to the shear in the webs. The design condition, Figure 20b, is therefore, a conservative approach.

5. Predicted Temperature Behavior

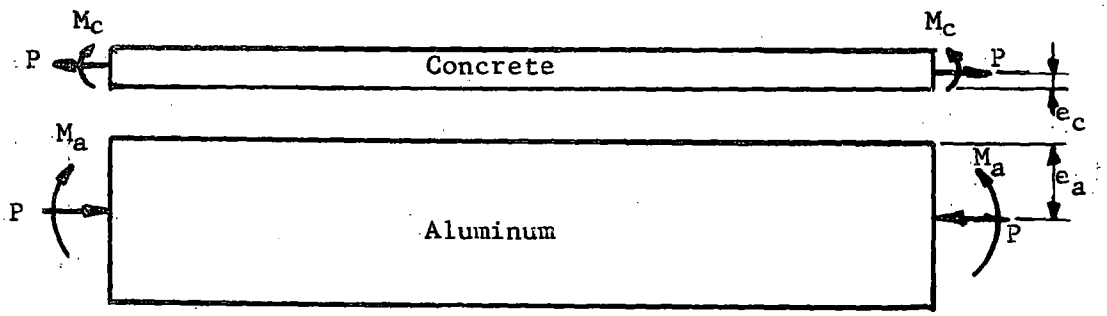

Because the concrete has a lower thermal coefficient of expansion than the aluminum, the span tends to deflect downward due to a temperature increase. If equilibrium is considered around the interface of the aluminum and concrete, then:

$$M_a + M_c = P\,(e_a + e_c).$$

Since the materials are working as a completely composite section, their curvature must also be equal.

$$\frac{1}{\rho_a} = \frac{1}{\rho_c}$$

$$\text{or} \quad \frac{M_a}{E_a I_a} = \frac{M_c}{E_c I_c}$$

At the interface, the adjacent strains must be compatible. These strains are:

$$\epsilon_{temp} = \alpha\ (\Delta t)$$

$$\epsilon_{axial} = \frac{P/A}{E}$$

$$\epsilon_{bending} = \frac{M}{E\ I}\ e$$

Equating the total strain in the concrete to the total strain in the aluminum:

$$\alpha_c\ (\Delta t) + \left[\frac{P/A}{E}\right]_c + \left[\frac{M}{E\ I}\ e\right]_c = \alpha_a\ (\Delta t) - \left[\frac{P/A}{E}\right]_a - \left[\frac{M}{E\ I}\ e\right]_a$$

This equation is simplified by substituting $\left[\frac{M}{EI}\right]_a = \left[\frac{M}{EI}\right]_c$

and the following relationships are evolved:

$$M_a = \frac{E_a I_a}{e_a + e_c}\left\{\Delta t\left[\alpha_a - \alpha_c\right] - P\left[\frac{1}{A_a E_a} + \frac{1}{A_c E_c}\right]\right\}$$

$$M_c = \frac{E_c I_c}{e_a + e_c}\left\{\Delta t\left[\alpha_a - \alpha_c\right] - P\left[\frac{1}{A_a E_a} + \frac{1}{A_c E_c}\right]\right\}$$

$$P = \left[\frac{E_c I_c + E_c I_a}{(e_a + e_c)^2}\right]\left[\Delta t\ (\alpha_a - \alpha_c) - P\left(\frac{1}{A_a E_a} + \frac{1}{A_c E_c}\right)\right]$$

The numerical values for the constants in these equations are as follows:

Material	E	e	I	α	A
Concrete	3×10^6	5.625	4,560	6×10^{-6}	1656
Aluminum	10.6×10^6	23.18	44,000	13×10^{-6}	87

where

e = distance from interface to centroid of material section (in)

α = coefficient of thermal expansion.

For a change in temperature of 100° Fahrenheit, substitution of the above yields:

$M_a = 6510 \times 10^3$ in-lb.

$M_c = 191 \times 10^3$ in-lb.

$P = 232 \times 10^3$ lb.

For the same temperature change the center line deflection is calculated to be:

$$\delta = \frac{ML^2}{8EI} = 0.628 \text{ in.}$$

The thermal stresses are predicted to be:

$$f = \frac{P}{A} \pm \frac{Mc}{I}$$

Top Concrete Fiber

$$f = \frac{232{,}000}{1656} - \frac{191{,}000 \times 2.375}{4560} = 41 \text{ psi Tension}$$

Bottom Concrete Fiber

$$f = \frac{232{,}000}{1656} + \frac{191{,}000 \times 5.625}{4560} = 376 \text{ psi Tension}$$

Top Aluminum Fiber

$$f = \frac{232{,}000}{87} + \frac{6510 \times 10^3 \times 23.18}{44{,}000} = 6097 \text{ psi Compression}$$

Bottom Aluminum Fiber

$$f = \frac{232{,}000}{87} - \frac{6510 \times 10^3 \times 21.82}{44{,}000} = 561 \text{ psi Tension}$$

6. Predicted Behavior Under Test Loading

a. Comparison of AASHO Loading and Test Condition (Figure 21)

(1) General

Practical considerations limited the test conditions to loading at the transverse centerline of the bridge. Concentric or eccentric

lane load could be accomplished by moving the loading jacks laterally at the centerline. As mentioned previously, the load pattern on the deck simulated the rear wheel spacing of an H15-44 truck.

(2) Bending

The 69,000 lbs applied at the centerline produced a bending moment equal to the live load plus impact moment required by AASHO specifications.

(3) Shear

With the truck in position to give maximum moment, the corresponding shear would have been 40,900 lbs; with the test loading the shear was 34,500 lbs. The test set-up did not permit application of an 81,000 lb load directly over the supports as required in the specification.

(4) Torsion

The specification condition required the span to withstand a torsional moment equal to 5,832,000 in-lb combined with a bending moment equal to 100% of design plus impact moment. Test conditions again precluded the possibility of achieving this loading. The maximum torsional moment was 6,220,800 in-lb combined with a bending moment equal to 125% of design plus impact moment applied at the centerline of the span. This loading produces 43,200 lbs shear and 3,110,400 in-lb. torsion in the span.

b. Predicted Test Behavior

(1) Deflection

For the loading used in the test set-up the following formulas

are used to calculate the centerline deflection:

$$\delta_{bending} = \frac{P\,L^3}{48\,E\,I}$$

$$\delta_{shear} = \frac{1}{2}\,\frac{V\,L}{A\,G}$$

where

A = area of web resisting shearing stresses

$A = 6 \times 0.081 \times 1.414 \times 45 = 31\ in^2$.

Substitution of values at test load yields:

$$\delta_b = \frac{69{,}000\ (600)^3}{48 \times 10.6 \times 10^6 \times 102{,}700} = 0.286 \text{ in.}$$

$$\delta_s = \frac{34{,}500 \times 600}{2 \times 31 \times 3.8 \times 10^6} = \underline{0.088}$$

Total 0.374 in.

Deflections for various loads are tabulated below:

Load % M_{LL}	Quarter Point Deflection (inches)			Centerline Deflection (inches)		
	Bending	Shear	Total	Bending	Shear	Total
50	.098	.022	.120	.143	.044	.187
100	.196	.044	.240	.286	.088	.374
150	.294	.066	.360	.429	.132	.561
200	.392	.088	.480	.572	.176	.748

(2) Bending Strains

Sample calculation for strains at centerline follow:

Bottom Fiber - Aluminum

$$f = \frac{M_{LL}c}{I} = \frac{10{,}313{,}000(45.6)}{102{,}700} = 4579 \text{ psi Tension}$$

$$f_t = E\epsilon_t;\ \epsilon_t = \frac{4579 \text{ psi}}{10.6 \times 10^6 \text{ psi}} = 432\ \mu\text{ "/"}$$

Top Fiber - Concrete

$$f_c = \frac{M_{LL}c}{I} = \frac{10,313,000\ (7.4)}{102,700} = 743 \text{ psi}$$

$$\epsilon_c = \frac{743}{3 \times 10^6} = 244\mu\text{"/"}$$

Top Fiber - Aluminum

The top aluminum fibers are located near the neutral axis, therefore, stresses are small and are not computed.

(3) Shear Flows and Stresses

The predicted shear flows for a concentrically applied load producing 100% M_{LL} at the centerline are equal to 3.45 times the unit solution for a vertical shear applied to the bridge with slab (Figure 22).

The predicted shear flows for the load eccentrically applied are 4.32 times the unit vertical shear solution plus 3.11 times the unit torsional moment solution (Figure 22).

The predicted web shear stresses for the above conditions are as follows:

(a) Concentrically applied load, V_z = 34,500 lbs.

Webs	Stress (psi)
AB,FE	1328
AC,FD	1322
GC,GD	1588

(b) Eccentrically applied load, V_z = 43,200 lbs., T = 3.11×10^6 in-lb.

Web	Stress (psi)	Web	Stress (psi)
AB	3080	GD	1453
AC	1944	FD	1367
GC	2525	FE	246

D. PRESENTATION OF RESULTS

1. Deflections

The applied concentric centerline load versus deflection curves for loads up to 138 kips (200% M_{LL} at the centerline) are shown in Figure 23 for measurements made at the centerline and quarter point. Also shown on this figure are the predicted deflection values which take into account both bending and shear.

For the eccentric loading case presented in Figure 24, the predicted bending curve for the center longitudinal member G is the same as for the concentric case.

2. Bending Stresses and Strains

The stress scale indicated at the tops of figures for the strains in the main longitudinal members A through G and the deck is based on a modulus of elasticity equal to 3,000,000 psi for concrete and 10,000,000 psi for the aluminum.

a. Top Flange

The five Whittemore strain gages located on the deck surface at Station 23 gave the concentrically applied load versus strain curves presented in Figure 25. The same information for the eccentric loading condition is presented in Figure 26.

The response of the strainometers located on the longitudinal centerline at mid-height between the steel reinforcing bars at Station 22 and the quarter point is given in Figure 27.

The strains recorded for each of the main longitudinal members B,C,D, and E are given in Figures 28 through 31. Comparison of strains for these four members is made in Figure 32. The eccentric loading case is presented in Figure 33.

Strains measured on the deck surface and top longitudinal members B, C, D, and E are presented in Figure 34 with respect to their physical location. Data is presented for a load of 69,000 lbs applied concentrically and eccentrically.

b. Bottom Flange

The strains recorded for each of the three main longitudinal members A, G, and F are presented in Figures 35 , 36 , and 37 . A comparison of strains in the three members is made in Figure 38 . The eccentrically applied load versus strain curves for these three members are presented in Figure 39 .

The concentric load-strain curves as recorded for the three individual gages of a strain rosette on the bottom sheet are given in Figure 40. The gage parallel to the longitudinal bridge axis gave the strains due to bending. The eccentric load-strain curves for the bottom sheet rosettes are given in Figure 41.

c. Webs

The strains in the webs due to bending are derived from the data recorded from the horizontal gage of the 45^{0} rosette at the mid-height of the web. The strains for all three gages of each web rosette are shown in Figures 42 through 47 and Figure 48 for the eccentric loading.

d. Comparison of Strains at the Quarter Point Cross Section

After test 15 additional gaging was placed on the span to determine a more complete vertical strain distribution at the quarter point cross section. Since the load-strain curve was linear for all gages up to the applied 200% M_{LL} at the centerline, data for Figure 49 was taken for the highest load increment of Test 16, 138 kips, which gave 200% M_{LL}. The bending moment at the quarter point was one-half the bending moment at the centerline. Figure 49 gives the strains as a function of their vertical location at the cross section.

3. Shear Stresses and Strains

The measured shear strains for the bottom sheet were derived from Figure 40 for the concentric case and Figure 41 for the eccentric case by a Mohr's Circle reduction of data. The data for the webs presented in Figures 42 through 47 was reduced by the same method to get web shear strain values.

The shear strains converted to stresses (shear modulus equal to 3.8 x 10^6 psi) are compared with predicted shear stresses in Figure 50 for an applied concentric load equal to 69,000 lbs. The eccentric case for the same load is presented in Figure 51 .

4. Centerline and End Frames

Strains in the transverse centerline frame are considered to be induced by forces acting in the plane of the frame. Since the load-strain curve was linear for all gages up to an applied centerline load of 138 kips,

the strain distribution in this frame caused by a load of 69,000 lbs applied concentrically and eccentrically directly above the frame is plotted in Figure 52 relative to the location of the electrical strain gages. For clarity, the figure shows the bridge divided into the three triangular beams containing elements of the frame.

The end frame was also considered to be strained by forces in the plane of the frame. The distribution of strains at two cross sections of the end frame is shown in Figure 53 at an applied centerline load equal to 69,000 pounds for the span on roller bearings. Both the eccentric and concentric loading is shown.

5. Destruction Tests

The bending moments at the centerline and quarter point given in Table 10 were computed from the loading given in Table 2. Strains at the centerline and quarter point were used to determine the magnitude and location of the dead loads, with the shear strains at the quarter point used as a check.

The web shear strains listed are Mohr's Circle reductions of the data recorded for the three gages of the 45° rosettes. Tensile strains in the bottom members A, G, and F were averaged to arrive at the value given in Table 10. Variation of strains between gages was small enough to permit the use of these averaged values.

The centerline deflections as recorded at bottom members A and F were corrected for end support settlements and temperature deflections, then averaged to arrive at the value in Table 10.

Observations made during the final testing of the bridge are noted in Table 10 also.

6. Natural Frequency

Figure 54 is a tracing of the automatic recording tapes for the three trials made to determine the natural frequency of the bridge.

7. Temperature Deflections

Figure 55 presents the results of the deflection and temperature observations made between September 8 and November 6, 1958. The slope of the curves for centerline deflections, quarter point deflections, and end movement gives a measure of movement per degree temperature change.

E. DISCUSSION OF RESULTS

1. Dead Load Effects

a. Deflections

The dead load centerline deflection was predicted to be 0.664-in., based on an anticipated bridge dead weight of 183.3 pounds per inch. The actual loading condition closely approximated the following:

27 cubic yards concrete @ 110 pcf	80,200 lbs.
10% additional weight for moisture content when poured	8,020
Aluminum	11,360
Reinforcing steel	6,700
Total	106,280 lbs.

Dead weight per linear inch equals

$$\frac{106,280}{51.15' \times 12} \cong 173 \text{ pounds per inch.}$$

Based on this dead weight, the actual bridge deflection was predicted to be 0.627 inches. The predicted deflection due to the weight of the concrete alone was 0.520 inches.

Observations made during the pouring of the deck slab indicated that temperature effects due to direct sunlight and the heat of hydration of the freshly poured concrete on the aluminum top flange caused a non-uniform temperature differential of approximately 60 degrees between the top and bottom flanges of the bridge. This, in turn, caused an upward deflection of the span.

After placing of the aluminum structure and the steel reinforcing, deflections of the bridge were measured due to the effects of the wet concrete only. Upon completion of the deck pour the deflection at the centerline was measured at 0.504-inch.

b. Stresses

Twenty-four electrical strain gages were read at different time intervals during the pouring of the deck. The data from these gages was inconclusive as a check of the predicted dead load stresses because of the temperature influences on the behavior of the span.

Readings taken on the day following the deck pour indicated the span was acting as a composite member and reacting to changes of the ambient air temperature.

The predicted dead load stresses in the aluminum structure were:

Maximum compressive stress, top aluminum fiber - 4347 psi

Maximum tensile stress, bottom aluminum fiber - 4090 psi.

2. Live Load Effects

a. General

The original test installation placed the bridge on oil-impregnated bronze bearing pads, restrained from horizontal movement at the west end, but free to slide at the east end. Both ends allowed rotational movement. After 360,000 cycles of dynamic loading to 150% M_{LL} at the centerline (Test 7), it was noted that the bearings at the free end were not sliding, thus causing a partial restraint or horizontal reaction at the top of the footing pedestal. This reaction caused an eastward horizontal movement of 0.036-inch at the point of application under an applied centerline bridge load of 103.5 kips.

After completion of Test 8a, the bronze bearing pads were removed at the east end and each one replaced with a new bearing resting on a nest of seven 3/4-inch lubricated rollers. This eliminated the horizontal motion of the top of the pedestal. Before resumption of the dynamic testing, Test 8b was completed.

Test 8b and succeeding tests indicated the effect the bronze bearing pads had on the end of the span. Relative movement between the bridge and pedestal ranged from 0.152-inch for test 10 to 0.185-inch for test 16 (both tests under 103.5 kips centerline load).

All test results in which this condition of restricted end movement had an effect upon the bridge are presented together with the results obtained after replacement of the bronze bearing pads. For Tests 1 through 16 inclusive, all results gave a linear relationship between load and strains or deflections up to 138 kips applied at the centerline producing 200% M_{LL} at the point of load application.

b. Bending Behavior

(1) Deflections

AASHO Specifications [1] allow a deflection due to live load plus impact equal to 0.750-inch (1/800 of the span length). This deflection, based on a uniformly distributed and a concentrated load plus an impact factor, was calculated to be 0.303 inches.

The predicted deflections calculated for the test load applied concentrically at the centerline include the effects of bending and shear.

The same value is shown for the predicted deflection of the longitudinal centerline (member G) of the span under an eccentrically applied load.

Measured at the main longitudinal members A, G, and F with mechanical dial gages reading to 1/1000-inch, the deflections under the bridge showed a small variance in readings at the centerline or quarter point under concentric loading, allowing averaged readings to be used for each curve (Figure 23). From the numerical comparisons made in Figure 56 , the measured value at the centerline was 6.1% more than the predicted deflection. At the quarter point the difference was 8.3%.

The measured deflection under member G for an eccentrically applied load of 69,000 lbs was 4.3% greater than predicted at the centerline. At the same section, member A deflected 32% more than member G; member F deflected 27% less than member G. At the quarter point the measured deflection of member G was 8.8% greater than predicted with +27% and -28% variation in the deflections of A and F respectively. The measured deflections along member G were practically the same at the centerline and quarter point for the load applied either concentrically or eccentrically.

The deflections of the deck surface, measured with an engineer's level reading scales graduated to 1/100-inch, showed excellent agreement with the data obtained from the dial gages.

The three scales placed on the deck directly over the pedestals indicated negligible settlement of the footings (1% of the total centerline deflection) with a 138 kip load on the bridge. The magnitude of settlement was correlated in Test 16 by the data obtained from the dial gages which had been placed to measure footing settlements.

(2) Top Flange (Reference Figures 25, 26, 27, 32, 33, 34)

For the concentric loading tests, distribution of strains across the deck surface and in the top longitudinal members B, C, D, and E near the centerline indicated a slight "dishing" of the deck near the point of load application. This was evidenced by greater strains toward the center of the deck and greater strains in the inside top members C and D which were under two of the bearing plates of the loading beams. The strain distribution on the deck surface also indicated that the entire deck was active in bending.

After Test 15, the additional gaging placed on the deck surface at the quarter point to determine further the lateral strain distribution failed to give any additional information due to scatter of the test results. Strains in the top longitudinal members at the quarter point were small, but comparison with the centerline strains on corresponding members indicated that the centerline strains were influenced by localized effects. Additional gages placed on the outside of members B and E after Test 15 confirmed these results.

The same conclusions can be drawn from the data for the eccentric load tests; that is, (1) there were localized increases in strain near the point of load application and (2) the entire deck was active in bending.

The strainometer at Station 22, placed at mid-height between the top and bottom reinforcing bars along the longitudinal centerline, also showed a slight increase in strain due to its proximity to the point of loading; it gave strains approximately 2 1/2 times greater than the strains recorded at a corresponding gage at the quarter point.

For the eccentric loading condition the strains measured by the

strainometers very closely followed the curve obtained for the concentric loading case.

The strains recorded from the strain rosettes mounted at the center of top sheets BC, CD, and DE at the quarter point were very small and scattered. The gage in the rosette parallel to the longitudinal axis of the span measured strains due to bending; results from all three gages of a rosette were used to determine the magnitude of principal strains, and hence, the shear strains. Since none of the gages gave any strain readings which were consistent and of any magnitude, it can be concluded that (1) the gage was near the neutral axis of the bridge cross section and (2) there were no shear strains at the point the gage was affixed to the top sheet. The results from the gages on members B, C, D, and E at the quarter point also help verify the location of the neutral axis.

(3) Bottom Flange

The gages on the outer longitudinal members A and F gave slightly (2 1/2%) greater strains than the gage on center member G. The centerline strains were twice the quarter point strains on the same member, indicating there were no local effects, such as the location of the bearing pads of the loading beams, influencing centerline strains.

Gaging of the bottom sheets AG and GF indicated that tension strains in the sheets due to bending of the bridge were slightly less than, but proportional to, the strains in the bottom longitudinal members. The gages applied to the top and bottom of the sheets perpendicular to the longitudinal bridge axis indicated there was no bending of the bottom sheets in this direction.

For the eccentric tests the strains at the centerline obtained in longitudinal member G were 14% higher than the strains obtained for the 69 kip load applied concentrically and equal to the predicted strain for the member. Member A was strained 10% higher than member G and member F was strained 27% less than member G. At the quarter point the strains in members G and F differed by 2.7% and were approximately 18% less than the strains in member A.

The data for the bottom longitudinal members under an eccentric load indicated a slightly unequal distribution of the load to the components of the span; that is, triangular beam ABC carried slightly more load than the other two sections.

(4) Vertical Strain Distribution at the Quarter Point

An overall comparison of the strains in the deck, top aluminum, webs, and bottom aluminum was made in Figure 49 to arrive at the vertical strain distribution at a quarter point cross section. It can be seen from the figure that the entire cross section is active in bending and the strains are proportional to their distance from the neutral axis.

By obtaining the slope of the line connecting these points, the vertical location of the neutral axis for each web section was determined with respect to the location of the bottom gage. The average of the six vertical heights so obtained gave the location of the neutral axis as 47.4 inches above the plane of the gages on members A, G, and F. The predicted height, measured from the same reference plane, was 46.6 inches. Physically, the neutral axis was located in the plane of the top sheet CD.

c. Shear Behavior

Electrical 45° rosette strain gages were placed on the top sheets, webs, and bottom sheets to determine the principal shear strains and hence, stresses at selected points of the quarter point cross section.

Gage readings for the rosettes at the centerline of the top sheets, although small and scattered, indicated strains in the magnitude of 10 microinches per inch under a centerline load of 138 kips (200% M_{LL}). This meant that the gage was located at a point of zero bending and shear strains, a condition which would occur along the longitudinal centerline of sheets BC, CD, or DE at the neutral axis of the bridge cross section.

Reduction of the data from the individual gages of the web rosettes by the Mohr's Circle method gave strains very close to the predicted for the concentric loading condition (Figure 50). The agreement between measured and predicted strains for the eccentric loading condition was not as close, but was within approximately 10% (Figure 51).

If the entire web had been active in bending as indicated in Figure 49 , then the shear distribution along each web would have been parabolic, with a small variation, rather than uniform as predicted. Thus, the gages may not have been located at a point of maximum shear stress, which would partially account for the differences between predicted and measured, particularly for the eccentric case. Due to the large ratio of flange to web areas, the uniform distribution as predicted is close to the measured value.

The assumption that areas were concentrated at the centroids of elements having 22 1/2-inch horizontal projections was used to predict the shear flows in the bottom sheet. This led to a solution which gave uniform

shear flows between centroids of flange elements with an increase or decrease occuring at the centroids. Actually, the shear in the bottom sheet varies linearly with the only sharp breaks occuring at the main longitudinal members A,G, and F. This condition would lead to disagreement between the predicted and measured shears (Figures 50 and 51).

d. Centerline and End Frame Behavior

The loads induced in the frame members due to the applied load on the deck were reacted by (1) a uniformly varying load, in pounds per inch of length of the sheet to which the frame member is attached, and (2) an axial load taken out at the ends of the frame member.

Under a concentrically applied centerline load of 69 kips (100% M_{LL} at the centerline) the maximum live load stress in any portion of this frame was approximately 1900 psi in compression. For an eccentric load of 69 kips, the maximum compression stress was approximately 3200 psi.

The strain distribution in the diagonals of the end frame indicated there was possible bending at the upper cross section due to the method of loading - that is, the shear in the webs pulling on the inside edge of the frame as a uniform load (pounds per inch of length of the frame diagonal). This was also discussed in connection with the frame design procedure.

At a lower cross section the load was almost equal in the channel sections, indicating a more uniform distribution of load across the section and, therefore, a uniform distribution of load on the bearing block.

The magnitude of axial load transmitted to the bearing blocks by each of the frame diagonals could not be determined without additional data,

but the relative magnitude can be seen in Figure 53. In general, the same relations existed between load distribution in the outside channel, doubler plate, and inside channel at each corresponding cross section of the six different diagonal frame members.

The stresses under a concentric centerline load of 69 kips (100% M_{LL} at the centerline) were only in the magnitude of 1350 psi. For the eccentric condition under the same 69 kip load the maximum stress was 3300 psi. Comparing the measured stresses with a design stress (live load only) of approximately 6150 psi assumed to be acting over the entire length of the member, it can be seen that the design approach was conservative.

e. Destruction Test

Table 10 is the summary of the results of destruction Tests 17 and 18. Linear behavior of the span was indicated up to a shear of 241.8 kips (load increment 11) which caused elastic buckling of the outer webs visible at the end supports. The first buckling appeared near the bearing block, with additional buckles later appearing above these under increasing loads. At load increment 20, inelastic buckling had occured.

The highest load increment at which gage readings were taken was increment 20. With 85,100,000 inch-pounds moment at the centerline, 49,900,000 inch-pounds moment at the quarter point, and 328.0 kips shear, the centerline deflection was 3.87 inches and tensile stress in the bottom fiber was 38,000 psi.

After releasing the jack load of increment 21, an attempt to reload the span led to a sudden and complete collapse of the bridge (Figures 57 and 58). At the time of failure, the centerline moment was 885% M_{LL}.

f. Temperature

Calculation of the slope of the long time temperature-deflection curves (Figure 55) by the method of least squares gave a relationship for movement per degree change in temperature as follows:

1. Centerline deflection = 0.0062 in.
2. Quarter point deflection = 0.0042 in.
3. Relative end movement (between bridge and pedestal) =0.0068 in.

According to the theory used to predict temperature effects caused by differences of coefficients of thermal expansion for concrete and aluminum, deflections would be caused by a moment acting at the ends of the span. End movements would be the total effect of strains due to temperature, axial load, and bending moment. The theoretical movements per degree change in temperature were calculated to be:

1. Centerline deflection = 0.00628 in.
2. Quarter Point deflection = 0.00471 in.
3. Relative end movement = 0.0081 in.

Analysis of the electrical strain gage data for temperature changes only gave very inconclusive results. The change in strain per degree temperature change varied from one test to another, precluding the possibility of getting an accurate picture of the temperature-strain behavior.

Over a short period of time, such as during one complete test, most gages were consistent and allowed reduction of data as described in Appendix B. Continuity of readings between tests over longer periods of

time was obtained with the mechanical dial gages; but, due to sensitivity to direct heat and sunlight, gage creep, and the variable temperature and humidity conditions at the test site, no continuity of readings was obtained for the electrical strain gages from one test to another. Even the use of temperature compensated electrical gages mounted opposite selected SR-4 gages failed to give any pertinent information regarding strain behavior due to temperature changes.

Measurements made to determine the temperature distribution within the span indicated the following:

1. Bottom sheet and deck surface responded more quickly to sunlight and temperature change than did the internal members of the span such as the diagonal webs GC, GD, and top aluminum sheet CD supporting the deck.

2. In general, the temperature was not uniform, nor was there a uniform gradient, within the span. Only when the air temperature started to drop and the direct rays of the sun were not acting on the span did the temperature distribution tend to become uniform across a section of the span.

g. Natural Frequency

The predicted frequency of the span was computed to be approximately 400 cycles per minute. The results of three tests gave the natural frequency equal to 333 cycles per minute.

F. SUMMARY AND CONCLUSIONS

1. Dead Load

The predicted dead load deflection of the aluminum structure due to the weight of the wet concrete only was 0.520 inches. The maximum measured dead load deflection was 0.504 inches, which was influenced by temperature effects of direct sunlight and hydration of the concrete.

Test results did not provide a satisfactory measure of the dead load stresses to check the predicted stresses of 4347 psi compression in the top aluminum fiber and 4090 psi tension in the bottom aluminum fiber.

After initial curing of the concrete during the 24 hour period immediately following the pouring of the deck, observations indicated changes in the deflected shape of the structure with changes of the ambient air temperature. This indicated composite action between the concrete and aluminum responding to the different rates of thermal expansion.

2. Static Live Load Effects

a. Loading

The AASHO Specification truck loading on this span produced a design moment due to live load plus impact equal to 10,313,000 in-lbs at a point 21 inches from the center of the span. A 69,000 lb test load applied at the centerline produced the same bending moment.

The concentric loading of each lane at the center of the span produced a shear load of 34,500 lbs on each half of the span. Specification

requirements of 81,000 lbs shear directly over an end support could not be duplicated due to limitations at the test site.

With eccentric loading, the maximum specification condition would have produced a torsional moment equal to 5,832,000 in-lbs and a bending moment equal to the live load plus impact design moment of 10,313,000 in-lbs. The maximum eccentric test loading condition produced moments of 6,220,800 in-lbs torsion and 12,891,000 in-lbs bending combined with a shear of 53,200 lbs.

b. Bending Behavior

The predicted deflection due to an applied load of 69,000 lbs producing 100% M_{LL} at the centerline compared with measured deflections as follows:

	Deflections (inches)		
Location	Predicted	Measured	
	Concentric Loading	Concentric Loading	Eccentric Loading
Centerline	Bending .286 Shear .088 Total 0.374	0.397	A 0.500 G 0.369 F 0.256
Quarter Point	Bending .196 Shear .044 Total 0.240	0.260	A 0.317 G 0.243 F 0.168

The predicted stresses due to the design live load plus impact moment at the centerline compared with stresses derived from the measured strains, using a modulus of elasticity E of 10,000,000 psi, as follows:

Bottom Longitudinal Members	Stress (psi)			
	Centerline		Quarter Point	
	Predicted	Measured	Predicted	Measured
A	4579	4210	2290	2070
G		4040		1900
F		4210		2030

For the same load (69,000 lbs) eccentrically applied, the stresses were as follows:

Bottom Longitudinal Members	Stress (psi)			
	Centerline		Quarter Point	
	Predicted	Measured	Predicted	Measured
A	--	5050	--	2200
G	4579	4600	2290	1850
F	--	3350	--	1800

Stresses in the top longitudinal members were negligible.

Test data indicated a localized increase in strain in the deck and top longitudinal members near the point of load application. Top longitudinal members and the deck exhibited highest strains toward the longitudinal centerline of the deck, indicating a very slight dishing effect near the point of load application.

The stresses in the deck at Station 23 varied from 280 psi eight feet on either side of the longitudinal centerline to 360 psi along the centerline. Data from this area (near the load point) also indicated the entire deck was active in bending. For the eccentric loading condition, stresses varied from 390 psi in the loaded lane to 180 psi in the unloaded lane. All concrete stresses were based on a modulus of elasticity of 3,000,000 psi for the material.

Test results indicated the location of the neutral axis was in the plane of the top sheet, approximately 47.4 inches above the gages on the bottom members. The calculated height of the neutral axis, from the same reference, was 46.6 inches.

c. Shear Behavior

The predicted shear stresses at the quarter point due to a concentric 34,500 lb shear force (69,000 lbs applied at the centerline) compared with the stresses derived from the measured strains using the shear modulus G equal to 3,840,000 psi as follows:

Web	Stress (psi) Predicted	Measured
AB	1328	1555
AC	1322	1344
GC	1588	1574
GD	1588	1555
FD	1322	1294
FE	1328	1467

For the maximum eccentric condition of 86,400 lbs and 6,220,000 in-lbs applied at the centerline the comparison was as follows:

Web	Stress (psi) Predicted	Measured
AB	3080	3302
AC	1944	1890
GC	2525	2642
GD	1453	1290
FD	1367	1498
FE	246	695

d. Centerline and End Frames

The maximum measured stress in any member of the centerline frame was approximately 3200 psi under an eccentrically applied load of 69,000 lbs. The maximum measured compressive stress in the end frame also occured under the eccentric loading condition and was equal to approximately 3300 psi. The measured stresses were considerably less than the 6150 psi used for design.

e. Destruction Test

Up to a shear load of 241,800 lbs and a bending moment of 63,500,000 in-lbs (load increment 11 of the destruction test) there was a linear relationship between static load and stresses or deflections.

The highest load sustained by the bridge produced a bending moment equal to 970% of the live load plus impact design moment at the centerline with a shear force equal to 378,800 lbs. The shear load was 4.7 times the AASHO design requirement of 81,000 lbs. This load was held for ten minutes then partially released. Failure occured at 885% M_{LL} during another attempt to load the span.

f. Temperature

Observations indicated the centerline deflection of the span was 0.0062 inches downward for a one degree rise in ambient air temperature. This movement was predicted to be 0.00628 inches per degree temperature change. Analysis of the electrical strain gage data for temperature changes gave inconclusive results.

In general, the temperature distribution within the span was not

uniform. The bottom sheet and deck responded more quickly to sunlight and temperature changes then internal members.

g. Natural Frequency

The natural frequency was predicted to be approximately 400 cycles per minute and measured at 333 cycles per minute.

3. Dynamic Live Load Effects

The following program of repeated loads was applied to the structure:

a. 250,000 cycles producing 100% M_{LL}

b. 250,000 cycles producing 125% M_{LL}

c. 753,000 cycles producing 150% M_{LL}

d. 200,000 cycles producing 125% M_{LL} with a torsional moment of 6,220,000 in-lb.

Static tests before and after each dynamic test indicated the bridge did not suffer any visible damage or loss of structural integrity due to the repeated application of these loads.

4. Summary of Stresses

A summary of the primary stresses in the span is made in Table 11.

ACKNOWLEDGEMENTS

This investigation was carried out under the joint sponsorship of the Fairchild Airplane and Engine Corporation, Bureau of Public Roads, Aluminum Company of America, Reynolds Metals Company, Kaiser Aluminum Company, and Olin Mathieson Chemical Corporation.

The authors of this report wish to thank the sponsors' representatives composing the Fairchild Aluminum Bridge Technical Committee for their helpful suggestions in the planning and testing stages of this investigation. Gratitude is also expressed to Professor William J. Eney, Director of Fritz Engineering Laboratory, Dr. B. Thürlimann and other members of the laboratory staff for their cooperation, suggestions, and assistance in completing the test program and report.

The assistance of Mr. Frank Weaver, Assistant Superintendant of Buildings and Grounds, Lehigh University, in the preparation of the test installation is also gratefully acknowledged.

REFERENCES

1. American Association of State Highway Officials — "STANDARD SPECIFICATIONS FOR HIGHWAY BRIDGES," 1953.

2. Committee of the Structural Division on Design in Lightweight Structural Alloys — "SPECIFICATIONS FOR STRUCTURES OF ALUMINUM ALLOY 6061-T6", Proceedings ASCE, Paper 970, Vol. 82, No. ST 3, May 1956.

3. Smislova, A. Roesli, A. Brown, D. H., Jr. Eney, W. J. — "ENDURANCE OF A FULL-SCALE POST-TENSIONED CONCRETE MEMBER," Fritz Engineering Laboratory Report 223.6, Lehigh University, May 1954.

4. Kahn, H. J. — "STRESS ANALYSIS, ALUMINUM HIGHWAY BRIDGE, FAIRCHILD DESIGN TEST STRUCTURE OF 50 FOOT SPAN," Report No. 50-S1, Fairchild Kinetics Division, Fairchild Engine and Airplane Corporation, April 1958. (Not published)

5. Kuhn, P. — "STRESSES IN AIRCRAFT AND SHELL STRUCTURES," McGraw Hill Book Co., New York, New York, 1956.

NOMENCLATURE

These notations are used unless otherwise noted in text.

A = Area

A_e = Equivalent area

A_{eff} = Effective area

A_{total} = Total area

c = Distance from axis of bending to fiber at which stress is desired

E = Modulus of elasticity

f = Stress due to bending

G = Shear modulus of elasticity

I = Impact factor

I_x, I_y, I_z = Moment of inertia about X, Y, or Z - axis

L = Span length

M = Bending moment

M_{LL} = Bending moment due to live load plus impact = 10,313,000 in-lb.

n = Modular ratio of aluminum to concrete

P = Applied concentrated load

Q = Statical moment area about the neutral axis

q = Shear flow

q_n = Redundant shear flow, where n = cell number

T = Externally applied torsional moment

t = Thickness

t_e = Equivalent thickness

u_i = Internal energy for an infinitely small element

U_i = Total internal energy

U_e = Total external energy

V_x, V_y, V_z = Shear load applied in x, y, and z directions

w = Uniformly distributed live load

x, y, z = Coordinates of an element with respect to principal axes

$\bar{x}, \bar{y}, \bar{z}$ = Coordinates of the centroid of the cross-section with respect to the reference axes X', Y', Z'

γ = Shear strain

δ = Deflection

Δt = Increment of temperature change

ϵ = Strain

ϵ_{temp} = Strain due to temperature

ϵ_{axial} = Strain due to an axial load

$\epsilon_{bending}$ = Strain due to bending of the section

θ = Angle of twist due to an applied torsional moment

θ_n = Angle of twist of cell n

ρ_a, ρ_c = Curvature $\left(\frac{M}{E\ I}\right)$ of aluminum and concrete portions of the bridge

APPENDIX

A. MATERIAL PROPERTIES

1. Concrete

The concrete for the deck was designed for a minimum strength of 3,000 psi at 28 days. To maintain the concept of a lightweight structure, the concrete design embodied a lightweight slag aggregrate commercially known as Waylite.

The following mix, which had been tried and used previously by the Waylite Company, was used for the bridge deck:

Mix proportions (loose dry volume) - 1 : 1.5 : 2.25

Admixture - 6 oz. Darex per cubic yard

Cement - Lehigh Portland, Type I, 8 1/2 sacks per cubic yard

Dry materials were transported from the batch plant to the job site in ready-mix trucks of 4 to 5 cubic yard capacity. Batch slips indicated a total of 30 cubic yards of concrete was delivered to the bridge site. Upon arrival of a truck, water was added and thoroughly mixed with the dry materials. Before and during the unloading of each truck, a standard slump test was run to determine whether or not the concrete had the proper water content, a two to three inch slump was required.

The concrete was unloaded from the truck into a one cubic yard bucket, lifted to the deck level, placed, then vibrated for optimum compaction. The surface was raked smooth and finished with a screed spanning the 24-foot width of deck between forms.

After the proper surface was obtained by the screed, the deck was covered with wet burlap; curing was completed by keeping this burlap wet for seven days after the pour.

A total of 14 cylinders were poured and tested, four at 11 day strength and ten at 28 day strength. Results are compiled in Table 12 . The average twenty-eight day strength was 4150 psi with an average density of 108 pounds per cubic foot.

2. Reinforcing rods

The concrete deck contained 6700 pounds of intermediate grade, 18,000 psi design strength, reinforcing rods. Longitudinal reinforcement consisted of #4 rods (one-half inch diameter) at eighteen-inch centers top and bottom, using a total of 34 bars. Transverse reinforcing bars were #5 rods (five-eighths inch diameter) at six-inch centers top and bottom. Insulation was placed between the steel and the top aluminum to prevent corrosive action at points of contact and to insure proper bond between the steel and concrete.

3. Aluminum

All aluminum used in the structure was standard production quality 6061-T6 alloy. This material was chosen for its ability to resist corrosion as well as for its structural properties.

After completion of the test program, 10 specimens were cut from areas of the bridge where stresses did not exceed the proportional limit of the material. The specimens had a gage length of 8 inches and cross section

dimensions as shown in Table 13 . As the specimen was loaded, an inductance gage measuring elongation over the 8 inch gage length and an automatic recorder were used to plot a graph of load versus strain. The graphs were then used to determine the elastic modulus and the yield strength (stress that produces a permanent set of 0.2 per cent of the initial gage length). Table 13 summarizes the material properties and gives the locations from which specimens were taken.

APPENDIX

B. RECORDING AND REDUCTION OF DATA

When reading any one electrical strain gage, the SR-4 Strain Indicator showed a slight creep causing a continually changing reading. This was due to humidity and temperature effects acting directly on the strain gage. The strains on a specific gage could possibly change plus or minus 25 microinches during the short period required to balance the Indicator. Readings were therefore made to the closest 5 microinches in as short a time as possible.

During any of the test periods the continually changing temperature induced strains in the span which in turn changed the zero reading (under no load) for most strain gages and, at the same time, caused deflection of the bridge. Since it was impossible to maintain a constant temperature at the test site, it was necessary to separate the changes due to temperature, and the strains and deflections caused by the applied load.

The following load sequence was used to take data:

1. Under no load a full set of zero readings was taken.
2. A load increment was applied and a full set of readings was taken.
3. The span was unloaded and another full set of zero readings was taken.

The difference in the zero readings was assumed to be the net change due to temperature.

To evaluate the method used, Test 6N was conducted from 12:00 PM to 8:00 AM (the total temperature change equaled 1 1/2 degrees) and then

repeated as Test 6D from 8:00 AM to 3:30 PM on the same day (the temperature change equaled 15 1/2 degrees).

The test results shown in Figure 59 were taken from a strain gage mounted on the bottom longitudinal extrusion on the south edge of the span. The recorded and reduced data is presented in Table 14. The total strain increment due to applied load and temperature change (designated as a-b on Figure 59) had to be corrected for the average zero change (indicated as a-c on Figure 59) over the period of one load increment. Applying this correction amounted to averaging the total change due to loading and unloading. The results are plotted on Figure 60. It can be seen from this figure that the variations from a straight line load-strain relationship were small.

Reduction of all rosette data was accomplished with the use of the Mohr's Circle Method as illustrated in Figure 61.

TABLE 1 SUMMARY OF COMPLETED STATIC AND REPEATED LOAD TEST PROGRAM
(Completed Between July 28, 1958 and December 9, 1958)

Test No.	Description		Maximum Center Line LL+I Bending Moment		Remarks
	Type of Loading	Location	inch-kips	% design	
1	Static	Concentric	10 050	97.5	7 load increments
2	Dynamic	Concentric	10 313	100	250 000 cycles
3	Static	Concentric	12 900	125	6 load increments
4	Static	Eccentric	12 900 *6 220	125	6 load increments * torsional moment
5	Dynamic	Concentric	12 900	125	250 000 cycles
6N 6D	Static Static	Concentric Concentric	15 500 15 500	150 150	6 load increments: 12:00 A.M. to 8:00 P.M. Repeat Test 6N: 8:00 A.M. to 4:00 P.M.
7	Dynamic	Concentric	15 500	150	360 000 cycles: Bearings at free end changed
8a 8b	Static	Concentric	13 500	130	(a) deflections only - bronze bearings (b) all gages - roller bearings
9	Dynamic	Concentric	15 500	150	140 000 cycles
10	Static	Concentric	15 500	150	3 load increments
11	Dynamic	Concentric	15 500	150	253 000 cycles
12	Static	Concentric	15 500	150	3 load increments
13	Static	Eccentric	12 900 *6 220	125	3 load increments * torsional moment
14	Dynamic	Eccentric	12 900	125	200 000 cycles: dynamic record of ℄ of deflections and strains in bottom extrusions
15	Static	Eccentric	12 900	125	3 load increments
16	Static	Concentric	20 626	200	4 load increments
17	Static	Concentric	64 456	620	9 load increments for first attempted destruction test
18	Static	Concentric	91 270	885	Load at destruction. 970% M_{LL} reached before failure

TABLE 2 DESTRUCTION TEST - LOADING SEQUENCE

Applied Load Increment	Total Load (kips)	Ingot Weight on Deck Each Side of Center Line (kips)	Ingot Weight on Deck Each Side of Center Line (inches)	Jack Load Kips Applied at Center Line	Bending Moment ($\times 10^6$ in-lb.) Center Line	Bending Moment ($\times 10^6$ in-lb.) 1/4 Point	$\%M_{LL}$ at Center Line	Shear at 1/4 Point (kips)
1	152.6	76.3	76	0	17.1	11.5	165	76.3
2	221.6	76.3	76	69	27.4	16.7	265	110.8
3	152.6	76.3	76	0	17.1	11.5	165	76.3
4	290.6	76.3	76	138	37.7	21.8	365	145.3
5	152.6	76.3	76	0	17.1	11.5	165	76.3
6	242.2	121.1	74	0	27.4	18.2	265	121.1
7	345.7	121.1	74	103.5	42.9	25.9	415	172.85
8	380.2	121.1	74	138.0	48.0	28.5	465	190.1
9	414.7	121.1	74	172.5	53.2	31.1	515	207.35
10	449.20	121.1	74	207	58.4	33.7	565	224.6
11	483.7	121.1	74	241.5	63.5	36.2	615	241.85
12	242.2	121.1	74	0	27.4	18.2	265	121.1
13	380.0	190	71	0	43.8	29.3	425	190
14	518.0	190	71	138	64.4	39.6	625	259
15	380.0	190	71	0	43.8	29.3	425	190
16	552.8	190	71	172.8	69.6	42.2	675	276.4
17	380.0	190	71	0	43.8	29.3	425	190.0
18	587.0	190	71	207	74.7	44.8	725	293.5
19	380.0	190	71	0	43.8	29.3	425	190.0
20	656.0	190	71	276	85.1	49.9	825	328.0
21	757.6	190	71	377.6	100.2	57.5	970	378.8
22	380.0	190	71	0	43.8	29.3	425	190.0
23		190	71	317.6	91.3	53.0	885	348.8
Failure	697.6							

TABLE 3 SECTION PROPERTIES - WITHOUT SLAB

Element (Ref. Fig.15)	Area sq. in.	x (1) in.	z(2) in.	Az (3) in^3	Az^2(4) in^4
A	8.166	- 90.0	0	0	0
B	4.325	-135.0	45.0	194.445	8 750.0
1	1.823	-112.5	45.0	82.035	3 691.6
2	1.823	- 90.0	45.0	82.035	3 691.6
3	1.823	- 67.5	45.0	82.035	3 691.6
C	8.563	- 45.0	45.0	395.335	17 340.1
4	1.823	- 22.5	45.0	82.035	3 691.6
5	1.823	0	45.0	82.035	3 691.6
6	1.823	22.5	45.0	82.035	3 691.6
D	8.563	45.0	45.0	385.335	17 340.1
7	1.823	67.5	45.0	82.035	3 691.6
8	1.823	90.0	45.0	82.035	3 691.6
9	1.823	112.5	45.0	82.035	3 691.6
E	4.321	135.0	45.0	194.445	8 750.0
F	8.166	90.0	0	0	0
10	2.813	67.5	0	0	0
11	2.813	45.0	0	0	0
12	2.813	22.5	0	0	0
G	11.603	0	0	0	0
13	2.813	- 22.5	0	0	0
14	2.813	- 45.0	0	0	0
15	2.813	- 67.5	0	0	0
Totals	86.988			1897.875	85 404.6

Notes: (1) Due to symmetry about Z-axis
(2) With respect to reference axis
(3) Statical moment - with respect to reference axis
(4) Moment of inertia about x-reference axis

TABLE 4 SECTION PROPERTIES - WITH SLAB

Element (Ref. Fig.15)	Area sq. in.	$x = \bar{x}$ (1)	$A\bar{x}^2$	z	Az	$A\bar{z}^2$
A	8.166	- 90.0	66 144	0	0	0
B	20.825	-135.0	379 536	50.25	1 046.5	52 587
1	34.831	-112.5	440 830	50.25	1 750.3	87 953
2	34.831	- 90.0	282 131	50.25	1 750.3	87 953
3	34.831	- 67.5	158 699	50.25	1 750.3	87 953
C	41.571	- 45.0	84 181	50.25	2 088.9	104 967
4	34.831	- 22.5	17 633	50.25	1 750.3	87 953
5	34.831	0	0	50.25	1 750.2	87 953
6	34.831	22.5	17 633	50.25	1 750.3	87 953
D	41.571	45.0	84 181	50.25	2 088.9	104 967
7	34.831	67.5	158 699	50.25	1 750.3	87 953
8	34.831	90.0	282 131	50.25	1 750.3	87 953
9	34.831	112.5	440 830	50.25	1 750.3	87 953
E	20.825	135.0	379 536	50.25	1 046.5	52 587
F	8.166	90.0	66 144	0	0	0
10	2.813	67.5	12 817	0	0	0
11	2.813	45.0	5 696	0	0	0
12	2.813	22.5	1 424	0	0	0
G	11.603	0	0	0	0	0
13	2.813	- 22.5	1 424	0	0	0
14	2.813	- 45.0	5 696	0	0	0
15	2.813	- 67.5	12 817	0	0	0
Totals	483.084		2 898 182		22 023.5	1 106 685

Note: (1) Due to symmetry about z-axis

TABLE 5 CALCULATION OF UNIT SHEAR FLOWS - WITHOUT DECK

Element	Area	z	$Q_z = Az$	$\frac{V_z}{I_x} Q_z$	q	l	t	$\frac{l}{t}$	q $\frac{l}{t}$
A	8.166	-21.8177	-178.163	40.493	40.493	63.640	0.081	785.67	31 813.9
B	4.321	23.1823	100.171	-22.767	17.726	22.500	.081	277.78	4 923.9
1	1.823	23.1823	42.261	- 9.605	8.121	22.500	.081	277.78	2 255.7
2	1.823	23.1823	42.261	- 9.605	- 1.485	22.500	.081	277.78	- 412.4
3	1.823	23.1823	42.261	- 9.605	- 11.090	22.500	.081	277.78	- 3 080.5
C	8.563	23.1823	198.510	-45.118	- 56.207	22.500	.081	277.78	- 15 613.3
4	1.823	23.1823	42.261	- 9.605	- 65.813	22.500	.081	277.78	- 18 281.4
5	1.823	23.1823	42.261	- 9.605	- 75.418	22.500	.081	277.78	- 20 949.6
6	1.823	23.1823	42.261	- 9.605	- 85.023	22.500	.081	277.78	- 23 617.7
D	8.563	23.1823	198.510	-45.118	-130.141	22.500	.081	277.78	- 36 150.4
7	1.823	23.1823	42.261	- 9.605	-139.746	22.500	.081	277.78	- 38 818.6
8	1.823	23.1823	42.261	- 9.605	-149.351	22.500	.081	277.78	- 41 486.7
9	1.823	23.1823	42.261	- 9.605	-158.956	22.500	.081	277.78	- 44 154.9
E	4.321	23.1823	100.171	-22.767	-181.723	63.640	.081	785.67	-142 774.4
F	8.166	-21.8177	-178.163	40.493	-141.230	22.500	.125	180.00	- 25 421.5
10	2.813	-21.8177	- 61.373	13.949	-127.282	22.500	.125	180.00	- 22 910.7
11	2.813	-21.8177	- 61.373	13.949	-113.333	22.500	.125	180.00	- 20 399.9
12	2.813	-21.8177	- 61.373	13.949	- 99.384	22.500	.125	180.00	- 17 889.1
G	11.603	-21.8177	-253.151	57.536	- 41.848	22.500	.125	180.00	- 7 532.7
13	2.813	-21.8177	- 61.373	13.949	- 27.899	22.500	.125	180.00	- 5 021.9
14	2.813	-21.8177	- 61.373	13.949	- 13.951	22.500	.125	180.00	- 2 511.1
15	2.813	-21.8177	- 61.373	13.949	- .002	22.500	.125	180.00	- .25
A									
Web: AC; GC; GD; FD								785.67	

TABLE 6 CALCULATION OF UNIT SHEAR FLOWS - WITH DECK - V_z = 10 000 lb.

Element	Area	z	$Q_z = Az$	$\frac{V_z}{I_x} Q_z$	q	l	t	$\frac{l}{t}$	q $\frac{l}{t}$
A	8.166	-45.589	-372.280	36.262	36.262	67.454	0.081	832.765	30 197.6
B	20.825	4.661	97.065	- 9.455	26.807	22.500	1.548	14.535	389.6
1	34.831	4.661	162.347	-15.813	10.944	22.500	1.548	14.535	159.1
2	34.831	4.661	162.347	-15.813	- 4.869	22.500	1.548	14.535	- 70.8
3	34.831	4.661	162.347	-15.813	- 20.683	22.500	1.548	14.535	- 300.6
C	41.571	4.661	193.762	-18.873	- 39.556	22.500	1.548	14.535	- 574.6
4	34.831	4.661	162.347	-15.813	- 55.369	22.500	1.548	14.535	- 804.8
5	34.831	4.661	162.347	-15.813	- 71.182	22.500	1.548	14.535	- 1 034.6
6	34.831	4.661	162.347	-15.813	- 86.996	22.500	1.548	14.535	- 1 264.5
D	41.571	4.661	193.762	-18.873	-105.869	22.500	1.548	14.535	- 1 538.8
7	34.831	4.661	162.347	-15.813	-121.682	22.500	1.548	14.535	- 1 768.6
8	34.831	4.661	162.347	-15.813	-137.495	22.500	1.548	14.535	- 1 998.4
9	34.831	4.661	162.347	-15.813	-153.309	22.500	1.548	14.535	- 2 228.3
E	20.825	4.661	97.065	- 9.454	-162.763	67.454	.081	832.765	-135 543.4
F	8.166	-45.589	-372.280	36.262	-126.501	22.500	.125	180.	- 22 770.2
10	2.813	-45.589	-128.242	12.491	-114.010	22.500	.125	180.	- 20 521.8
11	2.813	-45.589	-128.242	12.491	-101.519	22.500	.125	180.	- 18 273.3
12	2.813	-45.589	-128.242	12.491	- 89.027	22.500	.125	180.	- 16 024.9
G	11.603	-45.589	-528.969	51.524	- 37.503	22.500	.125	180.	- 6 750.5
13	2.813	-45.589	-128.242	12.491	- 25.011	22.500	.125	180.	- 4 502.1
14	2.813	-45.589	-128.242	12.491	- 12.520	22.500	.125	180.	- 2 253.6
15	2.813	-45.589	-128.242	12.491	- .029	22.500	.125	180.	- 5.1

TABLE 7 CALCULATION OF UNIT SHEAR FLOWS - WITH DECK - V_x = 10 000 lb.

Element	Area	x	$Q_x = Ax$	$-\frac{V_x}{I_z} Q_x$	q	l	t	$\frac{l}{t}$	$q \frac{l}{t}$	$\Delta 2A$	$q\Delta 2A$
A	8.166	- 90.0	- 734.940	2.536							
B	20.825	-135.0	-2811.375	9.698	2.536	67.454	0.081	832.765	2111.5	6574.0	16 668
1	34.831	-112.5	-3918.488	13.518	12.234	22.500	1.548	14.535	177.8	104.9	1 283
2	34.831	- 90.0	-3134.790	10.815	25.752	22.500	1.548	14.535	374.3	104.9	2 701
3	34.831	- 67.5	-2351.093	8.112	36.567	22.500	1.548	14.535	531.5	104.9	3 836
C	41.571	- 45.0	-1870.695	6.452	44.679	22.500	1.548	14.535	649.4	104.9	4 687
4	34.831	- 22.5	- 783.698	2.703	51.131	22.500	1.548	14.535	743.4	104.9	5 364
5	34.831	0	0	0	53.833	22.500	1.548	14.535	782.5	104.9	5 647
6	34.831	22.5	783.698	- 2.703	53.833	22.500	1.548	14.535	782.5	104.9	5 647
D	41.511	45.0	1870.695	- 6.452	51.131	22.500	1.548	14.535	743.2	104.9	5 364
7	34.831	67.5	2351.093	- 8.112	44.679	22.500	1.548	14.535	649.4	104.9	4 687
8	34.831	90.0	-3134.790	-10.815	36.567	22.500	1.548	14.535	531.5	104.9	3 836
9	34.831	112.5	3918.488	-13.518	27.752	22.500	1.548	14.535	374.3	104.9	2 701
E	20.825	135.0	-2811.375	- 9.698	12.234	22.500	1.548	14.535	177.8	104.9	1 283
F	8.166	90.0	734.940	- 2.536	2.536	67.454	.081	832.765	2111.5	6574.0	16 668
10	2.813	67.5	189.878	- .655	0	22.500	.125	180.0	0	1025.7	0
11	2.813	45.0	126.585	- .437	- .655	22.500	.125	180.0	- 117.9	1025.7	- 672
12	2.813	22.5	63.293	- .218	- 1.092	22.500	.125	180.0	- 196.5	1025.7	-1 120
G	11.603	0	0	0	- 1.310	22.500	.125	180.0	- 235.8	1025.7	-1 344
13	2.813	- 22.5	- 63.293	.218	- 1.310	22.500	.125	180.0	- 235.8	1025.7	-1 344
14	2.813	- 45.0	- 126.585	.437	- 1.092	22.500	.125	180.0	- 196.5	1025.7	-1 120
15	2.813	- 67.5	- 189.878	.651	- .655	22.500	.125	180.0	- 117.9	1025.7	- 672
A					0	22.500	.125	180.0	0	1025.7	0
Web: AC; GC; GD; FD								832.765			Σ 74 100

TABLE 8 - SUMMARY OF SPECIFICATION SHEAR FLOWS

Element	Without Slab		With Slab							
			Unit Solutions		Live Load Plus Impact			Maximum Eccentric Loading		
	Unit Solution V_z=10 000 lb.	Dead Weight V_z=55 000 lb.	V_z=10 000 lb. q_z	T=1x10^6 in-lb. q_T	V_t=81 000 lb. 8.1 x q_z	T=0.972x10^6 in-lb. 0.972 x q_T	Total q	V_z=81 000 lb. 8.1 x q_z	T=5.832x10^6 in-lb. 5.832 x q_T	Total q
A-B	35.824	197.03	31.180	36.922	252.6	35.9	288.5	252.6	215.3	467.9
B-1	13.057	71.81	21.730	36.922	176.0	35.9	211.9	176.0	215.3	391.3
1-2	3.452	18.99	5.887	36.922	47.7	35.9	83.6	47.7	215.3	263.0
2-3	- 6.153	- 33.85	- 9.927	36.922	- 80.4	35.9	- 44.5	- 80.4	215.3	134.9
3-C	-15.759	- 86.67	-25.740	36.922	-208.5	35.9	-172.6	-208.5	215.3	6.8
C-4	14.408	79.24	23.720	58.392	192.1	56.8	248.9	192.1	340.5	532.6
4-5	4.803	26.41	7.907	58.392	64.0	56.8	120.8	64.0	340.5	404.5
5-6	- 4.803	- 26.42	- 7.907	58.392	- 64.0	56.8	- 7.2	- 64.0	340.5	276.5
6-D	-14.408	- 79.24	-23.720	58.392	-192.1	56.8	-135.3	-192.1	340.5	148.4
D-7	15.759	86.67	25.740	36.922	-208.5	35.9	-172.6	-208.5	215.3	6.8
7-8	6.153	33.83	9.927	36.922	80.4	35.9	116.3	80.4	215.3	295.7
8-9	- 3.452	- 18.99	- 5.887	36.922	- 47.7	35.9	- 11.8	- 47.7	215.3	167.6
9-E	-13.057	- 71.81	-21.730	36.922	-176.0	35.9	-140.1	-176.0	215.3	39.3
E-F	-35.824	-197.03	-31.180	36.922	-252.6	35.9	-216.7	-252.6	215.3	-37.3
F-10	-29.241	-160.83	-25.953	44.440	-210.2	43.2	-167.0	-210.2	259.2	49.0
10-11	-15.293	- 84.12	-13.462	44.440	-109.0	43.2	- 65.8	-109.0	259.2	150.2
11-12	- 1.343	- 7.40	- .970	44.440	- 7.9	43.2	35.2	- 7.9	259.2	251.3
12-G	12.605	69.32	11.522	44.440	93.3	43.2	136.5	93.3	259.2	352.5
G-13	-12.605	- 69.33	-11.522	44.440	- 93.3	43.2	- 50.1	- 93.3	259.2	165.9
B-14	1.343	7.39	.970	44.440	7.9	43.2	51.1	7.9	259.2	267.1
14-15	15.293	84.10	13.462	44.440	109.0	43.2	152.2	109.0	259.2	368.2
15-A	29.241	160.84	25.953	44.440	210.2	43.2	253.2	210.2	259.2	469.4
Web: AC	33.911	186.51	31.049	7.518	251.5	7.3	258.8	251.5	43.8	295.3
CG	41.373	227.55	37.284	13.952	302.0	13.6	315.6	302.0	81.4	383.4
GD	41.373	227.55	37.284	-13.952	302.0	-13.6	288.4	302.0	-81.4	220.6
DF	33.911	186.51	31.049	- 7.518	251.5	- 7.3	244.2	251.5	-43.8	207.7

TABLE 9 - PREDICTED SHEAR STRESSES FOR DEAD WEIGHT AND SPECIFICATION LOADING

Element	Thickness (in.)	Shear Flows (lb/in.)			Shear Stresses (psi.)	
		Dead Weight	Live Load & Impact	Eccentric Loading	Dead Weight + Live Load + Impact	Dead Weight + Eccentric Loading
A-B	0.081	197.0	288.5	467.9	5994	8209
B-1	1.55	71.8	211.9	391.3	183	299
1-2	1.55	19.0	83.6	263.0	66	182
2-3	1.55	- 33.9	- 44.5	134.9	- 51	65
3-C	1.55	- 86.7	-172.6	6.8	- 167	52
C-4	1.55	79.2	248.9	532.6	212	395
4-5	1.55	26.4	120.9	404.5	95	278
5-6	1.55	- 26.4	- 7.2	276.5	- 22	161
6-D	1.55	- 79.2	-135.3	148.4	- 138	45
D-7	1.55	86.7	-172.6	6.8	- 55	60
7-8	1.55	33.8	116.3	295.7	97	213
8-9	1.55	- 19.0	- 11.8	167.6	20	96
9-E	1.55	- 71.8	-140.1	39.3	137	- 21
E-F	0.081	-197.0	-216.7	-37.3	-5107	- 151
F-10	.125	-160.8	-167.0	49.0	-2622	-1678
10-11	.125	- 84.1	- 65.8	150.2	-1200	53
11-12	.125	- 7.4	35.2	251.3	222	1951
12-G	.125	69.3	136.5	352.5	1646	3374
G-13	.125	- 69.3	- 50.1	165.9	- 955	77
13-14	.125	7.4	51.1	267.1	468	22-
14-15	.125	84.1	152.2	368.2	1890	3618
15-A	.125	160.8	253.2	469.4	3312	5042
Web AC	.081	186.5	258.8	295.3	5498	5948
CG	.081	227.6	315.6	383.4	6706	7543
GD	.081	227.6	288.4	220.6	6370	5533
DF	.081	186.5	244.2	207.7	5317	4867

NOTE: Shear Stress at a point is equal to shear flow divided by thickness at that point

TABLE 10 - SUMMARY OF DESTRUCTION TEST RESULTS

Applied Load Increment (Ref. Table 2)	Bending Moment ($\times 10^6$ in-lb.)		Shear (kips)	Web Shear Strains (micro-in/in.)	Average Tensile Strains (micro-in/in.) Bottom Flange	Averaged ℄ Deflection (inches)	Remarks
	℄	1/4 point	1/4-point				
1	17.1	11.5	76.3	AB 748 AC 770 GC 918 GD 918 FD 760 FE 780	687	0.757	First dead weight increment
4	37.7	21.8	145.3	AB 1152 AC 1120 GC 1328 GD 1322 FD 1100 FE 1160	1459	1.73	Dead weight increment, plus applied jack load at ℄. Maximum for Test 17
6	27.4	18.2	121.1	AB 1324 AC 1203 GC 1382 GD 1402 FD 1158 FE 1304	1097	1.51	Additional dead weight placed on span
11	63.5	36.2	241.8	AB 2031 AC 1814 GC 2100 GD 2109 FD 1753 FE 1969	2415	3.29	Dead weight, plus jack load. Elastic buckling of outer webs visible at end supports
13	43.8	29.3	190.0	AB 1908 AC 2102 GC 2312 GD 2258 FD 1978 FE 1848	1745	2.45	Additional dead weight placed on deck

table continued on next page

TABLE 10- Summary of Destruction Test Results (Concluded)

Applied Load Increment	Bending Moment		Shear	Web Shear Strains	Average Tensile Strains	Averaged Deflection	Remarks
18	74.7	44.8	293.5		3084	3.51	Dead weight, plus jack load. Additional buckling at end frames
20	85.1	49.9	328.0		3802	3.87	Dead weight, plus jack load. Permanent buckling at end frames very pronounced
21	100.2	57.5	378.8				Maximum applied load held for 10 minutes, and then jack load released
23 Failure	91.3	53.0	348.8				Attempt to reload bridge caused a sudden and complete collapse at this load increment

NOTES: During the loading after Load Increment 18, the following signs of failure were noted:

(1) Web buckles at the supports were now permanent and visible on all webs

(2) Horizontal cracks appeared between the concrete deck and aluminum structure at the corners of the bridge

(3) Relative movement between the concrete and aluminum at the ends of the deck was measurable and visible. The concrete extended past the webs of the aluminum extrusion by 0.0153 in. at the east end and 0.0210 in. at the west end under Load Increment 20

(4) Noise within the span indicated possible rivet hole elongations and rivet failure

TABLE 11a - SUMMARY OF PRIMARY STRESSES, CONCENTRIC LOADING

	Dead Load		Design Load		
	Predicted (Based on 183.3 lb/in.)	Actual (Based on 173 lb/in.)	AASHO Spec. Live + Impact Loading	Test Loading Concentric	
			Predicted	Predicted	Measured
Maximum Moment (in-lb)	8 250 000	7 786 000	10 313 000	10 313 000	10 313 000
Maximum Shear (lb.)	55 000	51 910	81 000	34 500	34 500
Torsional Moment (in-lb.)	0	0	972 000	0	0
Tensile Stresses: Bottom Longitudinal Members A G F	4 091	3 861	4 580	4 580	4 210 4 040 4 210
Compressive Stresses: Top Longitudinal Members	4 347	4 103	0	0	0
Compressive Stresses: Concrete Deck Surface			468	468	357
Shear Stresses: Webs: AB AC GC GD FD FE	2 432 2 303 2 809 2 809 2 303 2 432	2 295 2 174 2 651 2 651 2 174 2 295	3 562 3 195 3 896 3 560 3 015 1 328	1 328 1 322 1 588 1 588 1 322 1 467	1 555 1 344 1 574 1 555 1 294 460

TABLE 11b - SUMMARY OF PRIMARY STRESSES, ECCENTRIC LOADING

	Dead Load		AASHO Spec. Live + Impact Loading	Test Loading Eccentric	
	Predicted (Based on 183.3 lb/in.)	Actual (Based on 173 lb/in.)	Predicted	Predicted	Measured
Maximum Moment (in-lb.)	8 250 000	7 786 000	10 313 000	12 890 000	12 890 000
Maximum Shear (lb.)	55 000	51 910	81 000	43 200	43 200
Torsional Moment (in-lb.)	0	0	5 832 000	6 220 000	6 220 000
Tensile Stresses: Bottom Longitudinal Members					
A	3 091	3 861			6 312
G					5 750
F					4 188
Compressive Stresses: Top Longitudinal Members	4 347	4 102	0	0	0
Compressive Stresses: Concrete Deck Surface					446
Shear Stresses:					
Webs: AB	2 432	2 295	5 777	3 080	3 302
AC	2 303	2 174	3 646	1 944	1 890
GC	2 809	2 651	4 733	2 525	2 642
GD	2 809	2 651	2 723	1 453	1 290
FD	2 303	2 174	2 564	1 367	1 498
FE	2 432	2 295	460	246	695

TABLE 12 - SUMMARY OF CONCRETE CYLINDER TESTS FOR DECK STRENGTH

	Specimen Number	Weight (lb.)	Height (in.)	Ultimate Load (lb.)	Density (pcf.)	Ultimate Stress (psi.)
11-day Strength	4	22.1	12	107 500	112.5	3800
	10	20.2	12	75 000	102.8	2650
	12	21.0	12	94 500	106.9	3340
	14	21.6	12	76 500	109.9	2700
28-day Strength	1	21.1	11-15/16	115 000	107.9	4060
	2	21.2	12	115 000	107.9	4400
	3	22.2	12	136 500	113.0	4820
	5	21.1	11-13/16	114 000	109.1	4030
	6	20.8	11- 7/8	110 000	107.0	3900
	7	20.9	11- 7/8	121 000	107.5	4300
	8	20.8	12	118 000	105.8	4200
	9	20.8	12	111 000	105.8	3900
	11	20.8	11-13/16	112 500	107.5	3960
	13	21.8	11- 7/8	112 000	112.1	3960

NOTE: All cylinders had a diameter of 6 in., with cross-sectional area equal to 28.3 sq in.

TABLE 13 - SUMMARY OF TENSILE TESTS OF 6061-T6 ALUMINUM ALLOY SPECIMENS

Specimen Number and Location	Width (in.)	Thickness (in.)	Modulus of Elasticity (10^6 psi.)	Yield Strength (psi.)	Ultimate Strength (psi.)
A-1 Bottom Longitudinal Extruded T-Section, South Edge	1.49	0.192	9.0	36 700	41 500
B-1	1.49	.195	10.1	36 200	40 500
A-2 Extruded Angle End Stiffener - Bottom Plate (AG)-East End	1.50	.163	9.7	37 700	41 500
B-2	1.49	.163	10.0	37 700	41 600
A-3 Bottom Sheet (AG) East End	1.49	.131	10.0	37 700	41 600
B-3	1.49	.130	10.3	37 900	41 900
A-4 Extruded Channel of East End Frame (Web GC)	1.49	.190	10.3	39 900	42 700
B-4	1.49	.190	10.1	38 700	42 500
A-5 Diagonal Web (EF) Sheet, Near Quarter Point	1.50	.080	10.1	40 800	44 500
B-5	1.50	.080	10.0	41 250	44 500

TABLE 14 - DATA FROM TESTS 6N & 6D

GAGE LOCATED ON LONGITUDINAL MEMBER A

	Load (kips)	Recorded Strain Readings (micro in/in.)	Strain Increments: Total (Reading — Zero)	Strain Increments: Successive Differences	Average - or Corrected Strain
Test 6N	zero	18 175			
	20	18 280	105	105	108
	0	18 170	- 5	-110	
	40	18 380	205	210	212
	0	18 165	- 10	-215	
	60	18 490	315	325	328
	0	18 160	- 15	-330	
	75	18 565	390	405	405
	0	18 160	- 15	-405	
	90	18 630	455	470	475
	0	18 150	- 25	-480	
Test 6D	103.5	18 710	535	560	560
	0	18 150	- 25	-560	
	20	18 270	95	110	105
	0	18 170	- 5	-100	
	40	18 405	230	235	218
	0	18 205	30	-200	
	60	18 550	375	345	325
	0	18 245	70	-305	
	75	18 670	495	425	400
	0	18 295	120	-375	
	90	18 790	615	495	492
	0	18 300	125	-490	
	103.5	18 880	705	580	570
	0	18 320	145	-560	

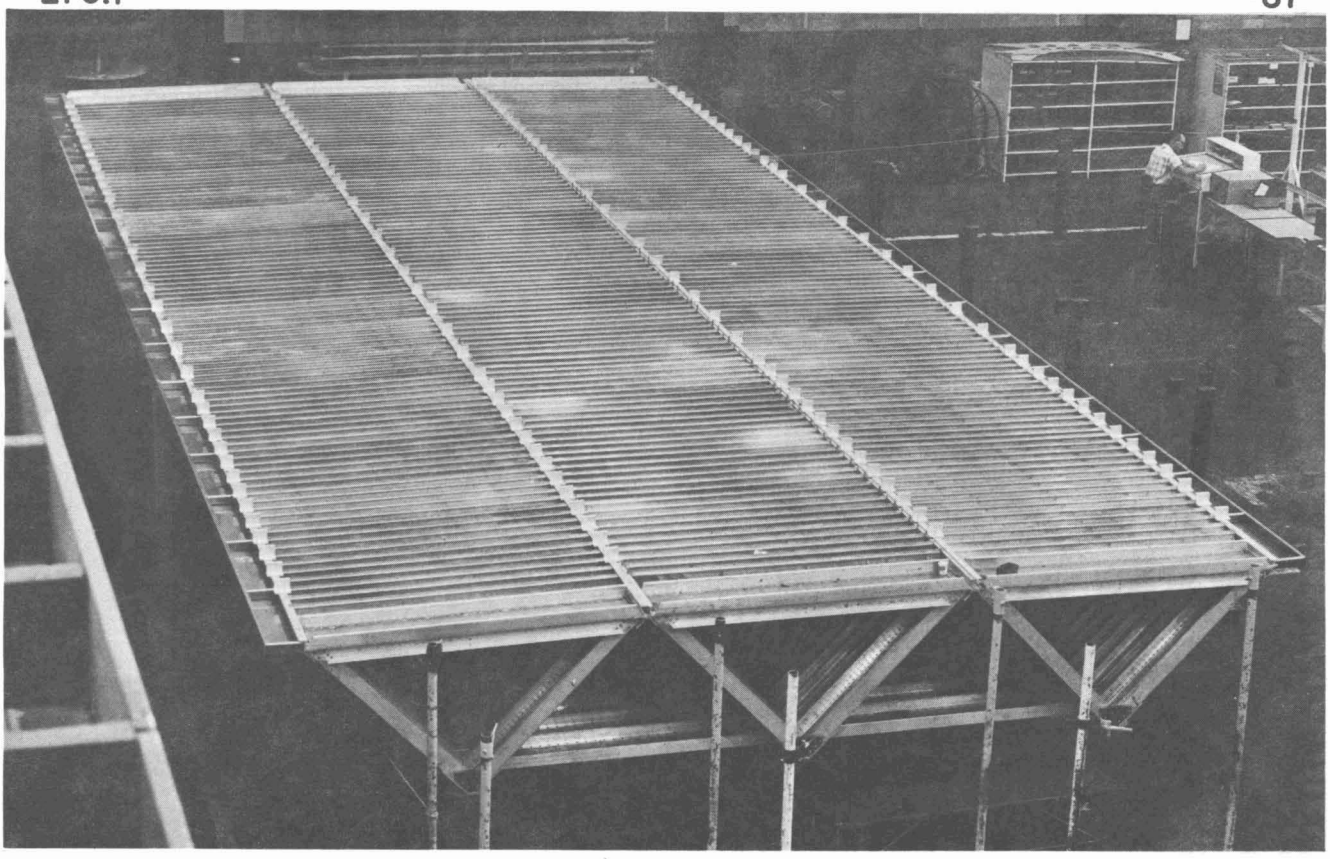

FIG. 1 PREASSEMBLY OF BRIDGE COMPONENTS BEFORE SHIPMENT

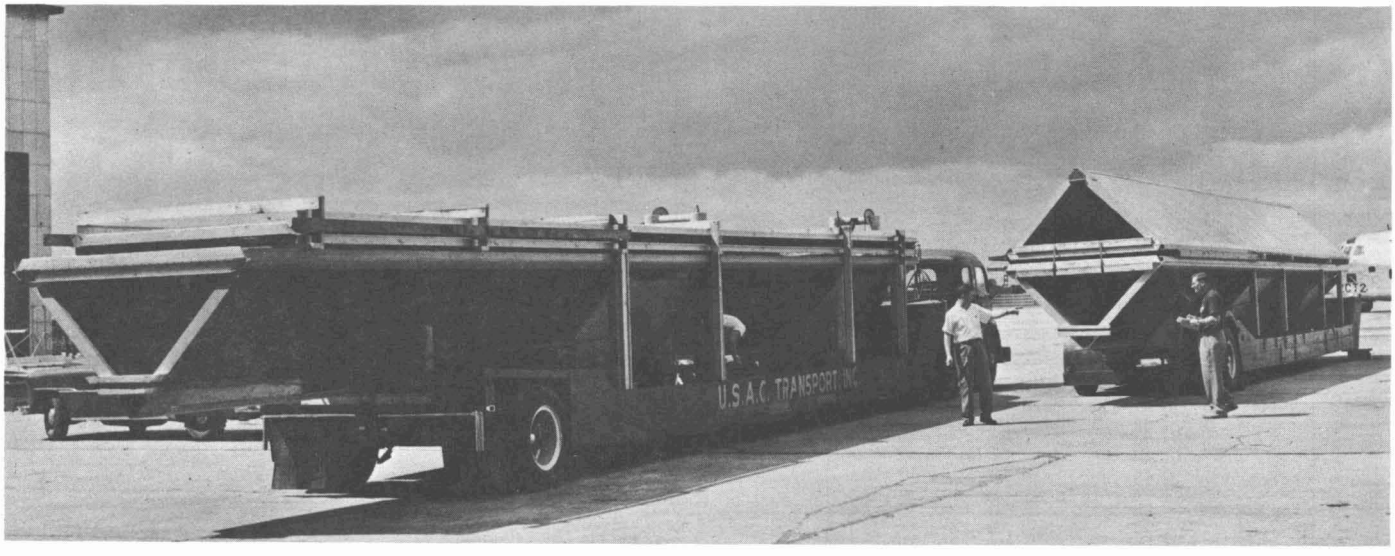

FIG. 2 BRIDGE SUBASSEMBLIES LOADED FOR SHIPMENT

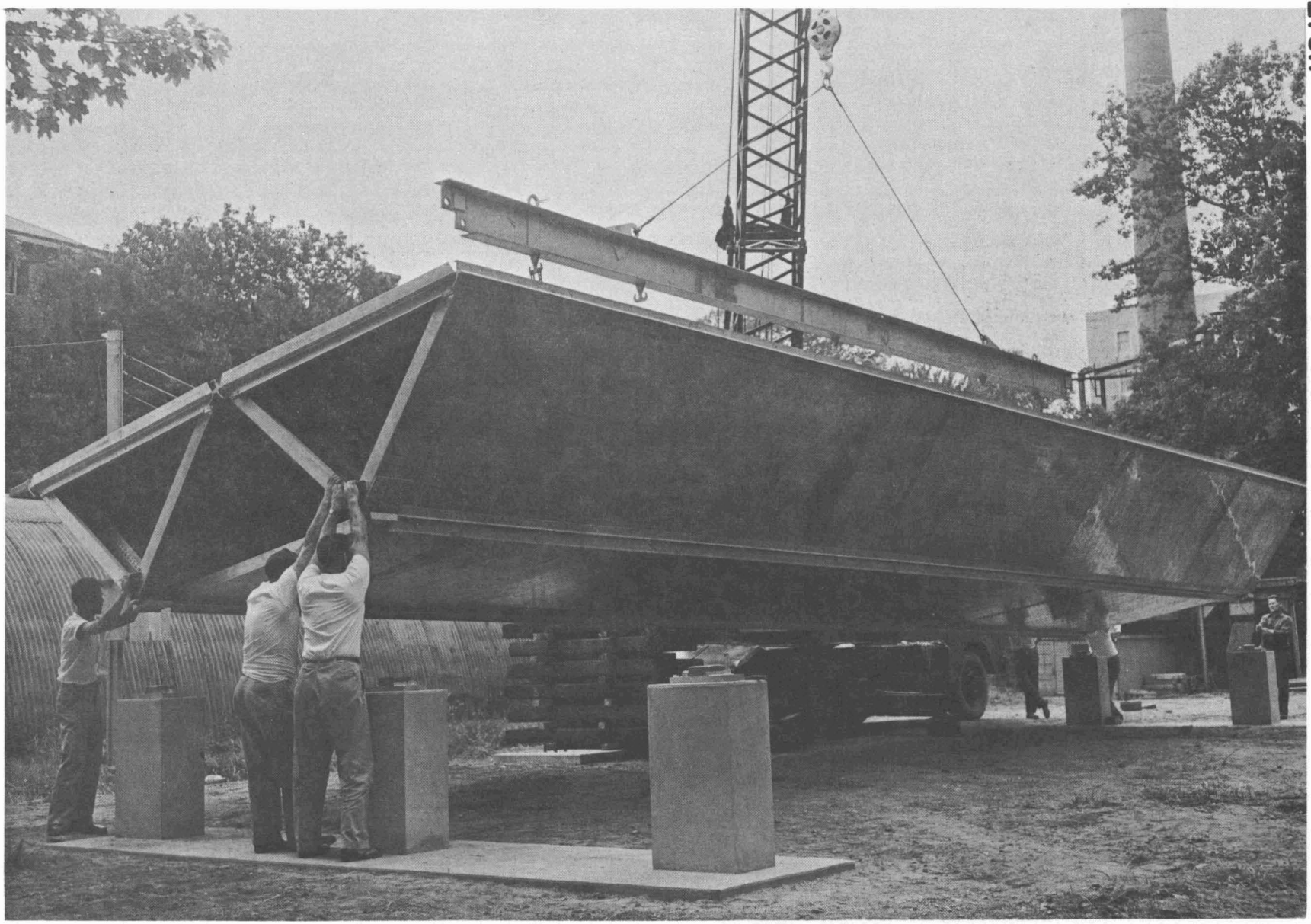

FIG. 3 START OF BRIDGE ERECTION

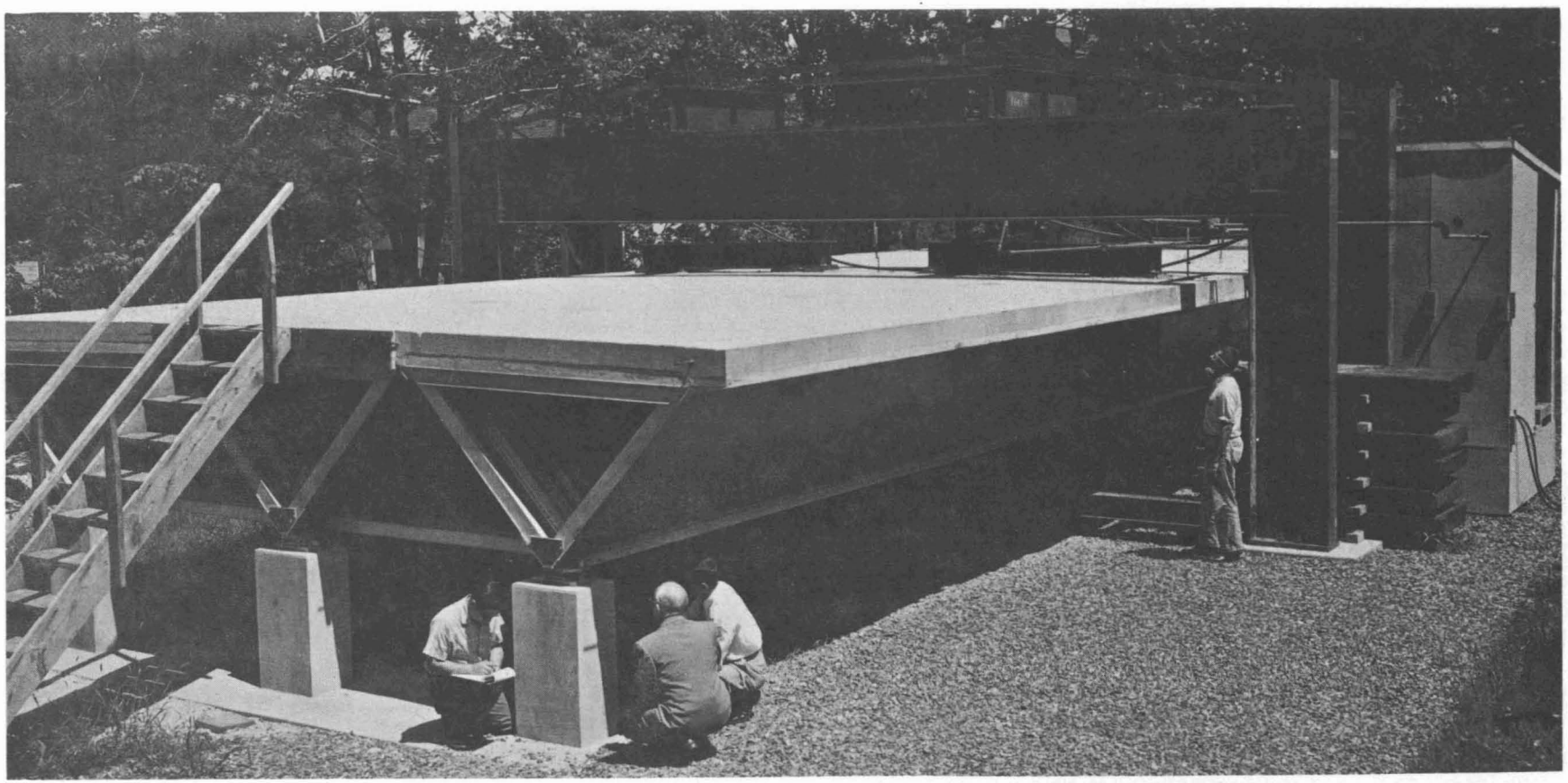

FIG. 4 OVERALL VIEW OF TEST BRIDGE

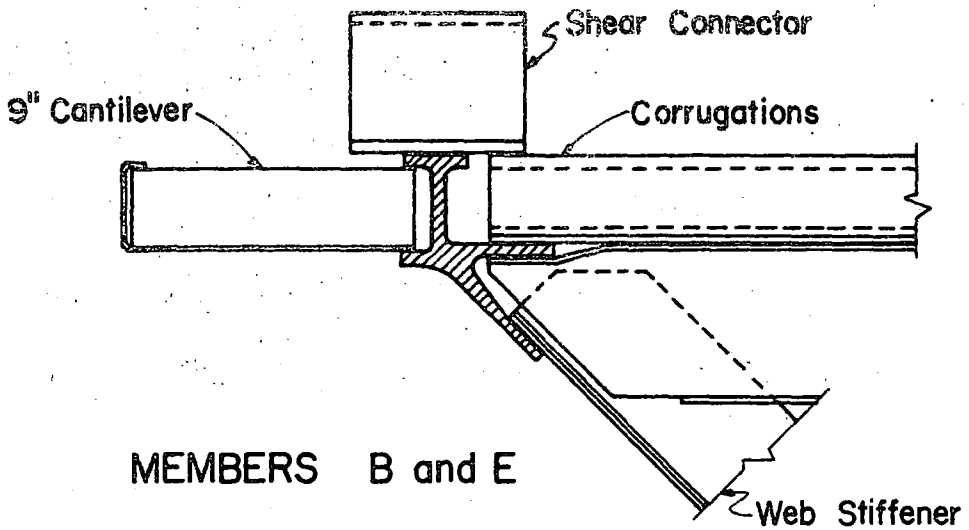

MEMBERS B and E

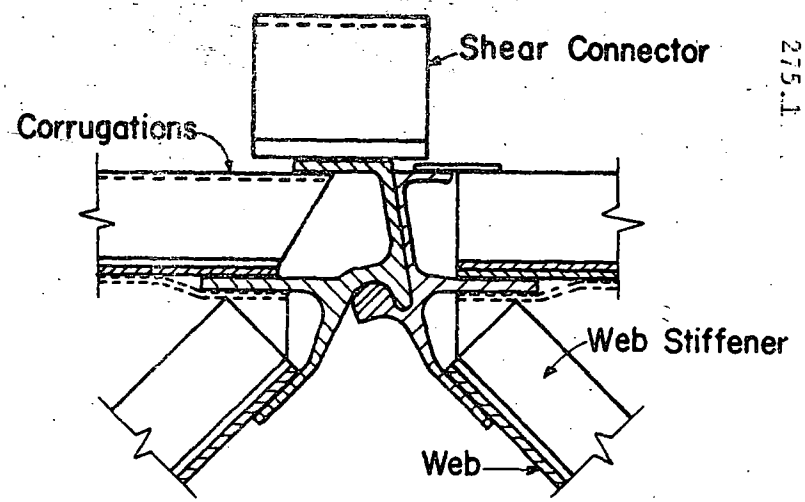

MEMBERS C and D

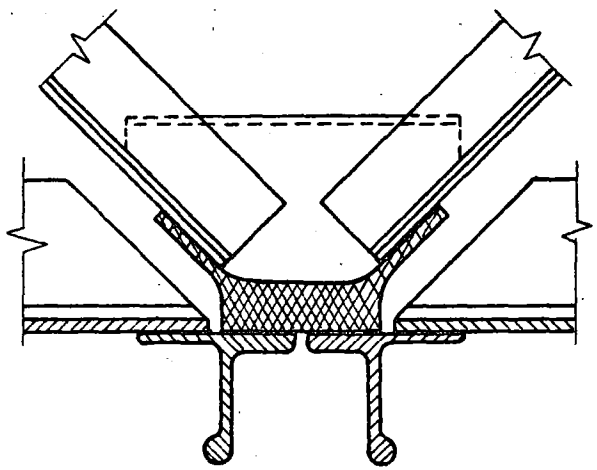

MEMBER G

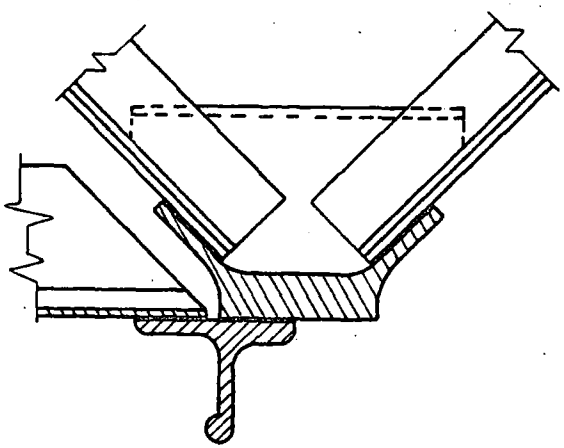

MEMBERS A and F

FIG. 5 DETAILS OF MAIN LONGITUDINAL MEMBERS

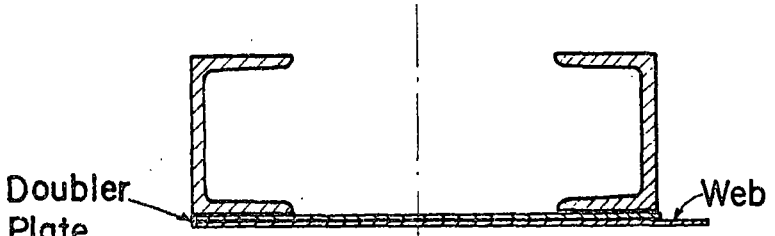

DIAGONALS
AB, AC, GC, GD, FD, FE

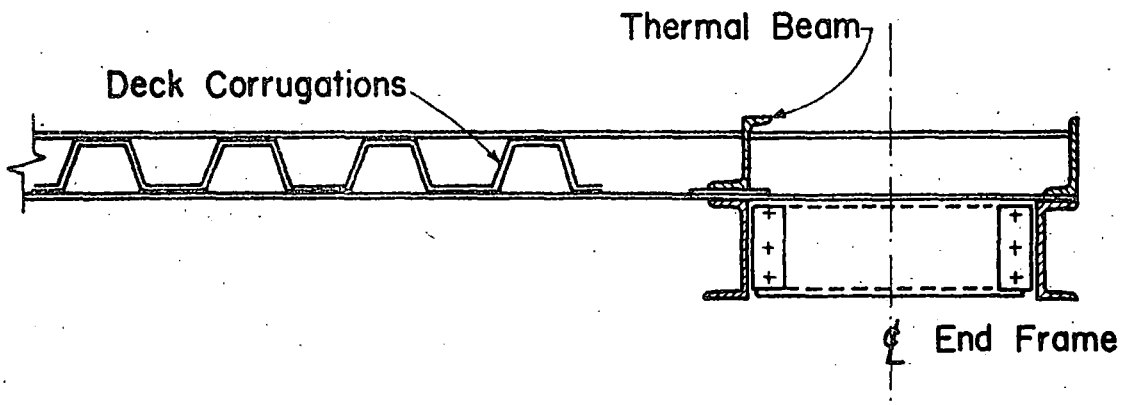

HORIZONTALS BC, CD, DE

FIG. 6 DETAILS OF END FRAME AND DECK SECTION

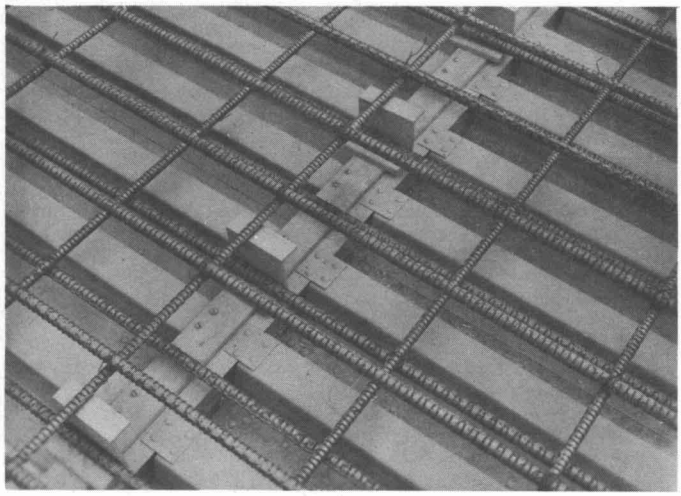

FIG. 7a
CENTER PORTION OF DECK

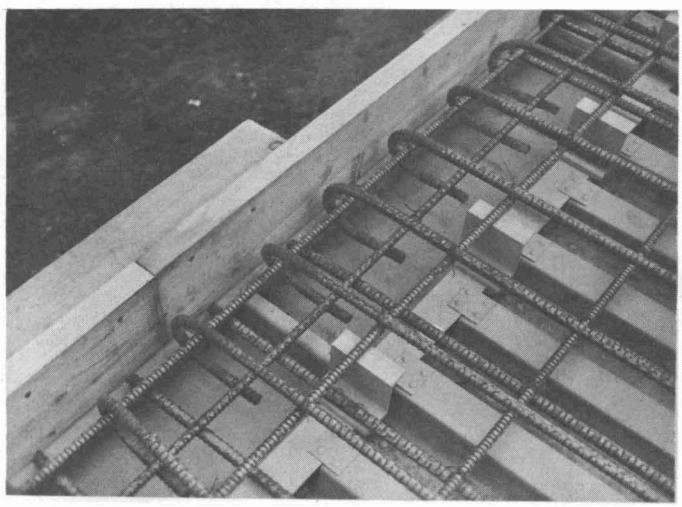

FIG. 7b
NINE INCH CANTILEVERED EDGE

FIG. 7 REINFORCING STEEL IN PLACE ON DECK

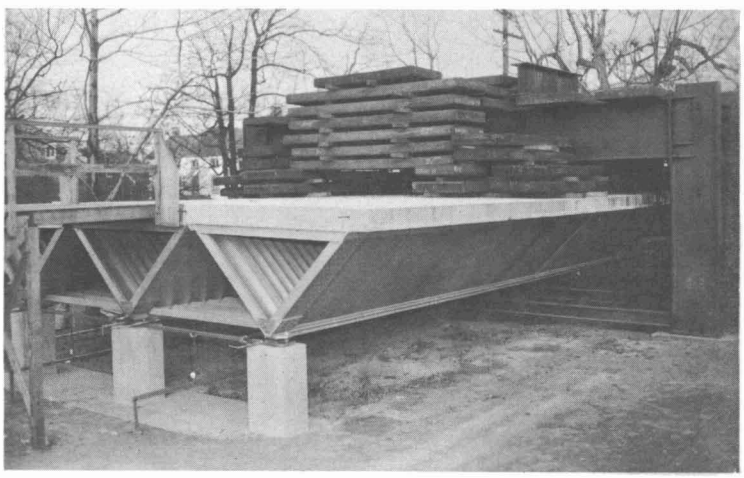

FIG. 9 STEEL SLABS PLACED ON BRIDGE DECK
FOR DESTRUCTION TEST

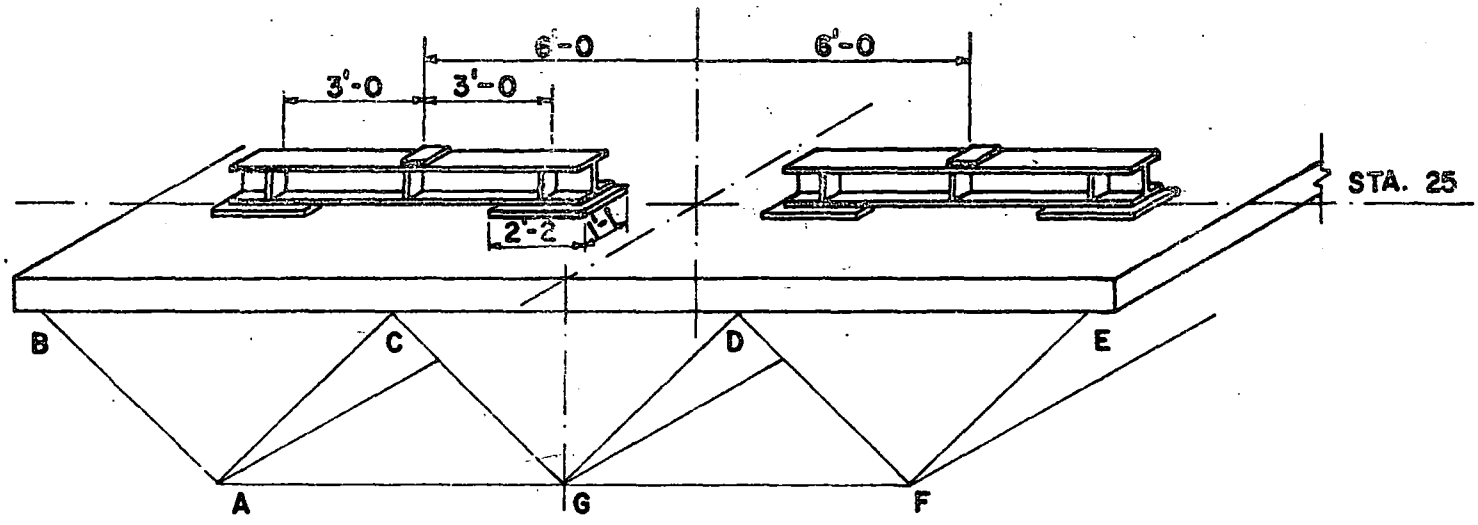

CONCENTRIC LOADING CONDITION

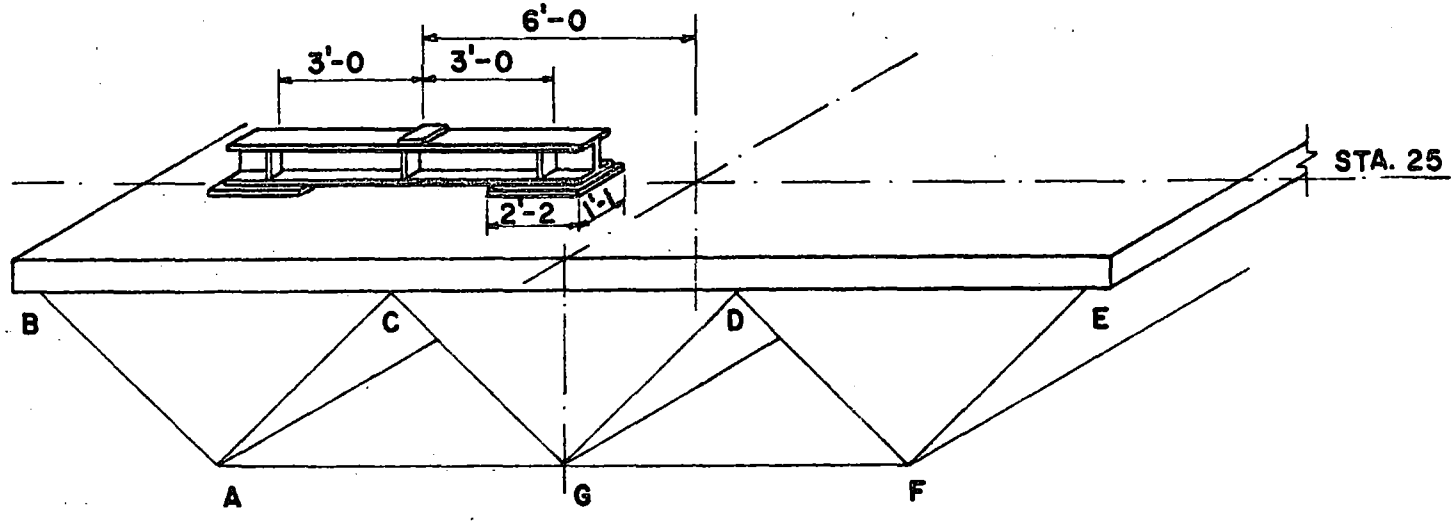

ECCENTRIC LOADING CONDITION

FIG. 8 LOCATION OF LOADING BEAMS

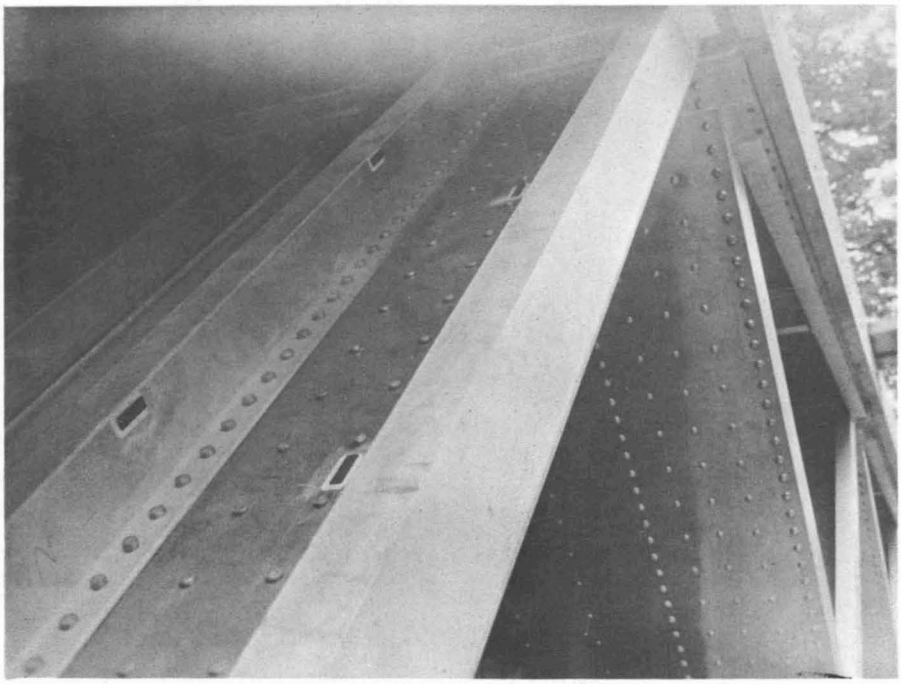

FIG. 10 END FRAME MEMBER AC WITH SR-4 ELECTRICAL STRAIN GAGES IN PLACE

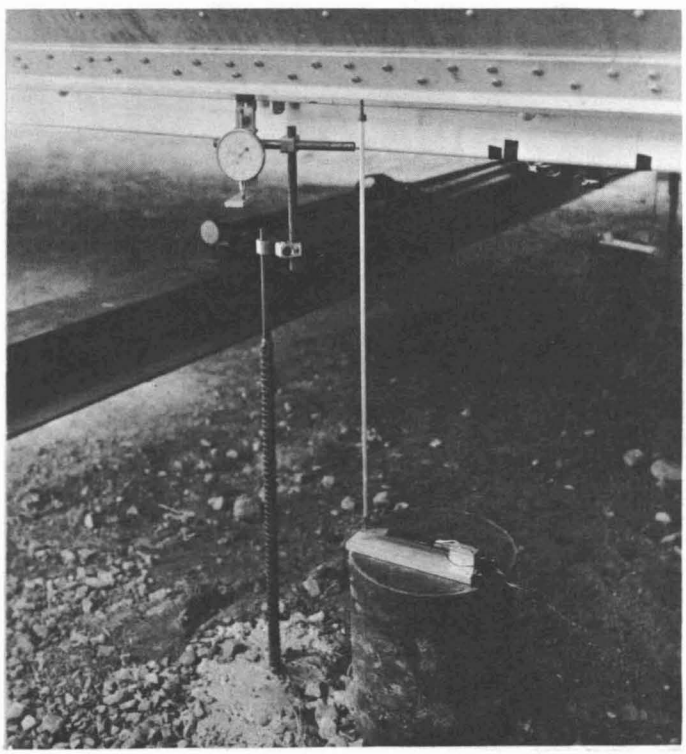

FIG. 14 SLIP GAGE AND TRANSDUCER USED FOR DYNAMIC DEFLECTION MEASUREMENTS

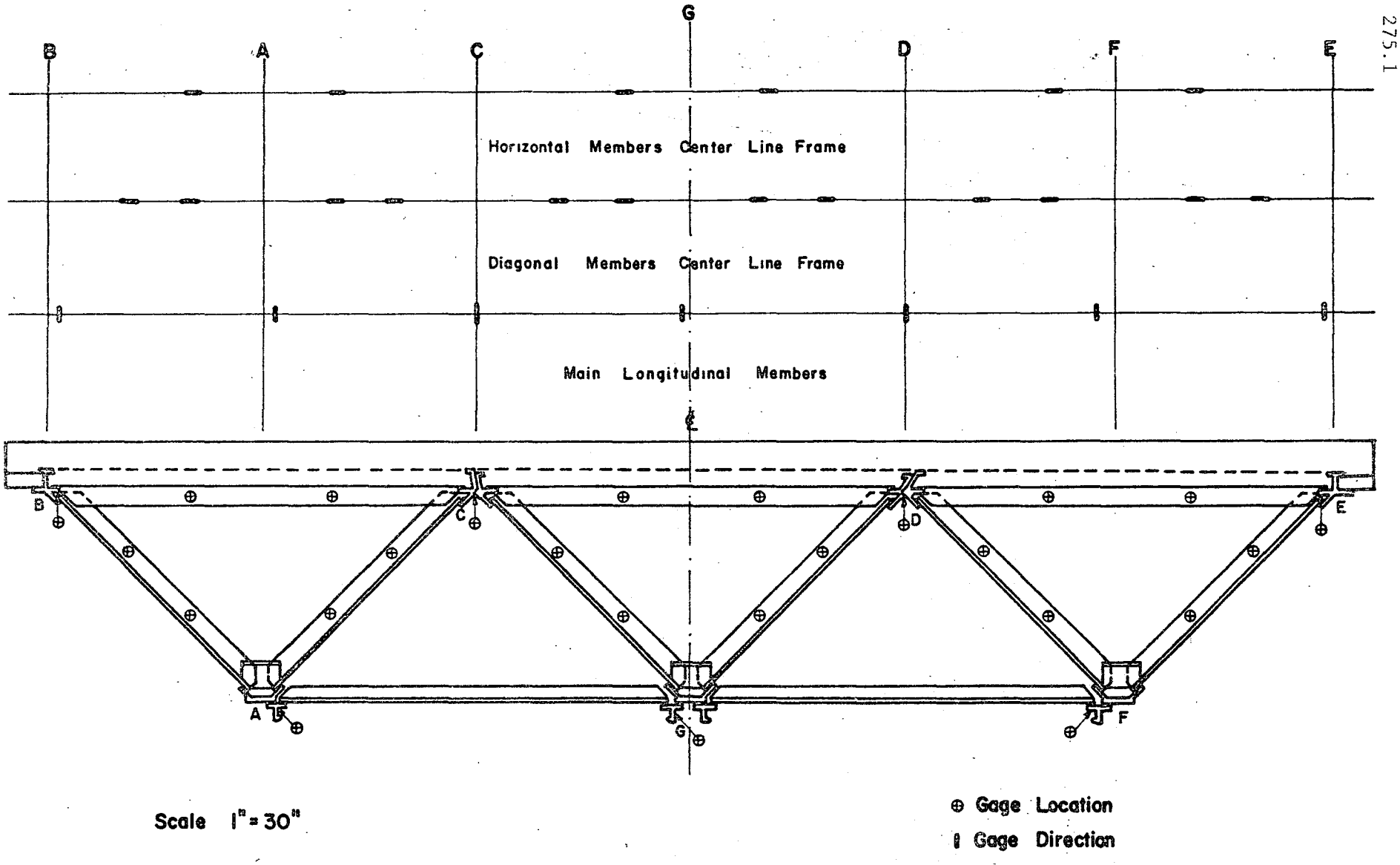

FIG. 11 LOCATION OF ELECTRICAL STRAIN GAGES ON CENTERLINE CROSS SECTION

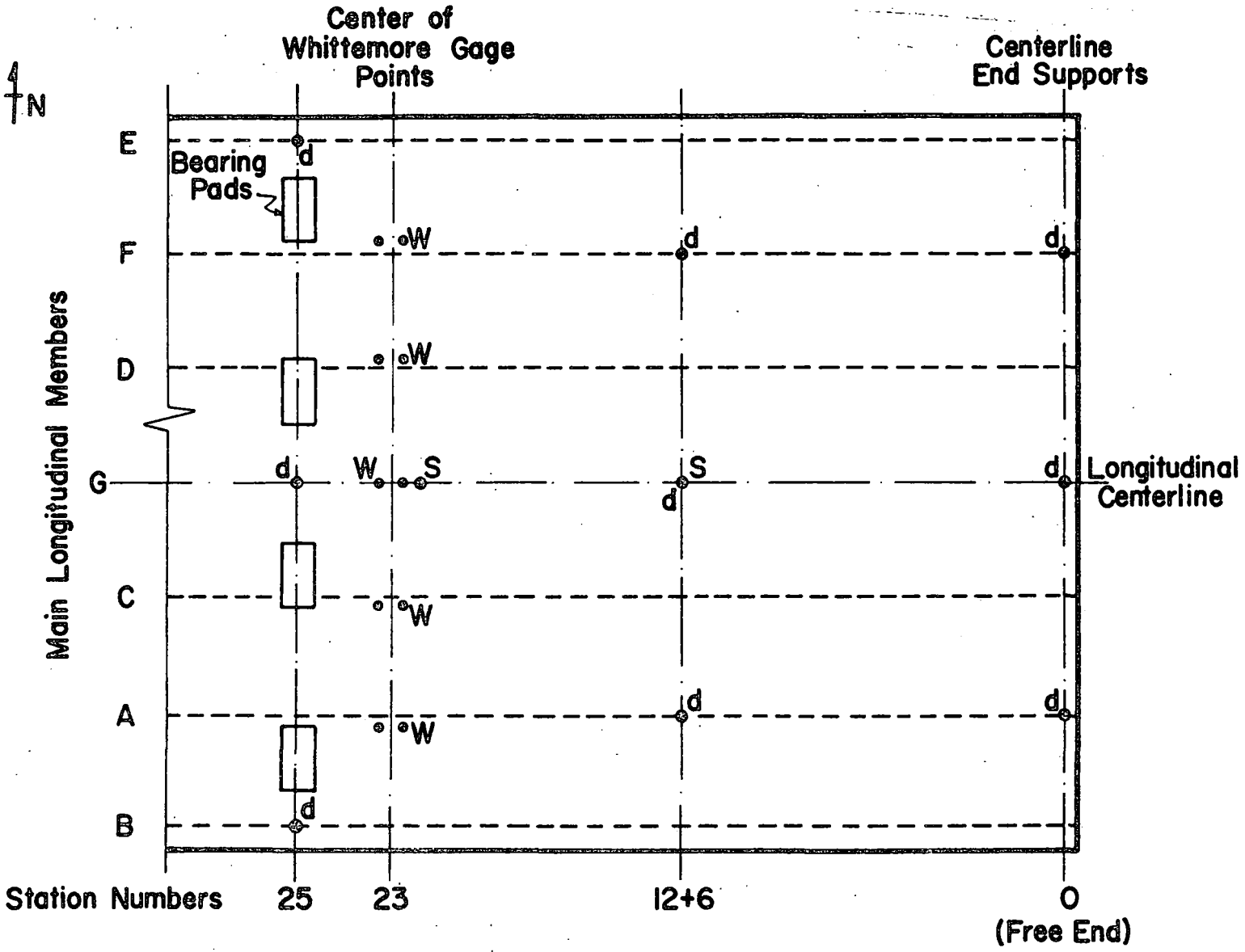

W - Whittemore Gage Points on Deck Surface

S - Strainometer at Mid-Height of Deck

d - Deflection Scale

FIG. 12 LOCATION OF GAGING FOR CONCRETE DECK

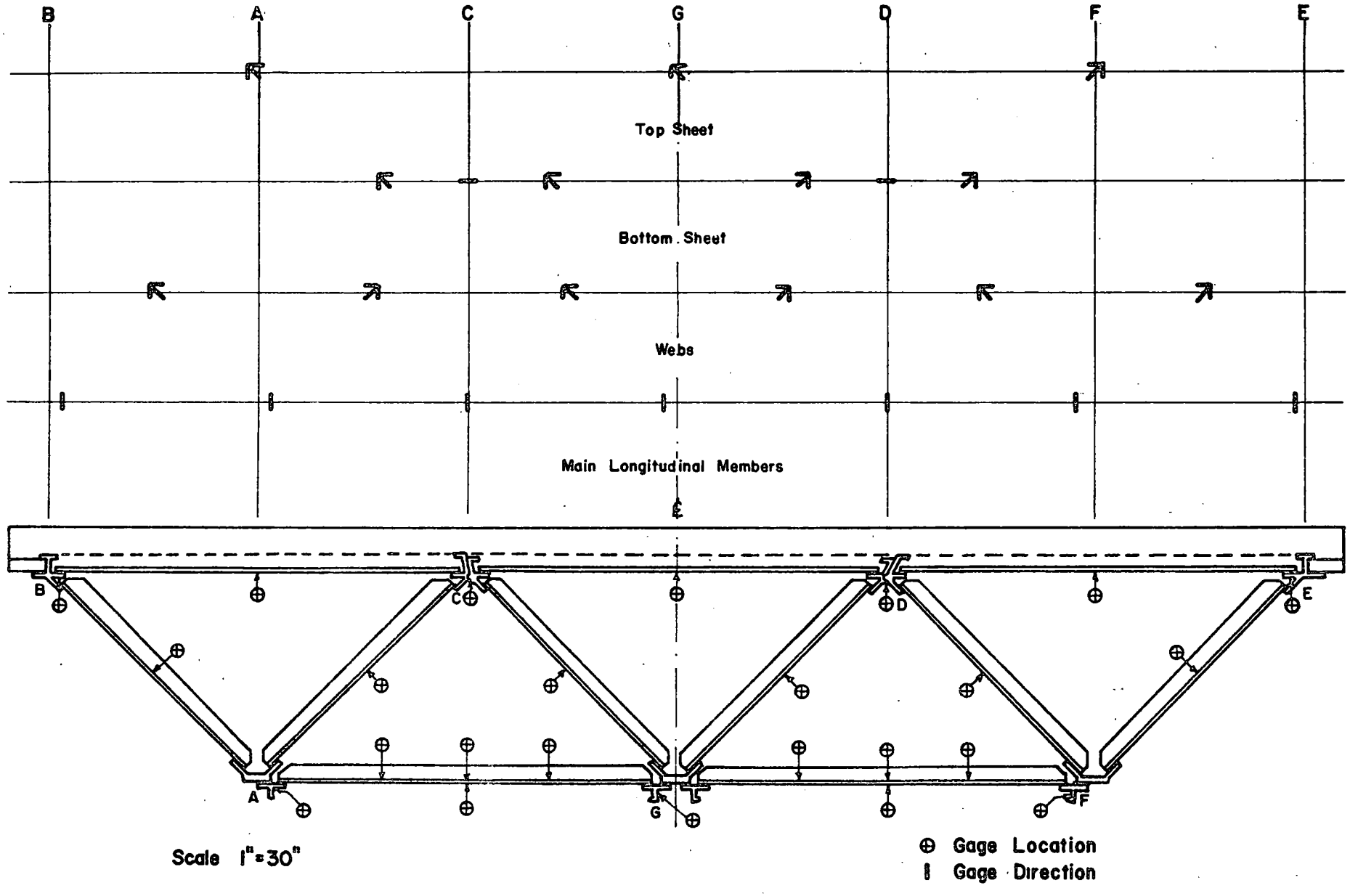

FIG. 13 LOCATION OF ELECTRICAL STRAIN GAGES ON QUARTER POINT CROSS SECTION

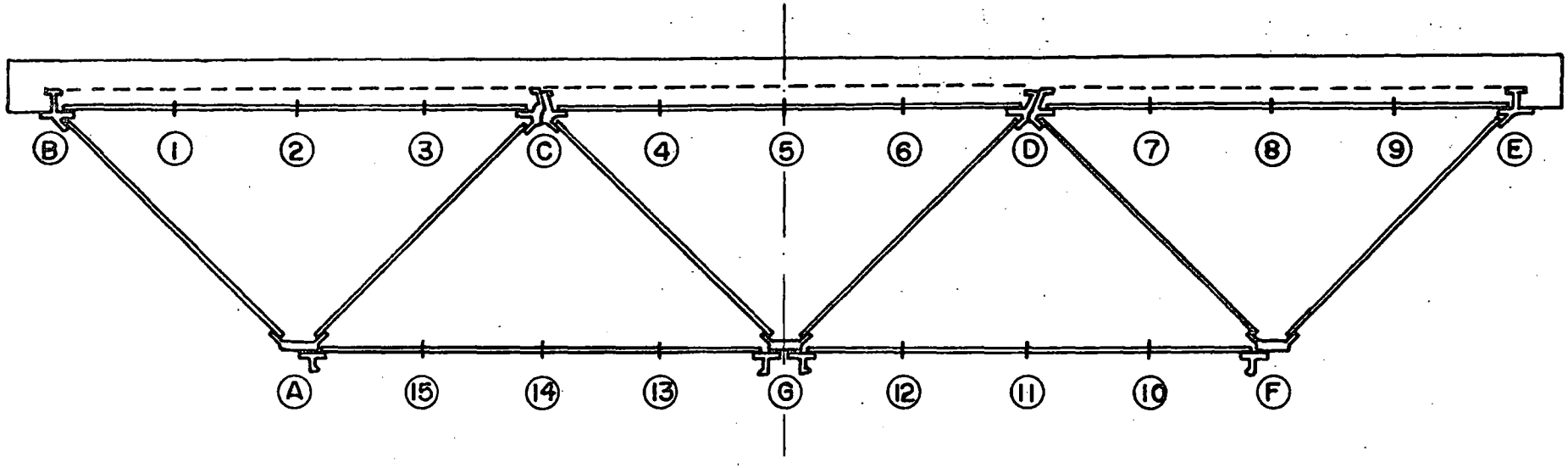

ELEMENT AREAS USED IN COMPUTATION OF SECTION PROPERTIES								
	WITHOUT SLAB (sq. in.)				CHANGES WITH SLAB (sq.in.)			
Element	Extrusions	Skin	Web	Total	Element	Skin	Slab	Total
A(F)	5.760	1.406	1.00	8.166				
G	7.790	2.813	1.00	11.603				
B(E)	3.410	0.911		4.321	3.410	0.911	16.504	20.825
C(D)	6.740	1.823		8.563	6.740	1.823	33.008	41.571
1-9		1.823		1.823		1.823	33.008	34.831
10-15		2.813		2.813				

Note: Elements are $22\frac{1}{2}$-inches center to center horizontally and 45-inches center to center vertically.

FIG. 15 CROSS SECTION OF SPAN USED TO COMPUTE GEOMETRIC SECTION PROPERTIES

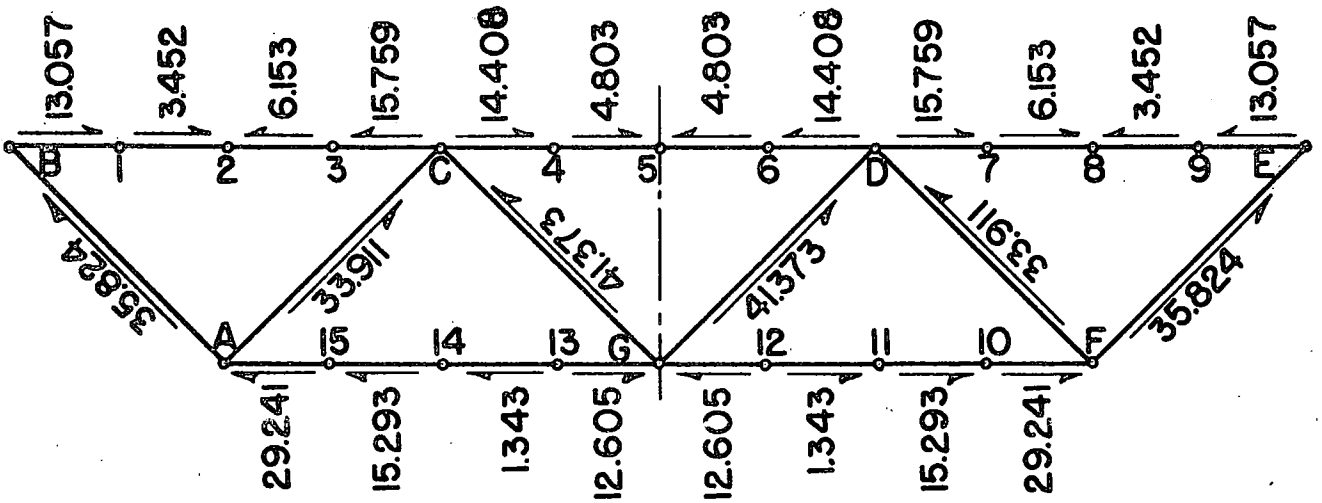

UNIT SOLUTION FOR V_z=10,000 LBS. THROUGH CENTROID OF CROSS SECTION

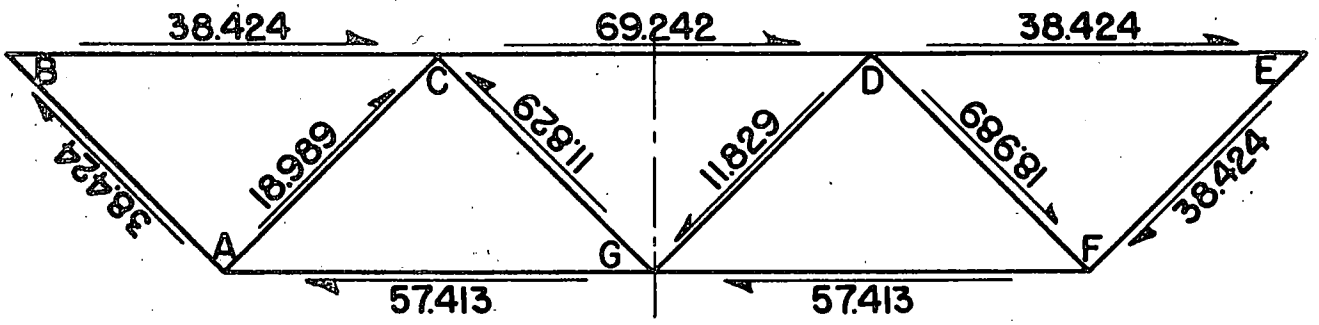

UNIT SOLUTION FOR T=1x10^6 IN. LBS.

FIG. 16 UNIT SHEAR SOLUTIONS FOR BRIDGE WITHOUT DECK

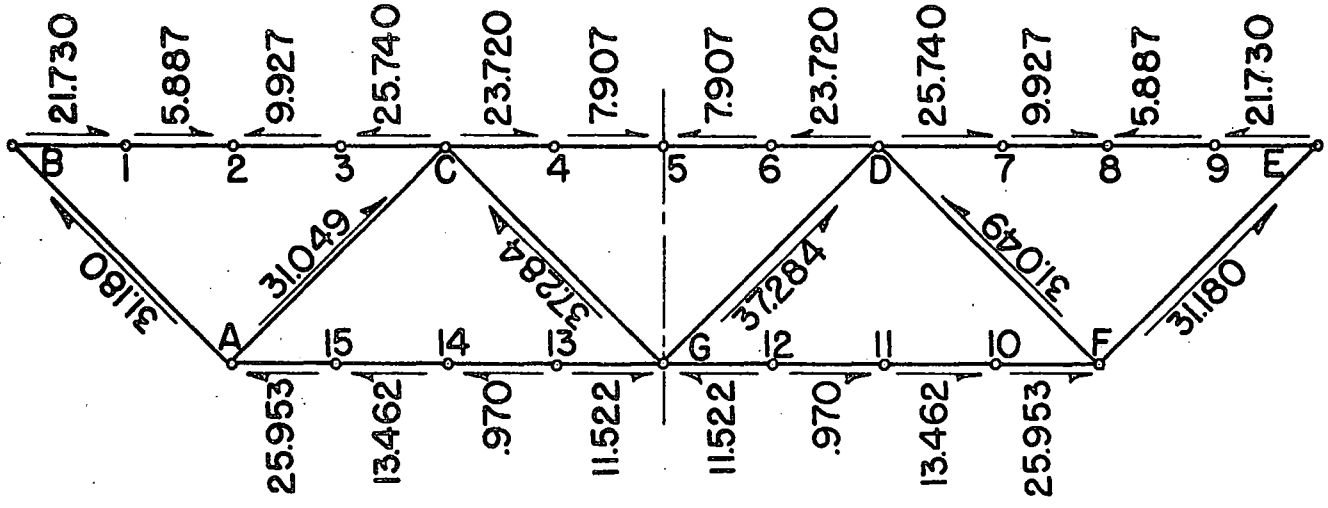

UNIT SHEAR SOLUTION FOR V_Z=10,000 LBS.
THROUGH CENTROID OF CROSS SECTION

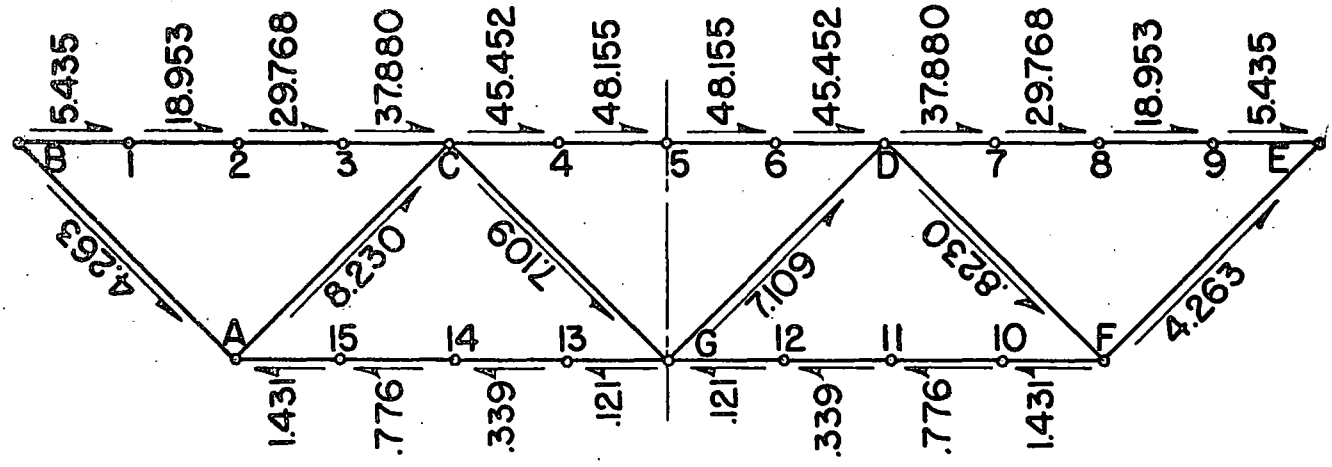

UNIT SHEAR SOLUTION FOR V_X=10,000 LBS.
THROUGH CENTROID OF CROSS SECTION

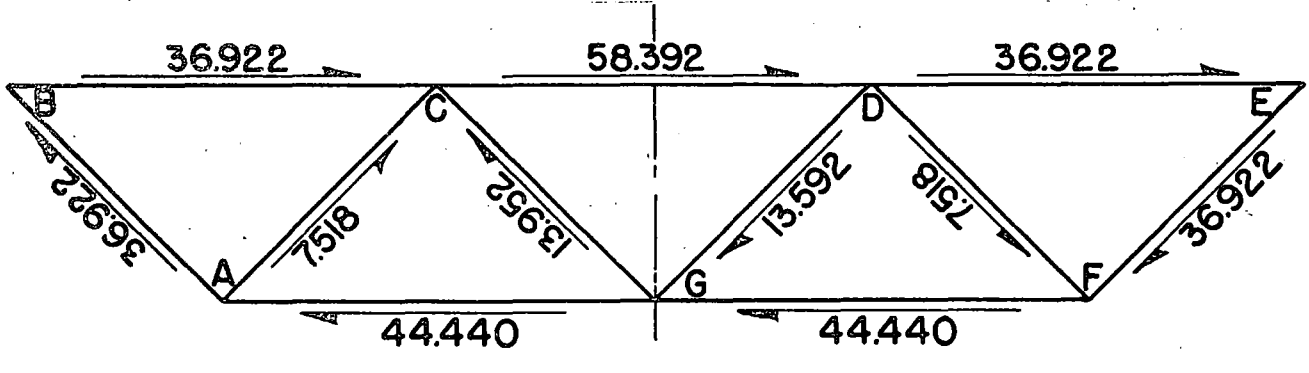

UNIT SHEAR SOLUTION FOR T = 1×10^6 IN. LBS.

FIG. 17 UNIT SHEAR SOLUTIONS FOR BRIDGE WITH DECK

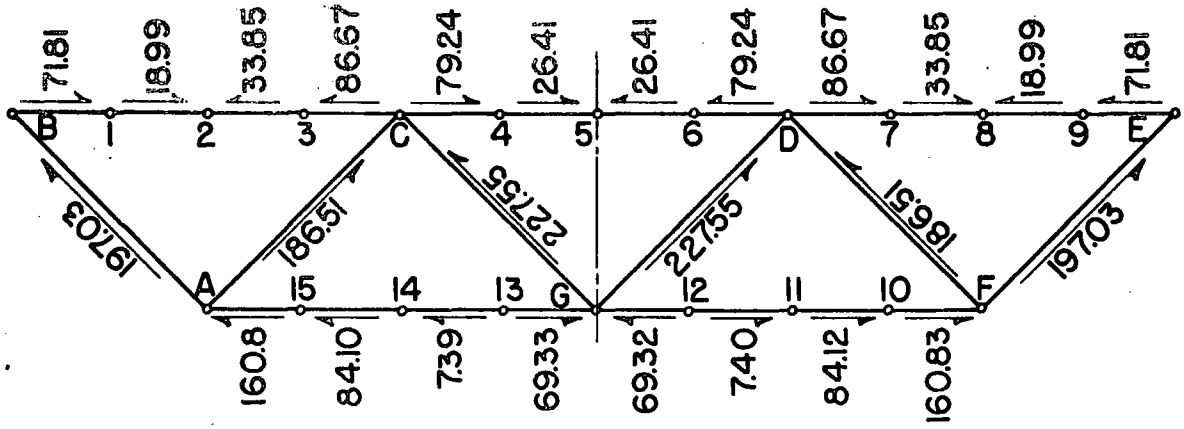

DEAD WEIGHT SHEARS. V_Z=55,000 LBS. ACTING ON BRIDGE WITHOUT SLAB

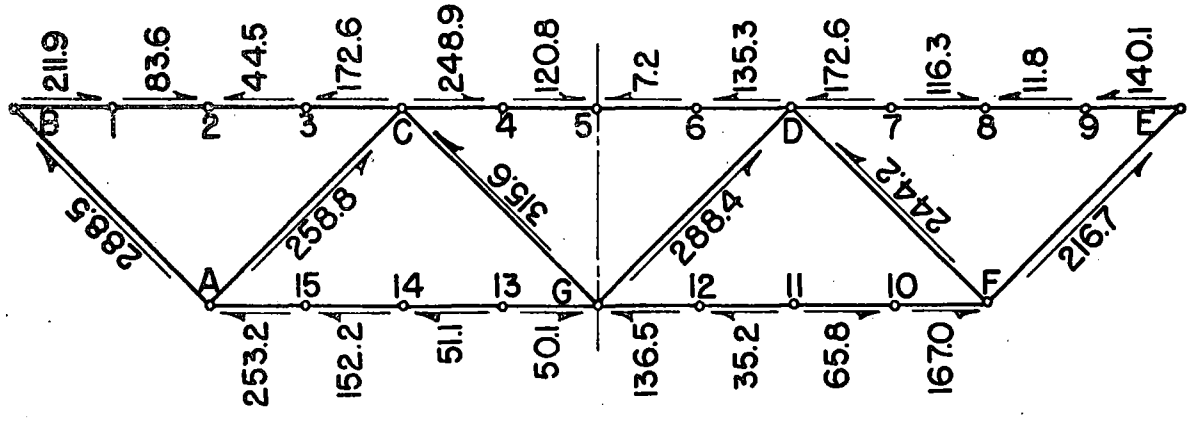

LIVE LOAD PLUS IMPACT SHEARS
V_Z=81,000 LBS. AND T=0.972×10^6 IN. LBS. ACTING ON BRIDGE WITH SLAB

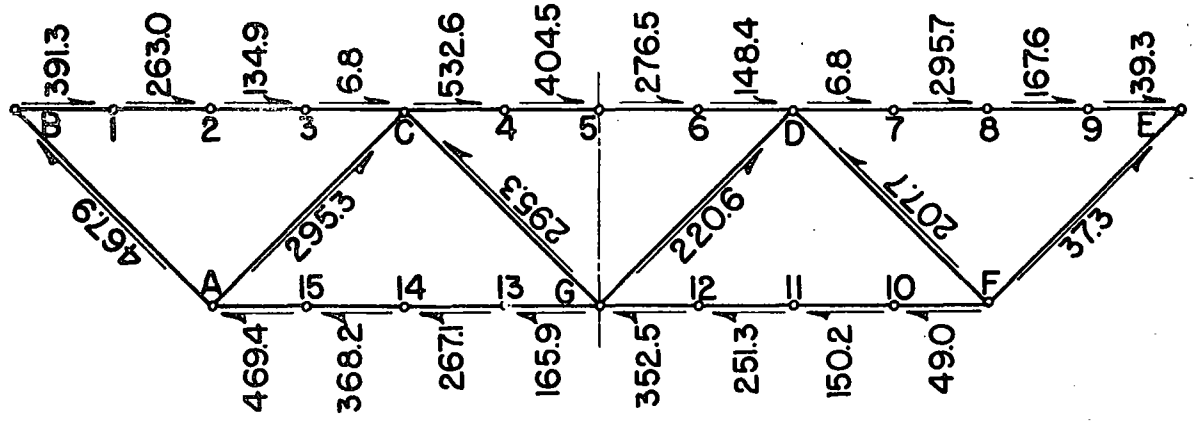

LIVE LOAD OVERLOAD SHEARS
V_Z=81,000 LBS. AND T=5.832×10^6 IN. LBS. ACTING ON BRIDGE WITH SLAB

FIG. 18 PREDICTED SHEAR FLOWS FOR DEAD WEIGHT AND AASHO SPECIFICATION LOADING

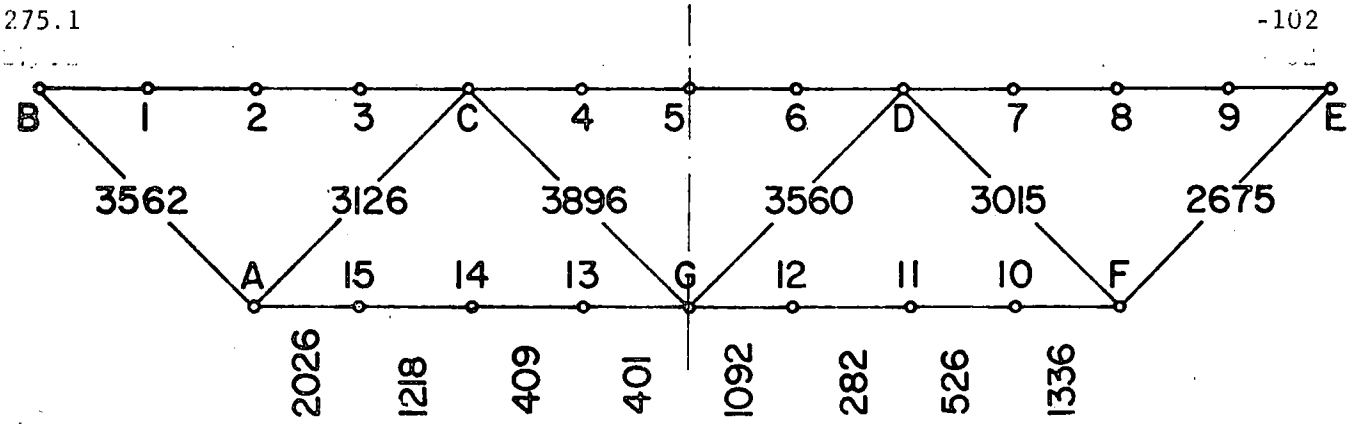

LIVE LOAD PLUS IMPACT LOADING

V_z = 81,000 LBS - ECCENTRICITY = 1 FOOT

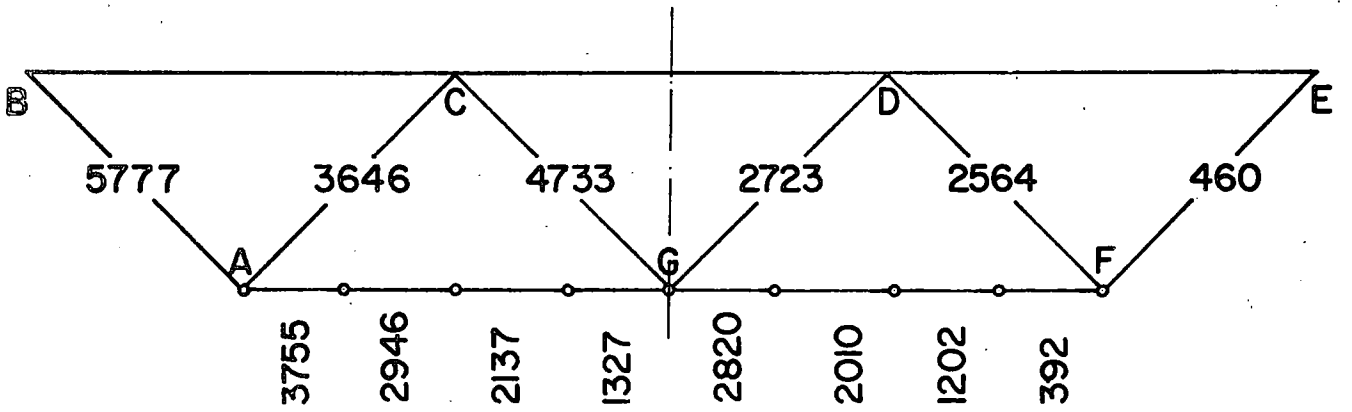

LIVE LOAD OVERLOAD

V_z = 81,000 LBS - ECCENTRICITY = 6 FEET

FIG. 19 PREDICTED SHEAR STRESSES (PSI) FOR AASHO SPECIFICATION LOADING

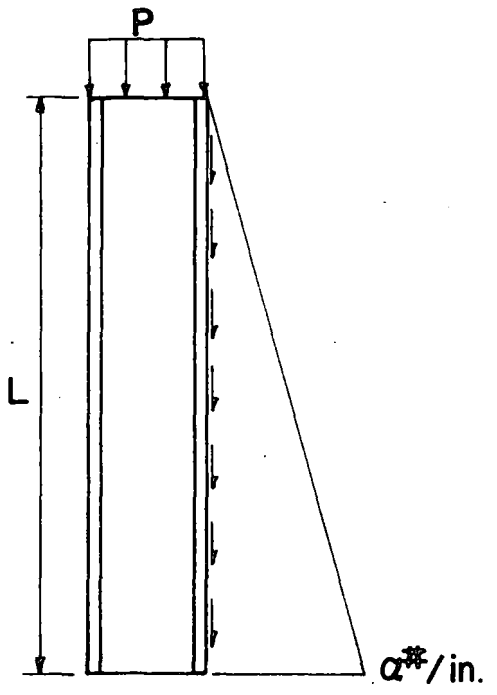

a. Theoretical Loading

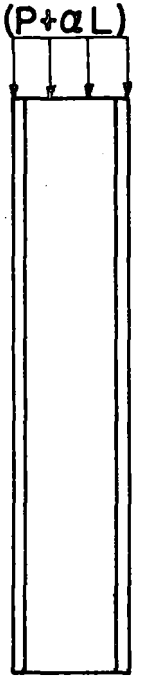

b. Design Loading

FIG. 20 COMPARISON OF THEORETICAL AND DESIGN LOADING CONDITIONS FOR END FRAME

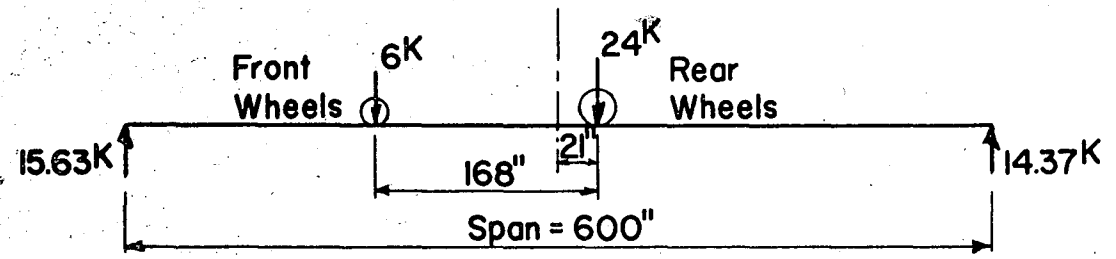

Truck position for maximum lane loading. Maximum moment under rear wheels.

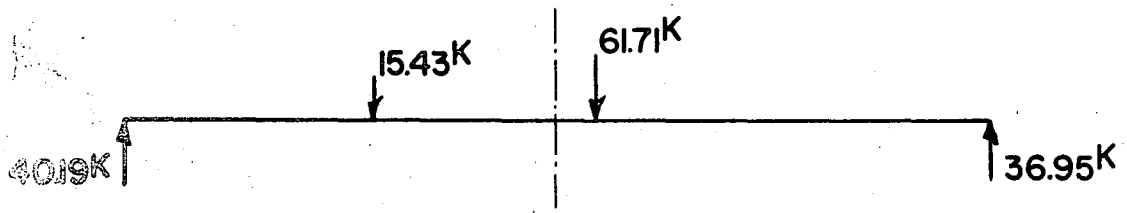

Specification loading for maximum moment due to live load plus impact. M_{LL} under rear wheels.

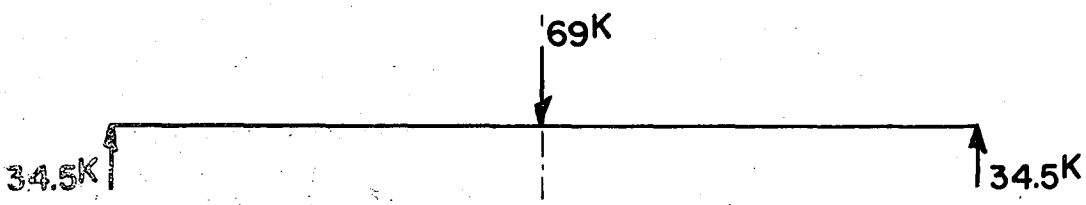

Test loading for 100% M_{LL} at center of span.

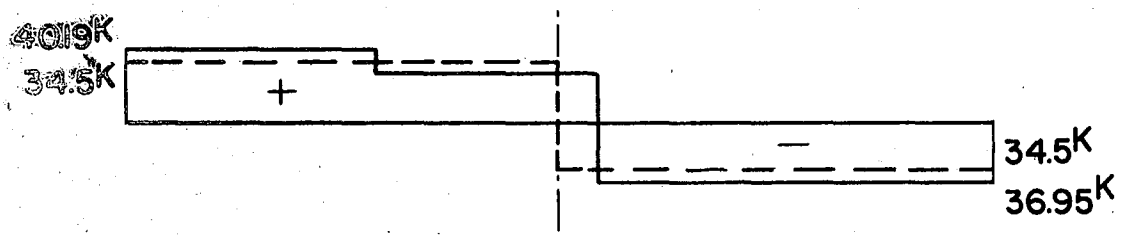

Shear diagram
———Specification
– – – –Test

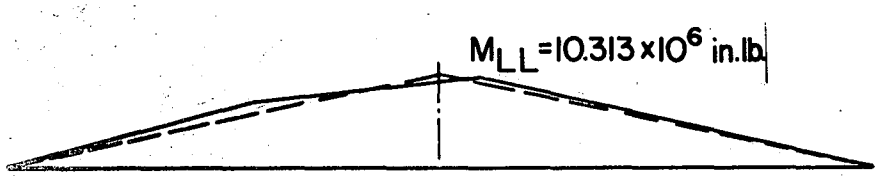

Moment diagram
———Specification
– – – –Test

FIG. 21 COMPARISON OF SPECIFICATION AND TEST VALUES FOR LOADING, SHEAR, AND MOMENT

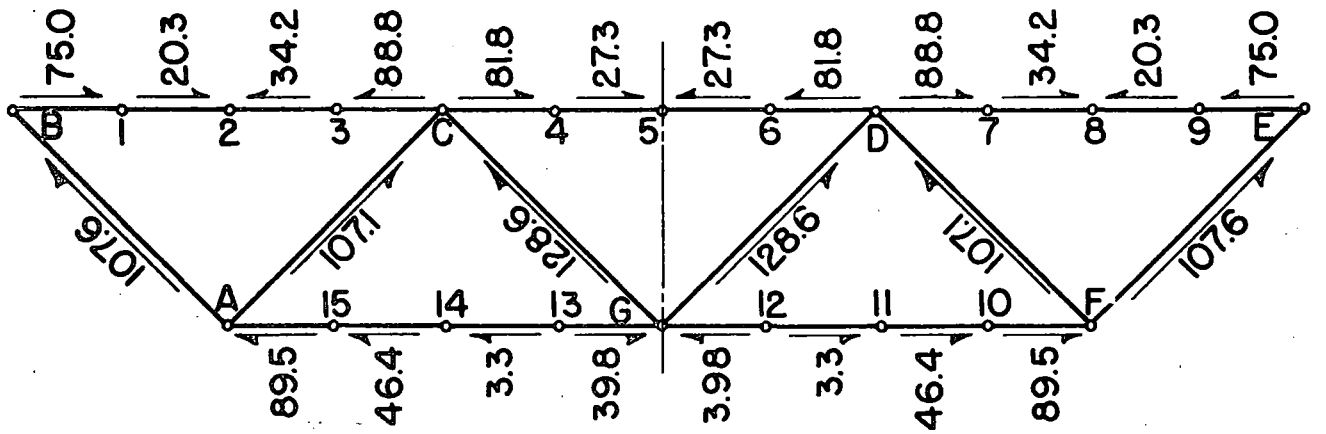

CONCENTRIC LOADING-100% M_{LL} AT CENTER LINE. V_Z = 34,500 LBS.

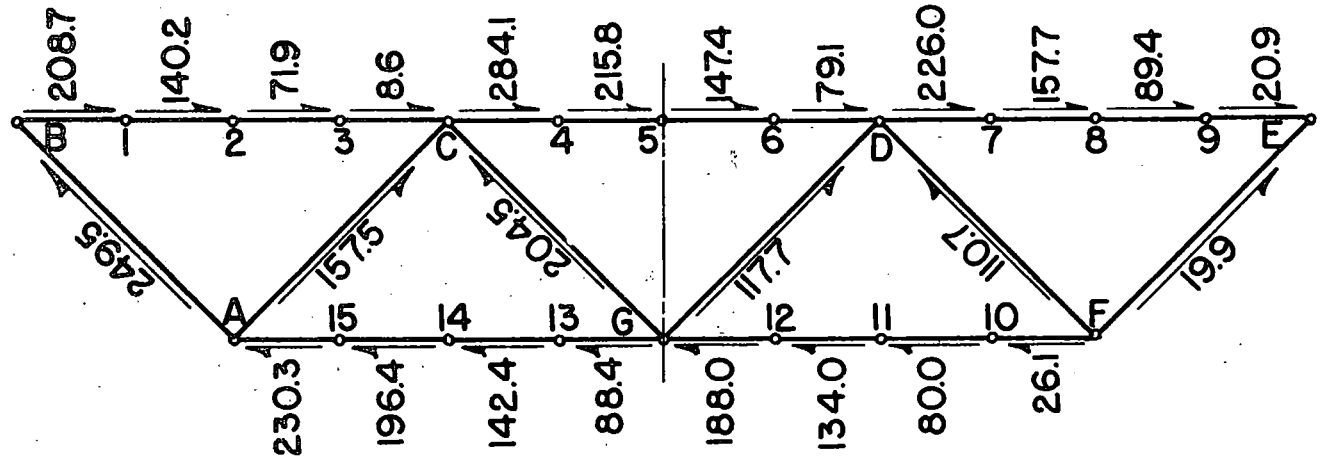

MAXIMUM ECCENTRIC LOADING-125% M_{LL} AT CENTER LINE
V_Z=43,200 LBS. AND T=3.11×10^6 IN. LBS.

FIG. 22 PREDICTED SHEAR FLOWS FOR TEST LOADING

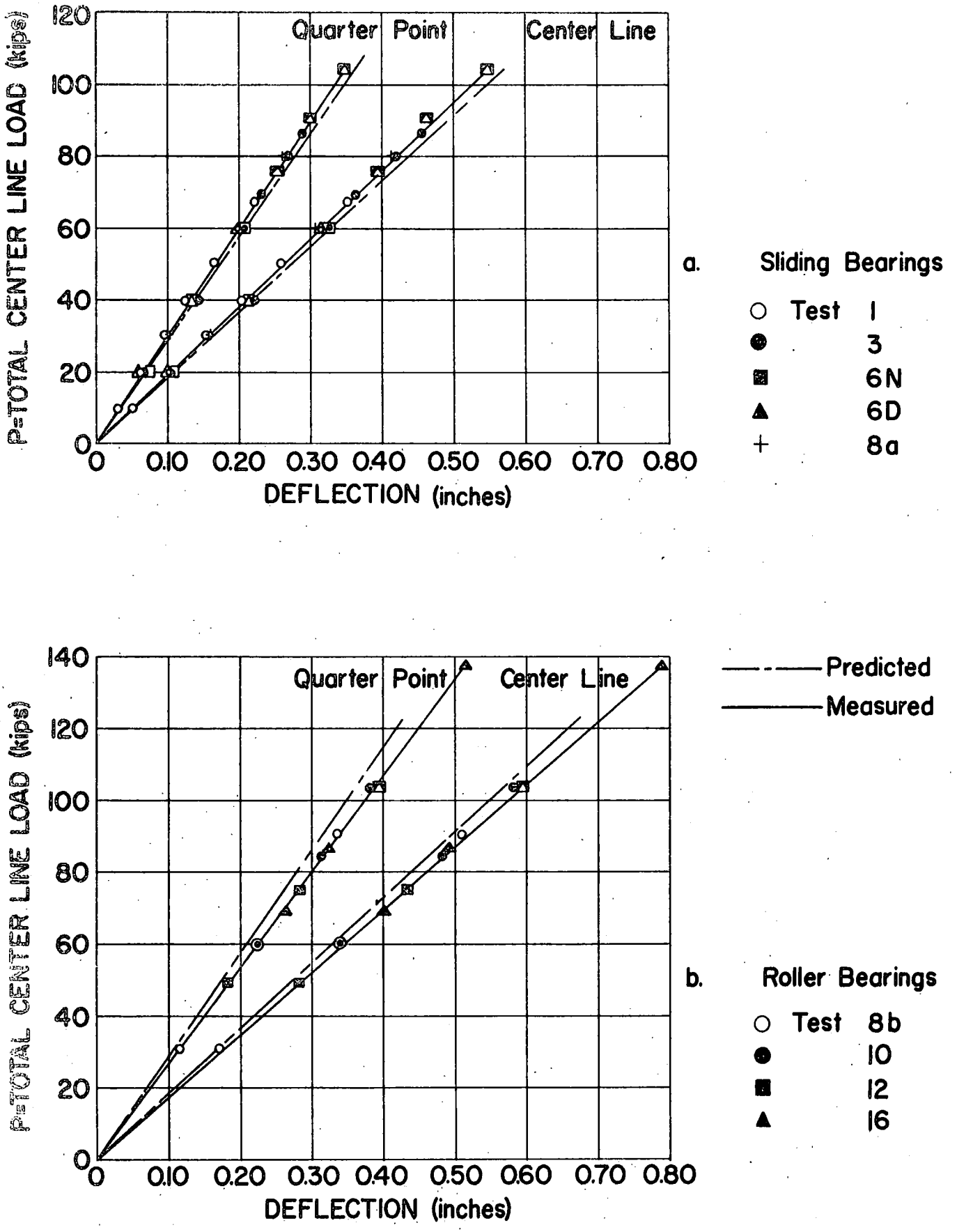

FIG. 23 CONCENTRIC STATIC LOAD-DEFLECTION CURVE

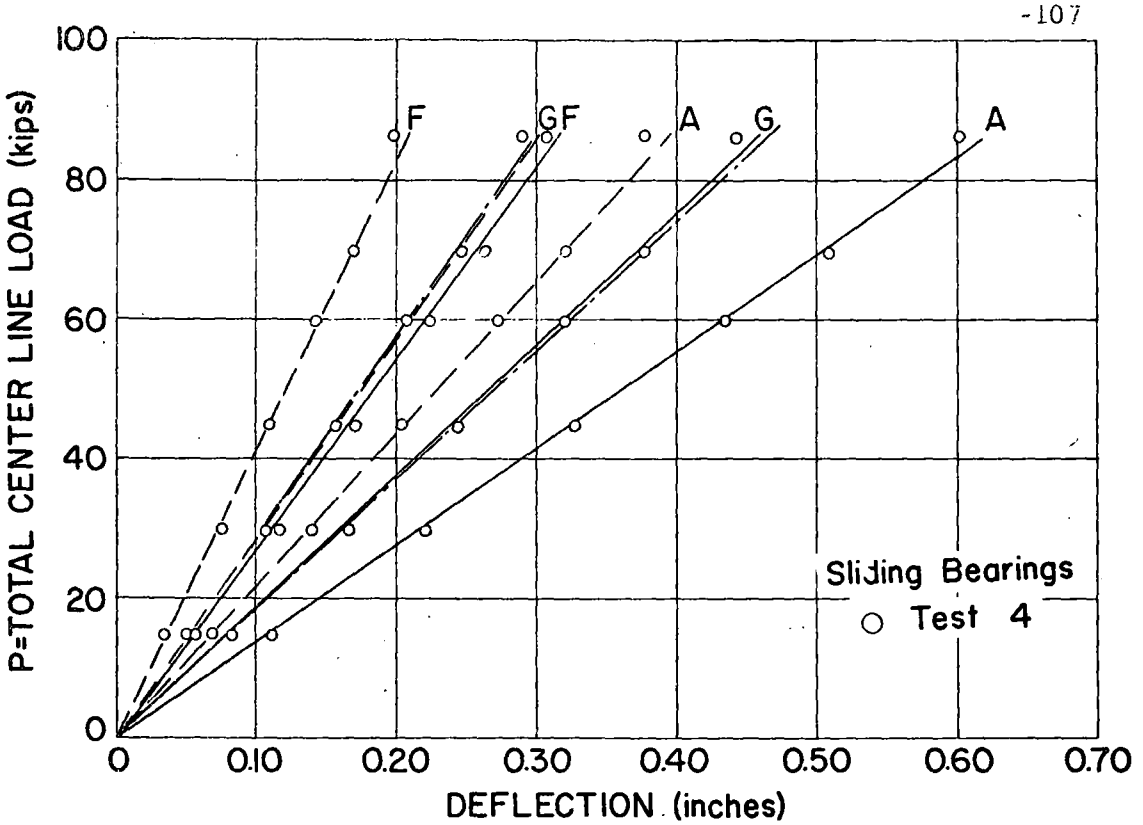

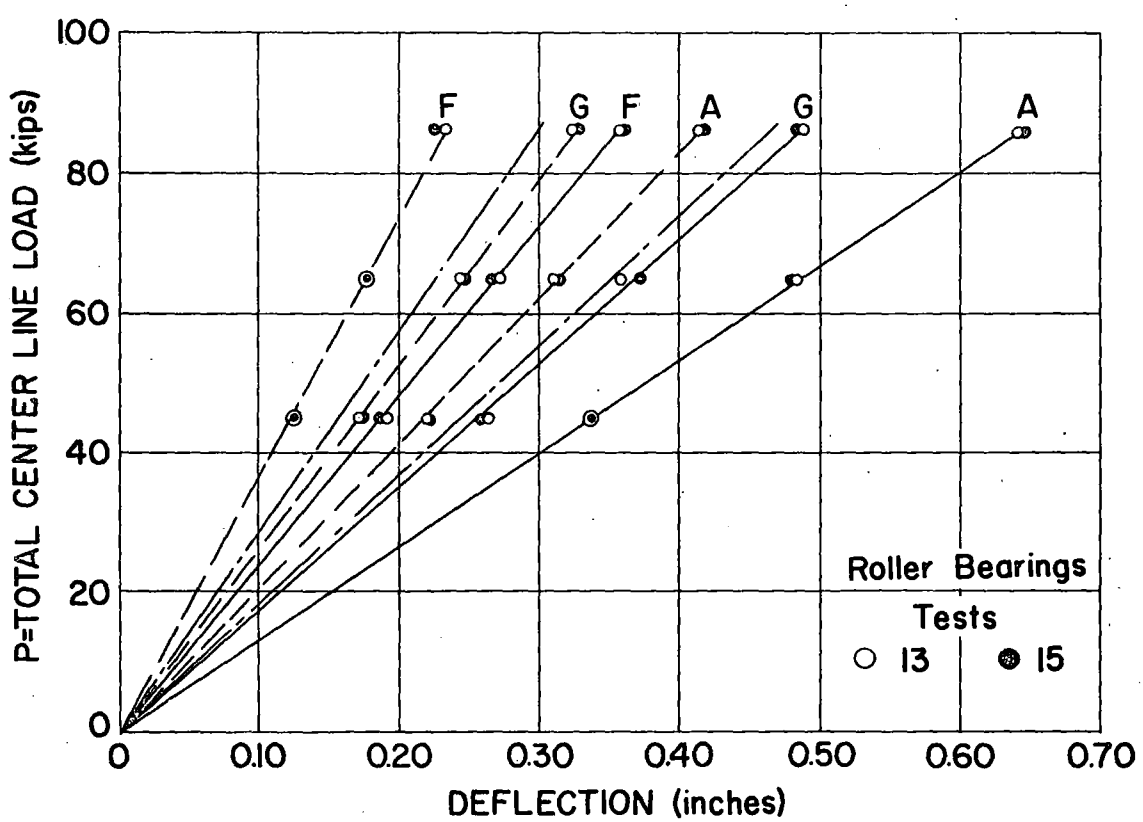

Measured

——— Center Line

– – – – Quarter Point

—·—·— Predicted (for G)

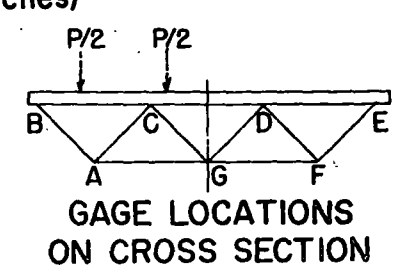

GAGE LOCATIONS ON CROSS SECTION

FIG. 24 ECCENTRIC STATIC LOAD-DEFLECTION CURVES

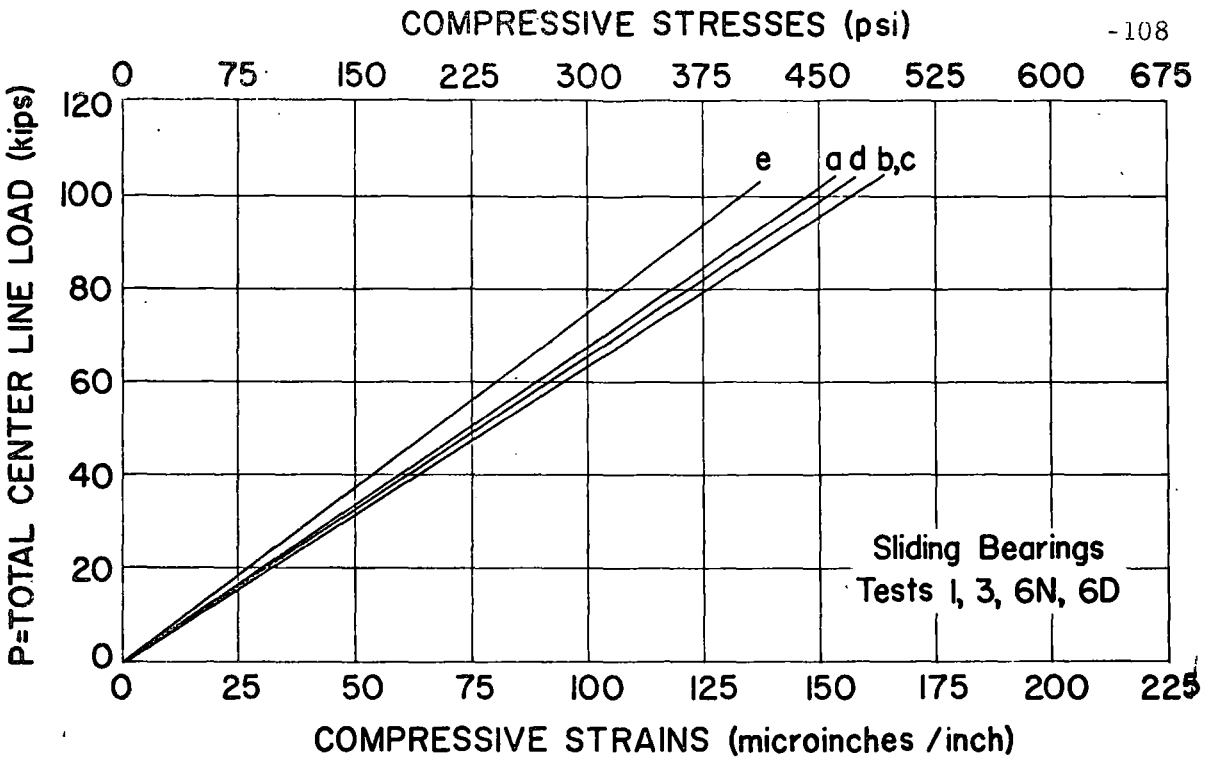

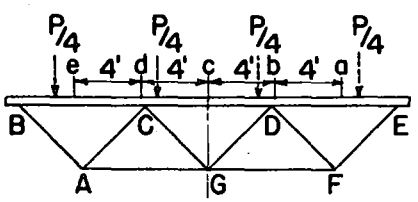

GAGE LOCATION
Station 23–Cross Section

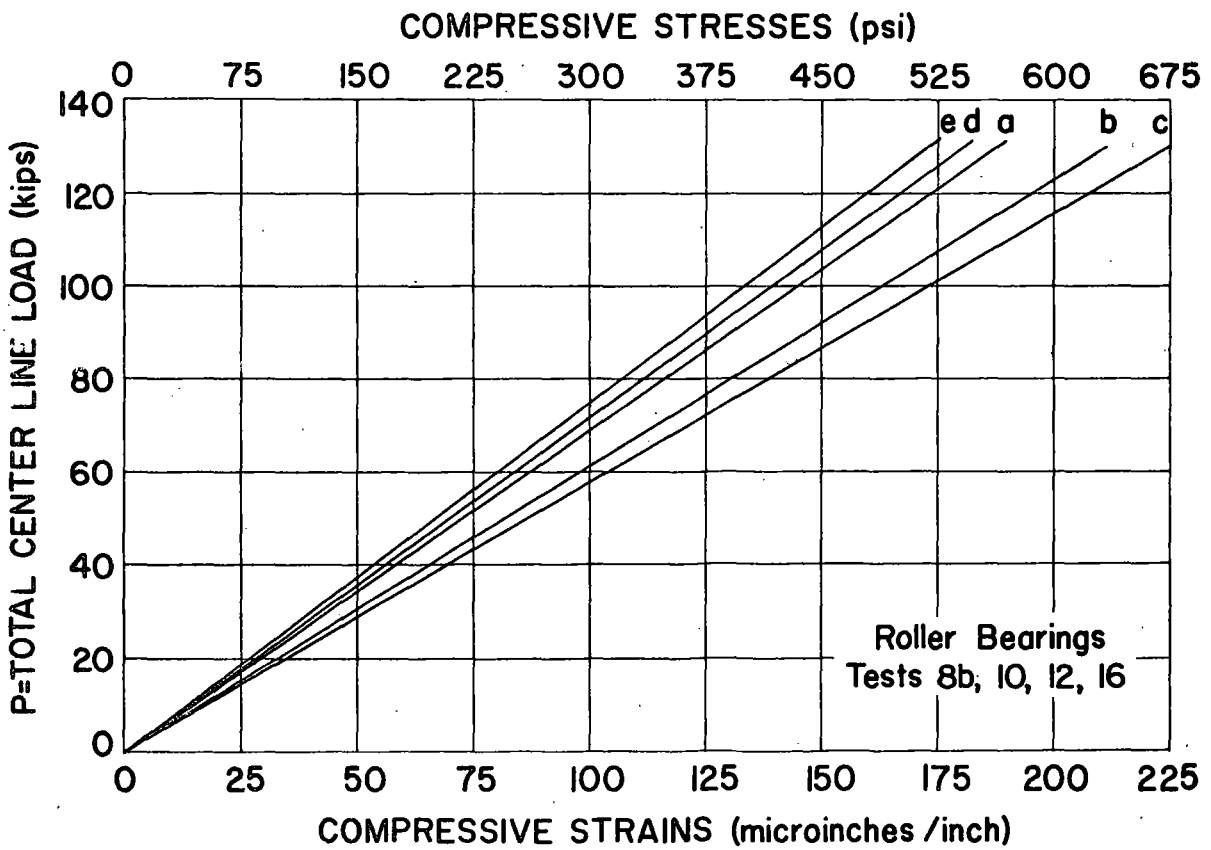

FIG. 25 CONCENTRIC LOAD-STRAIN CURVE FOR POINTS ON THE DECK SURFACE AT STATION 23

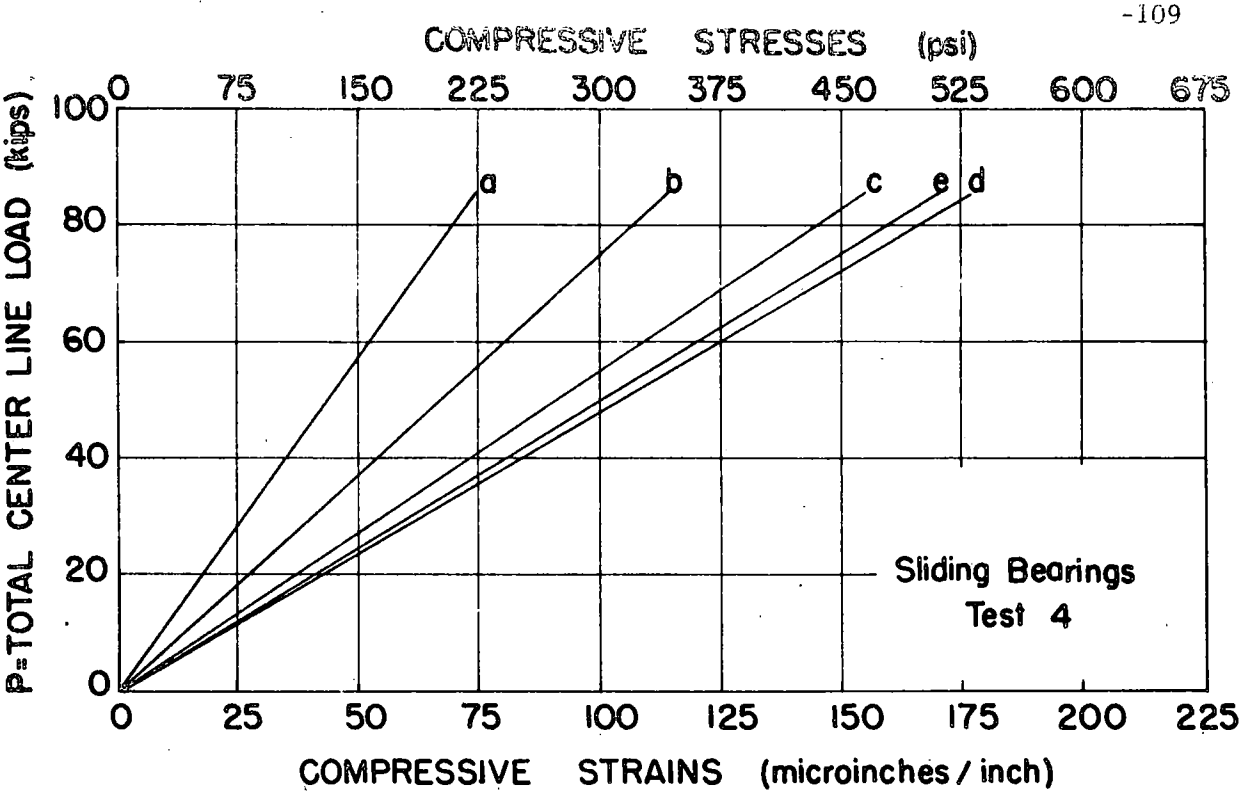

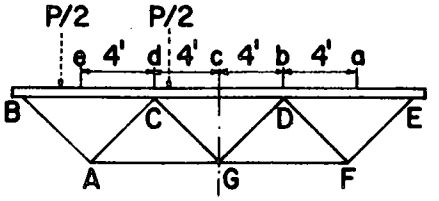

GAGE LOCATION
Station 23-Cross Section

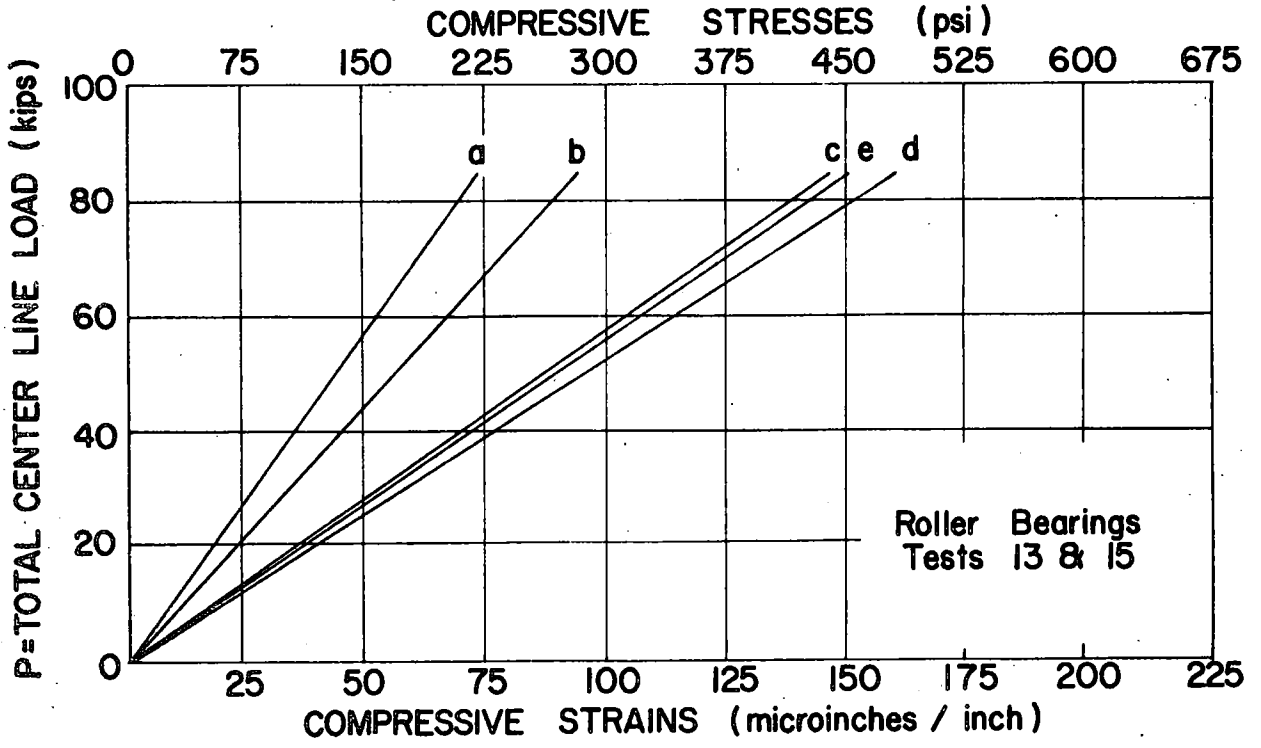

FIG.26 ECCENTRIC LOAD-STRAIN CURVE FOR POINTS ON THE DECK SURFACE AT STATION 23

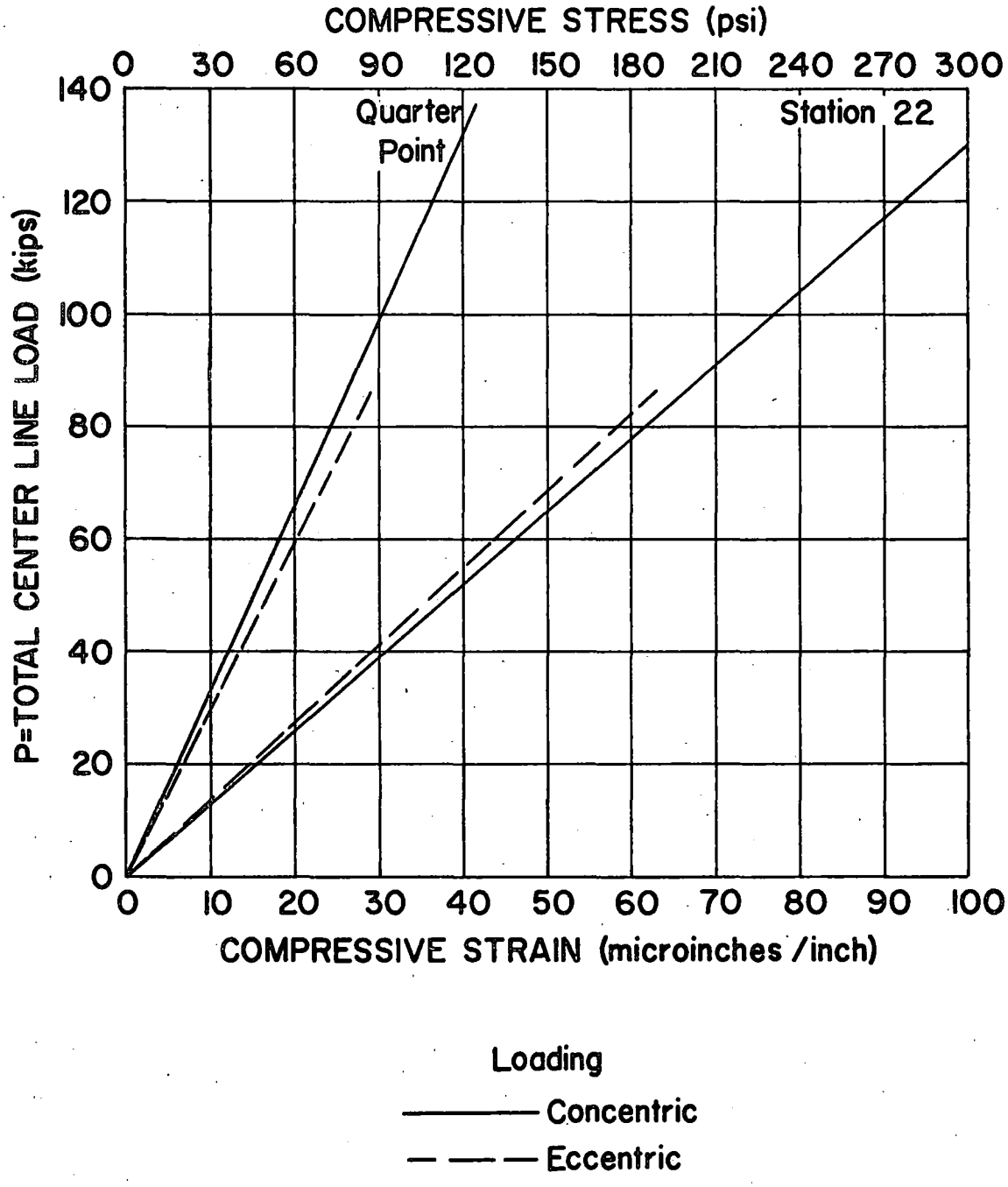

FIG. 27 LOAD-STRAIN CURVE FOR STRAINOMETERS IN DECK

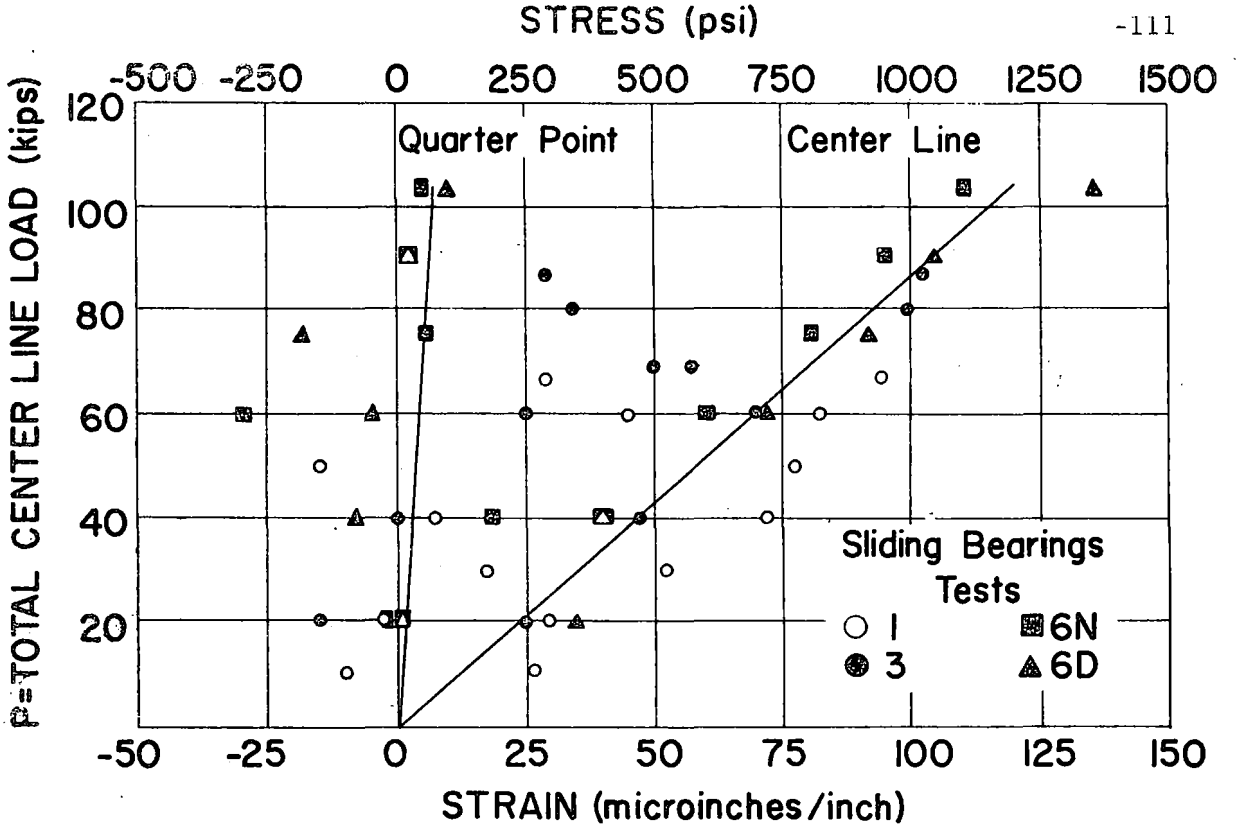

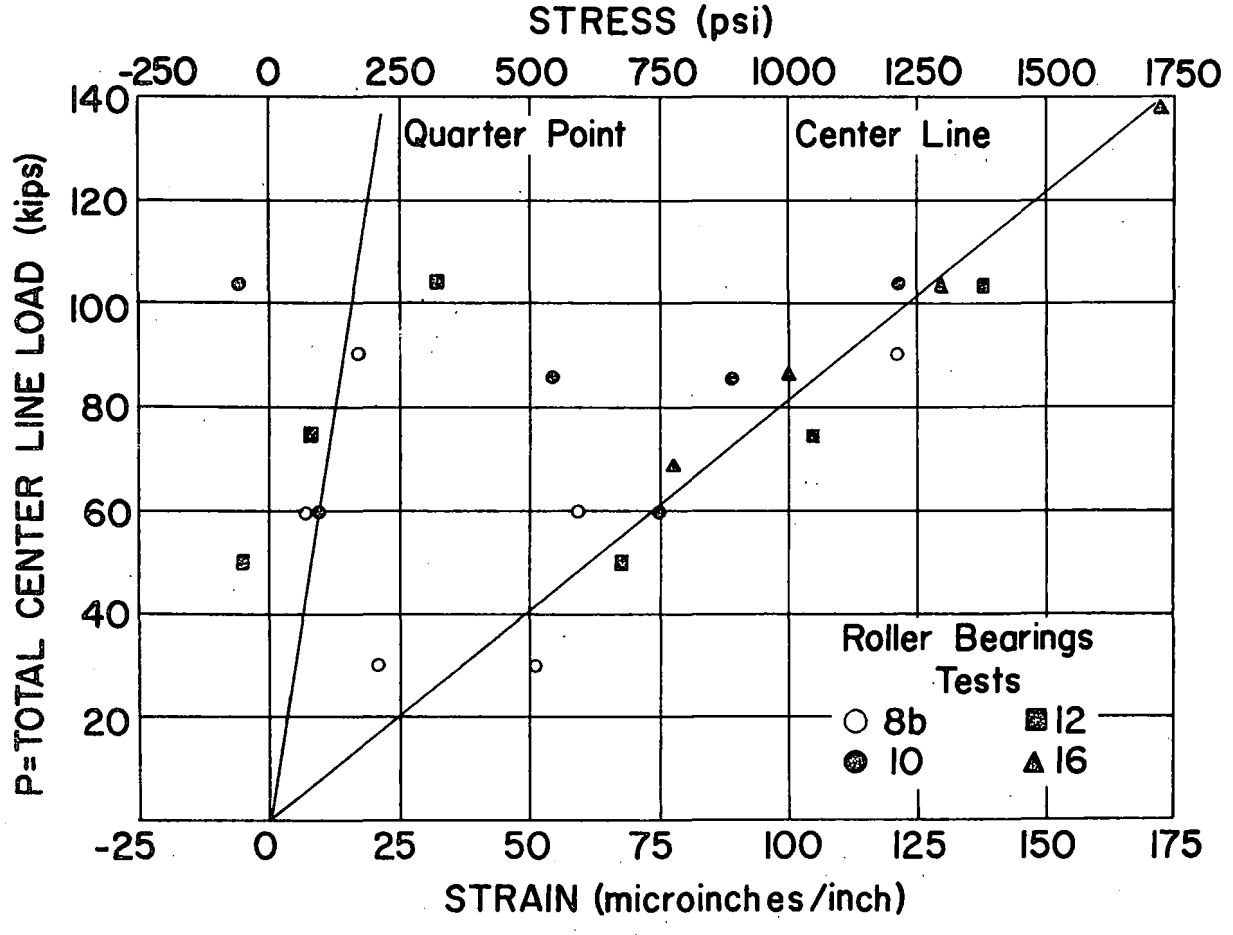

FIG. 28 CONCENTRIC LOAD-STRAIN CURVE FOR LONGITUDINAL MEMBER B

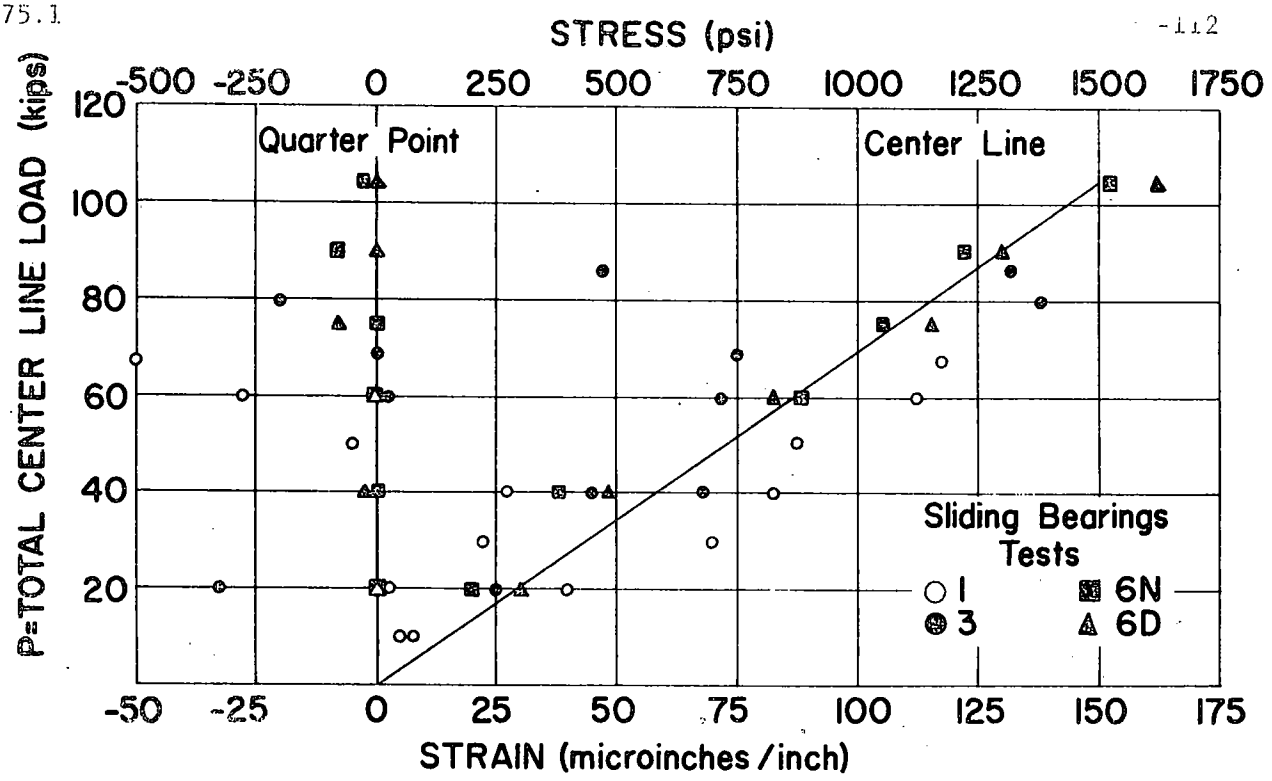

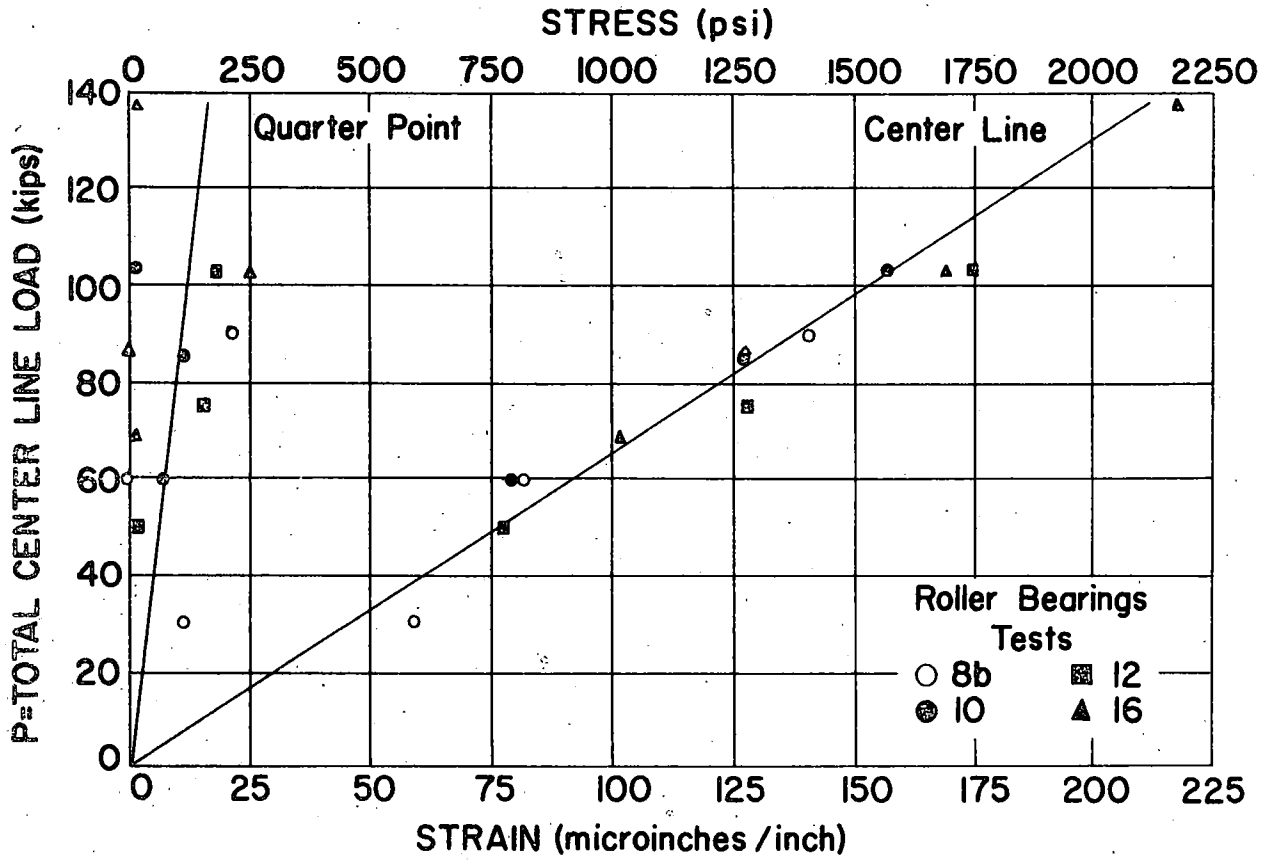

FIG. 29 CONCENTRIC LOAD-STRAIN CURVE FOR LONGITUDINAL MEMBER C

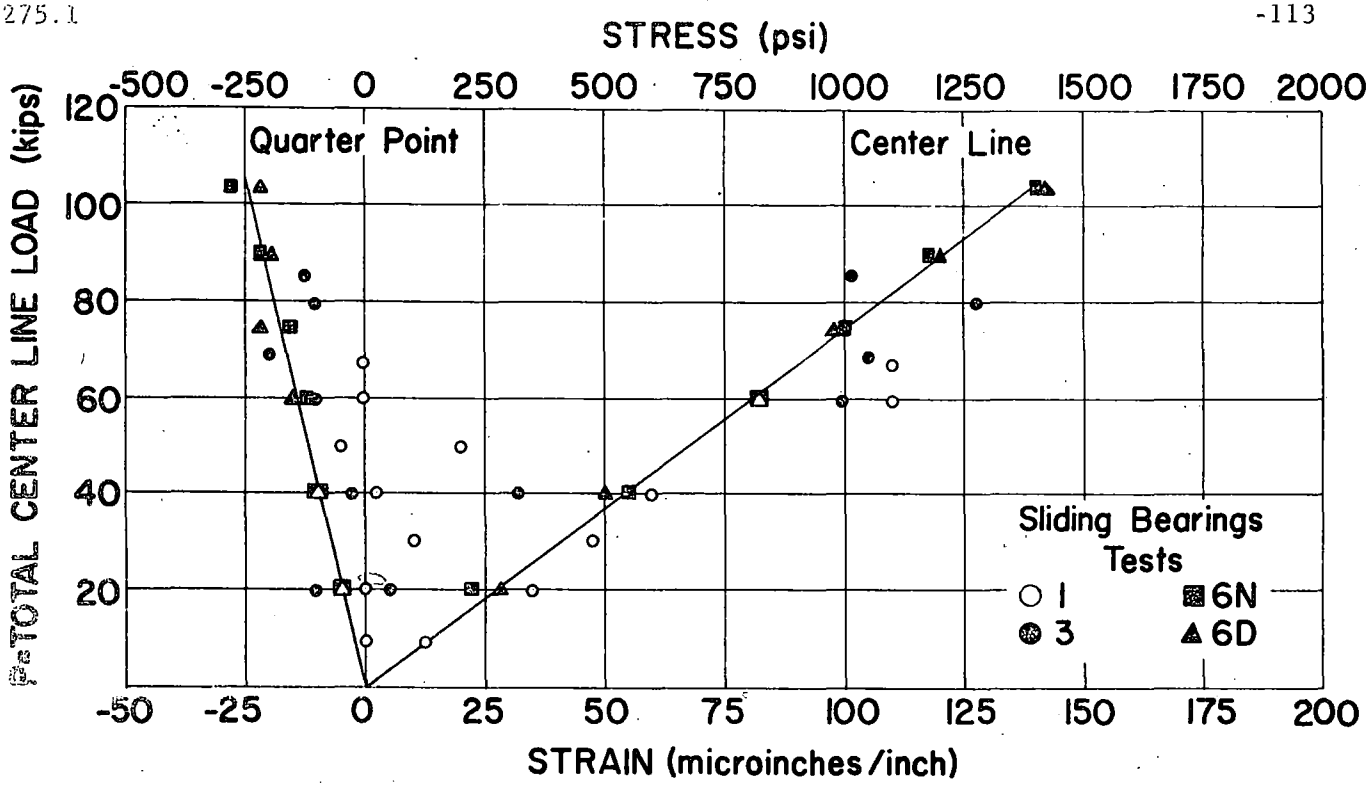

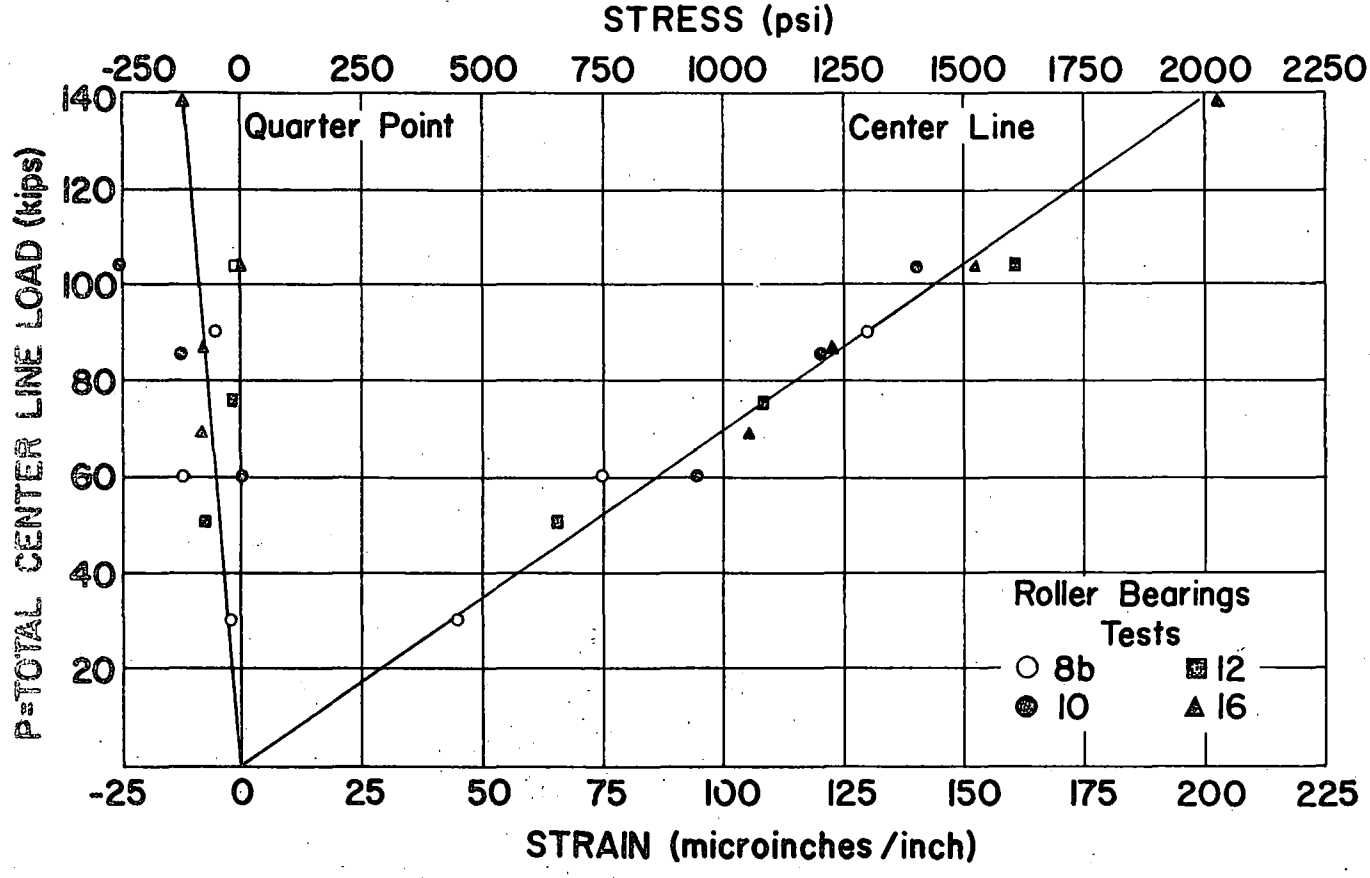

FIG. 30 CONCENTRIC LOAD-STRAIN CURVE FOR LONGITUDINAL MEMBER D

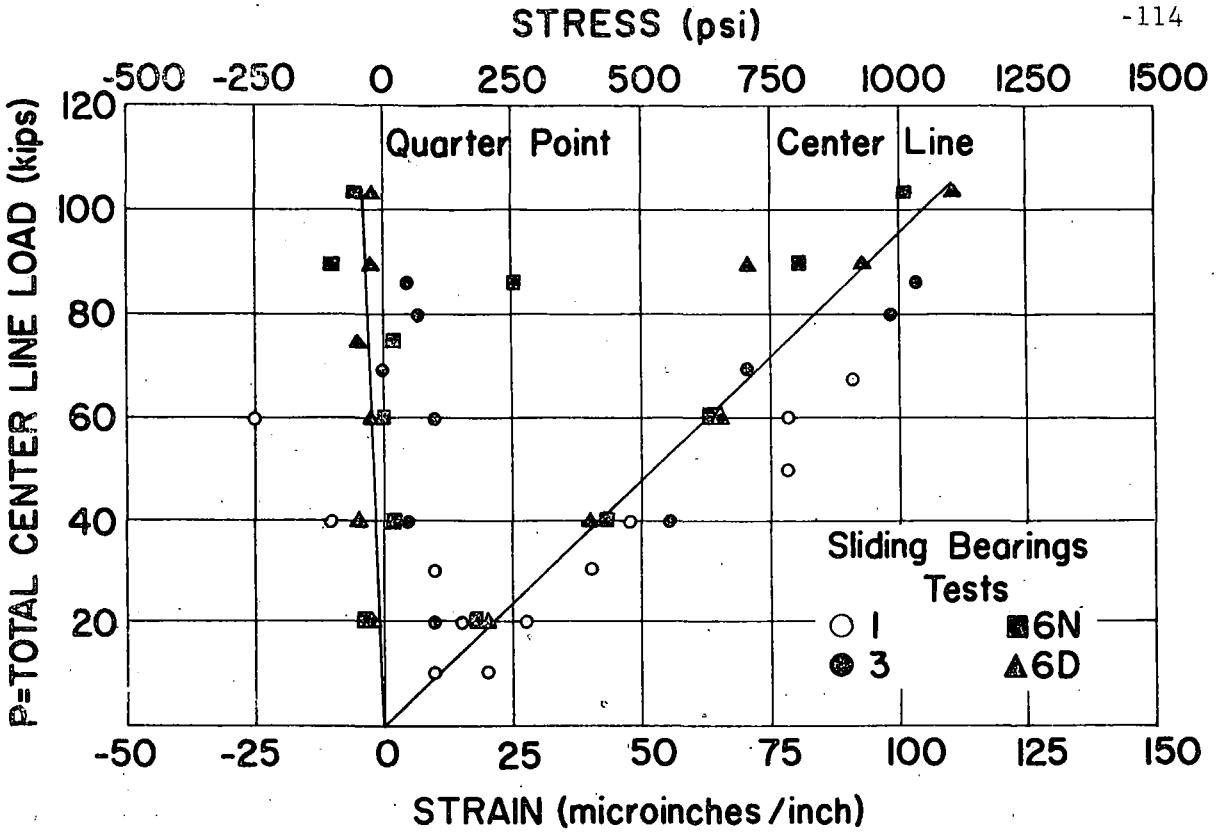

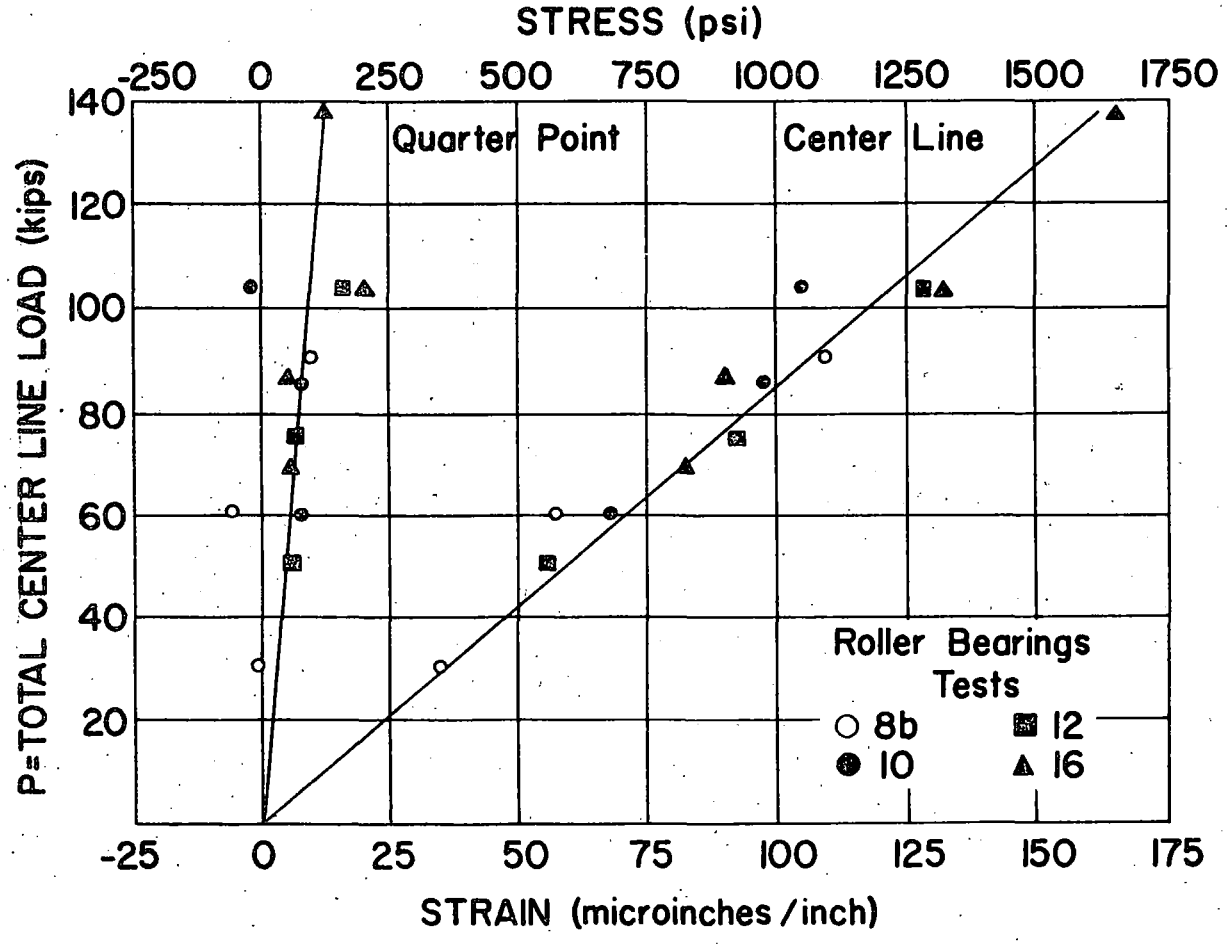

FIG.31 CONCENTRIC LOAD-STRAIN CURVE FOR LONGITUDINAL MEMBER E

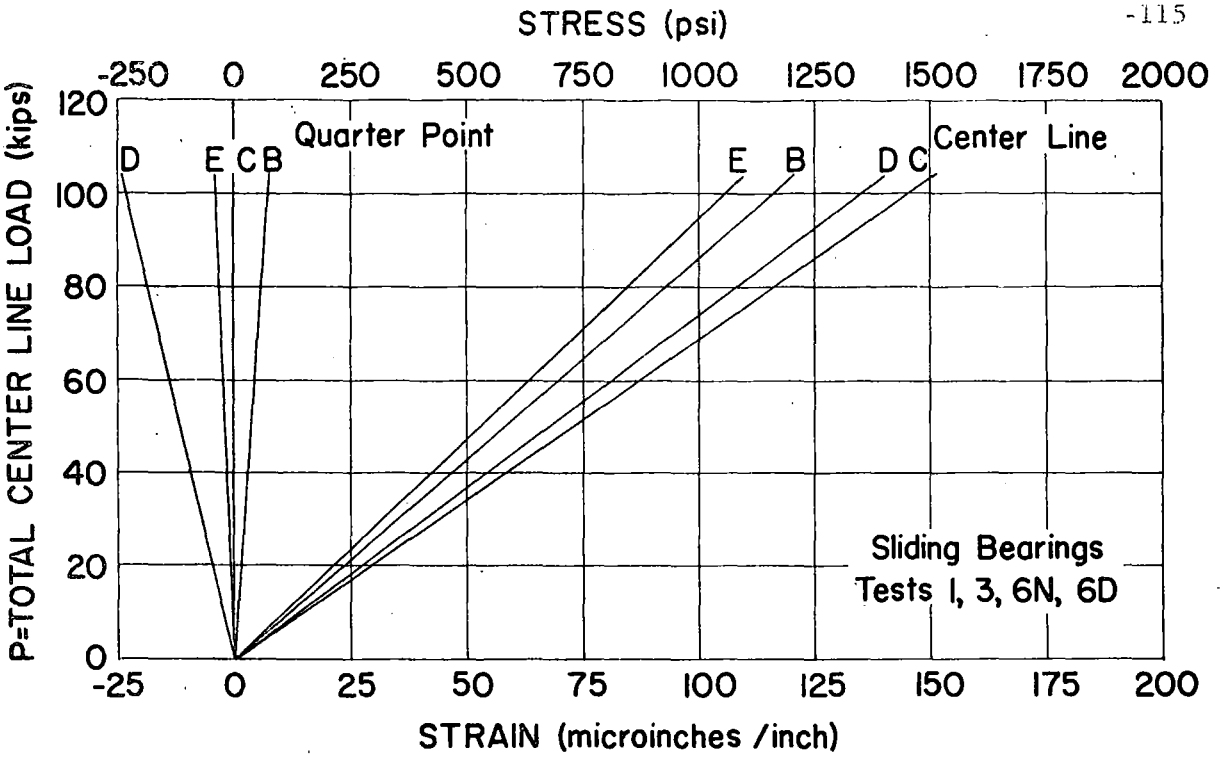

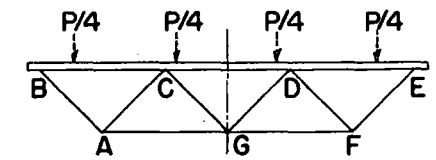

CROSS SECTION OF BRIDGE

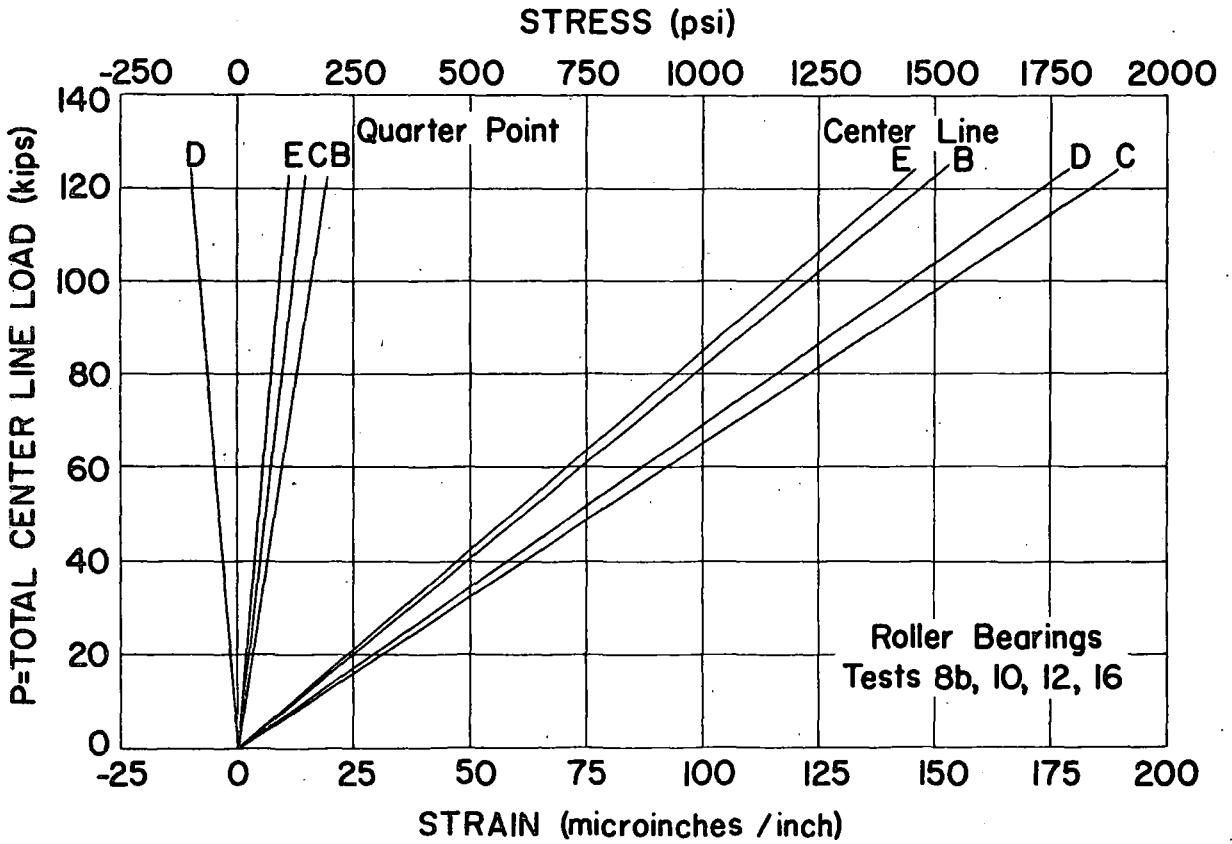

FIG. 32 COMPARISON OF STRAINS IN TOP LONGITUDINAL MEMBERS UNDER CONCENTRIC LOADING

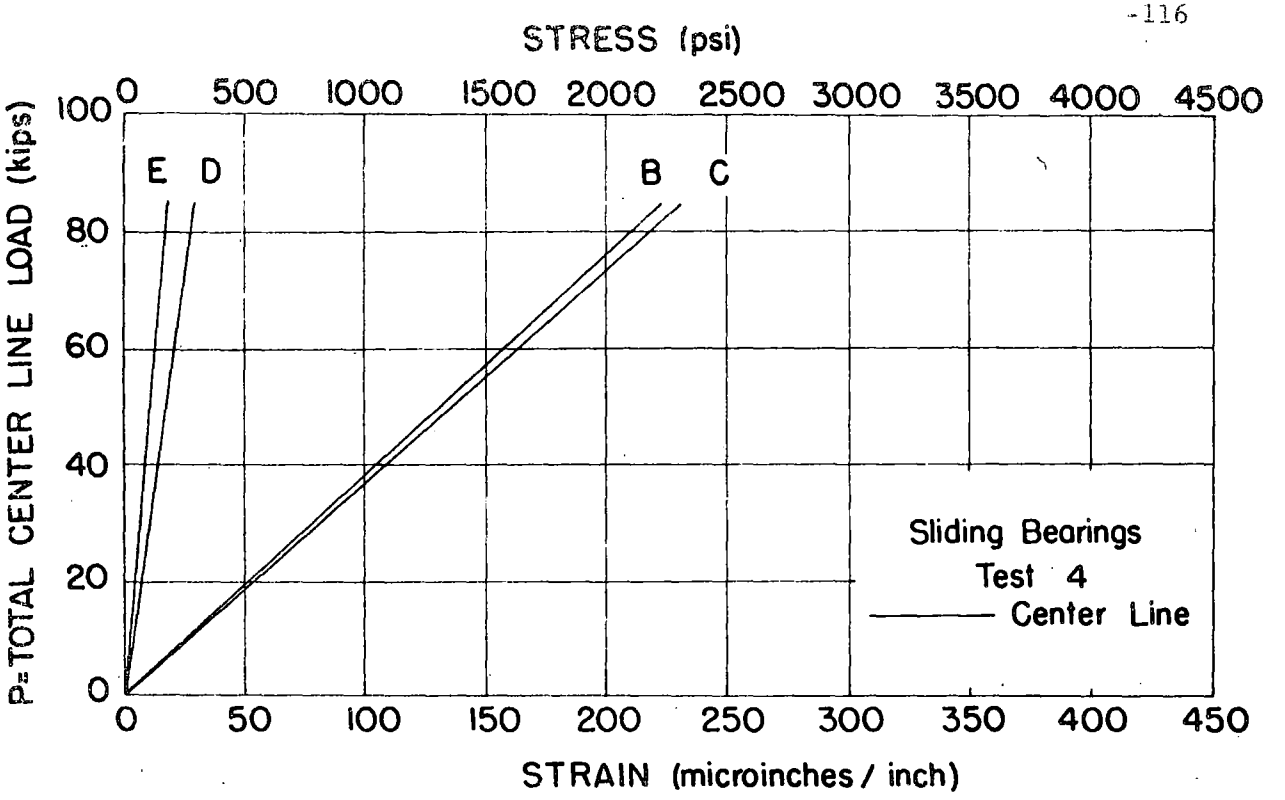

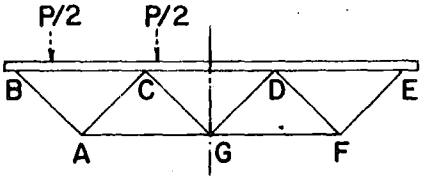

CROSS SECTION

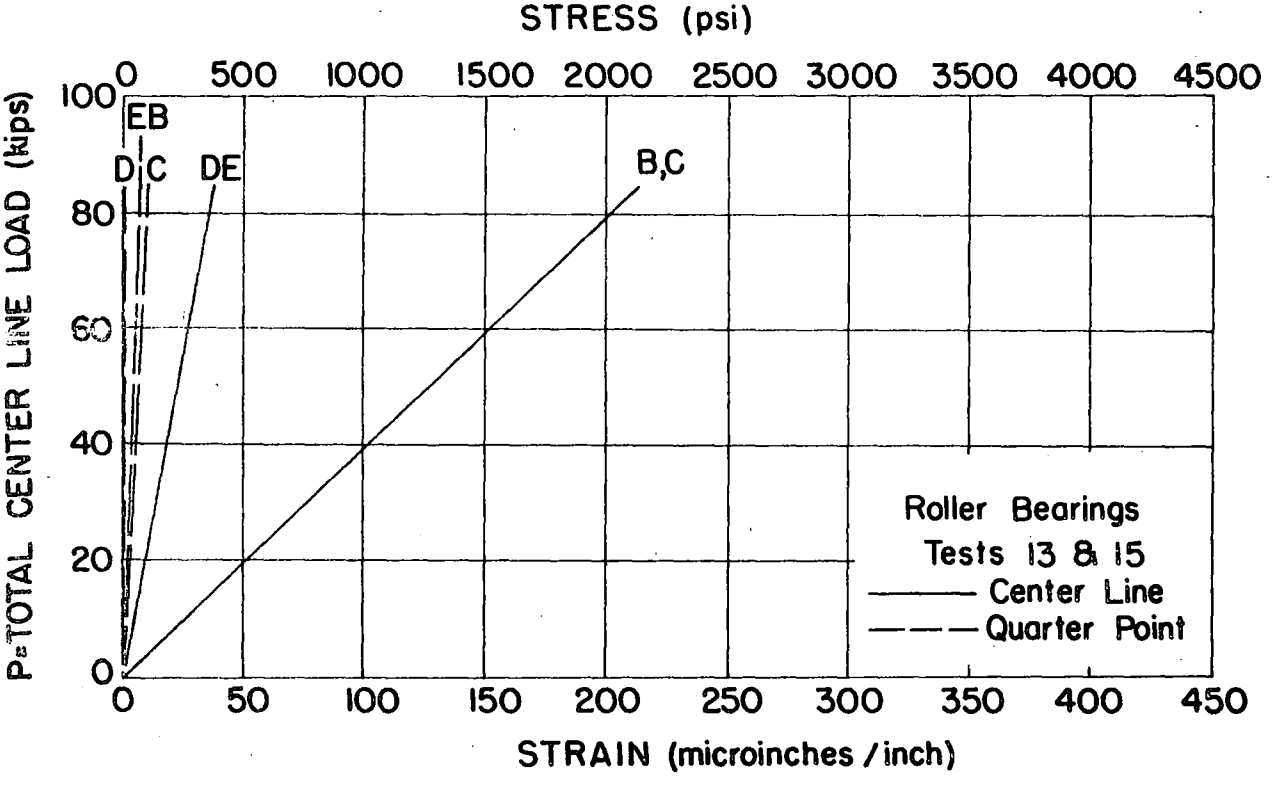

FIG.33 COMPARISON OF STRAINS IN TOP LONGITUDINAL MEMBERS UNDER ECCENTRIC LOADING

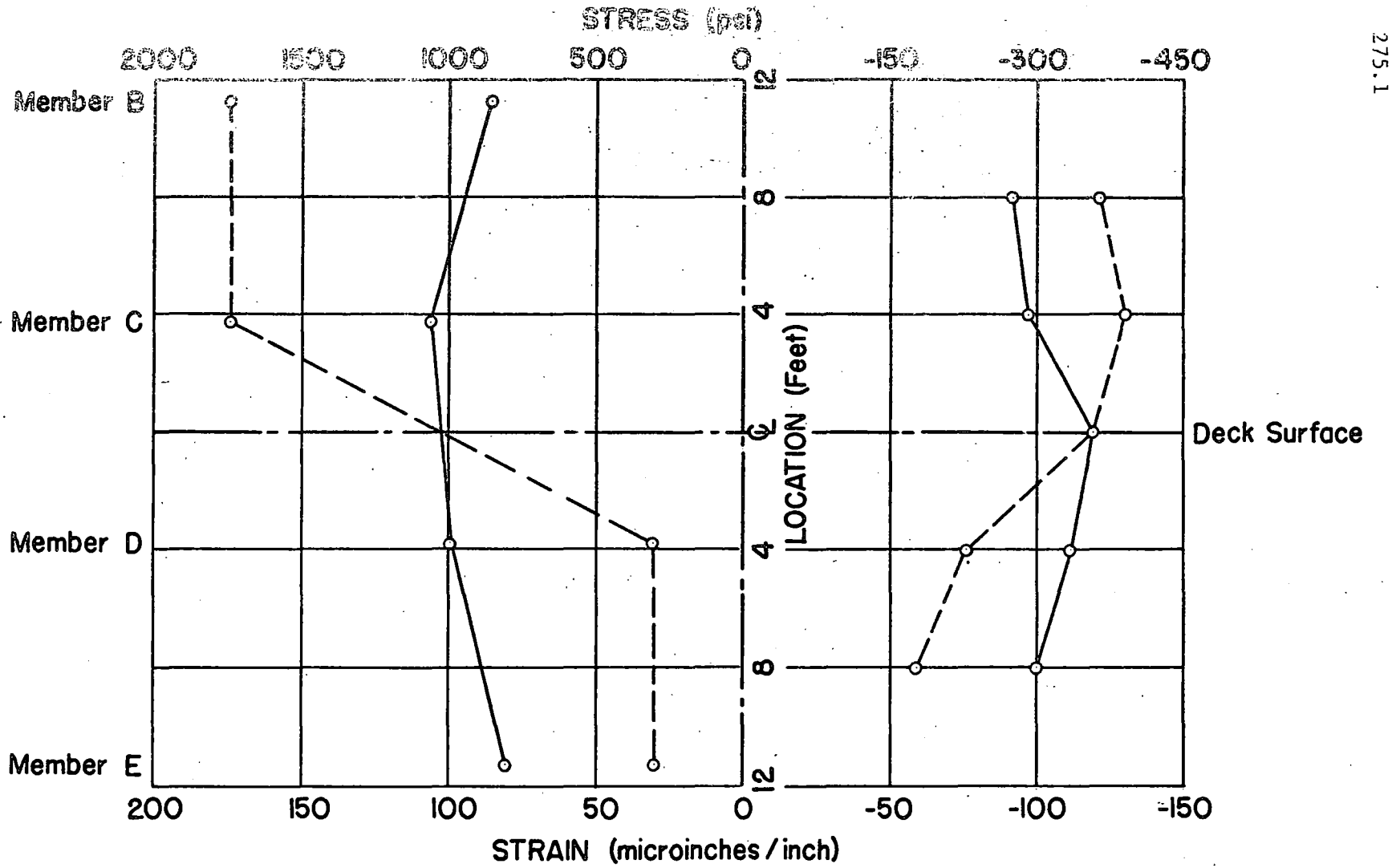

Notes: Main longitudinal members gaged at Station 25
Deck Surface gaged at Station 23
Vertical distance between gages was 9 in.
Applied load at transverse center line=69,000 lbs.

——— Concentric
— — — Eccentric

FIG. 34 COMPARISON OF STRAINS AT DECK SURFACE AND IN TOP LONGITUDINAL MEMBERS

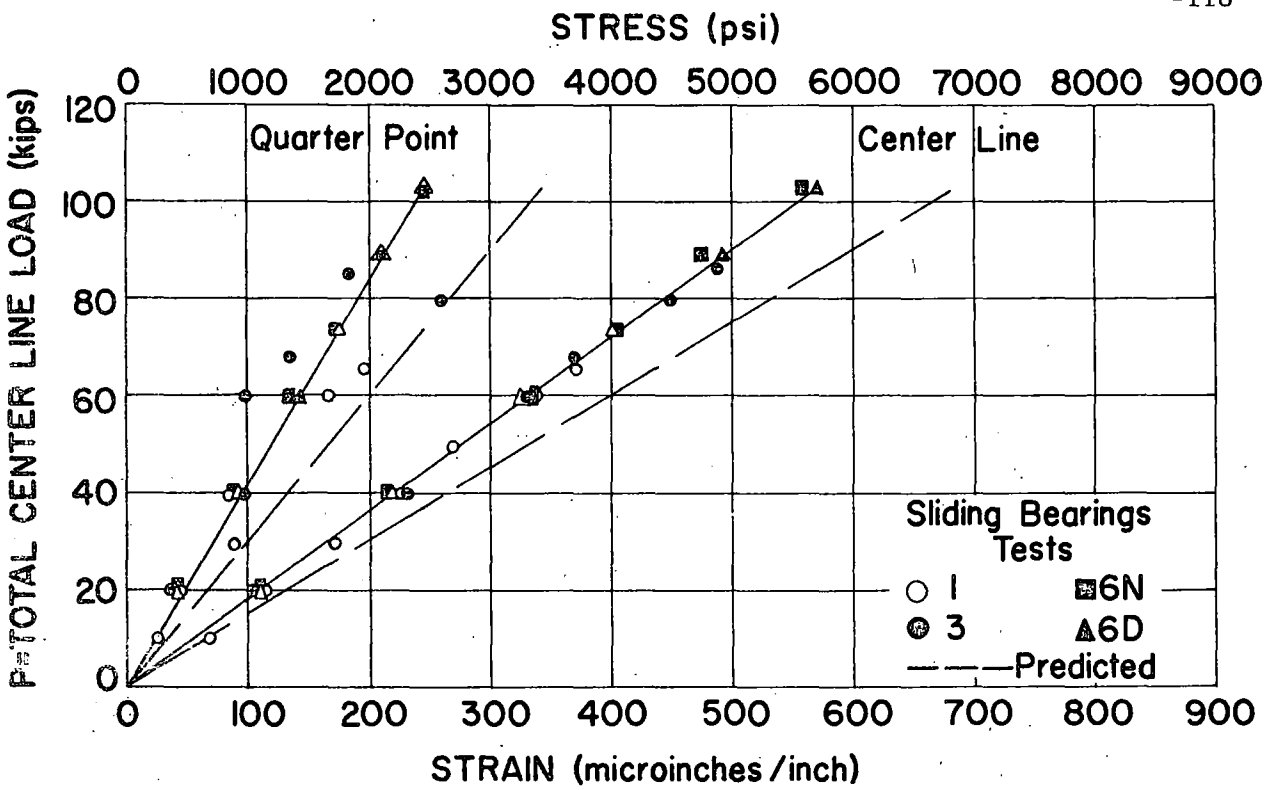

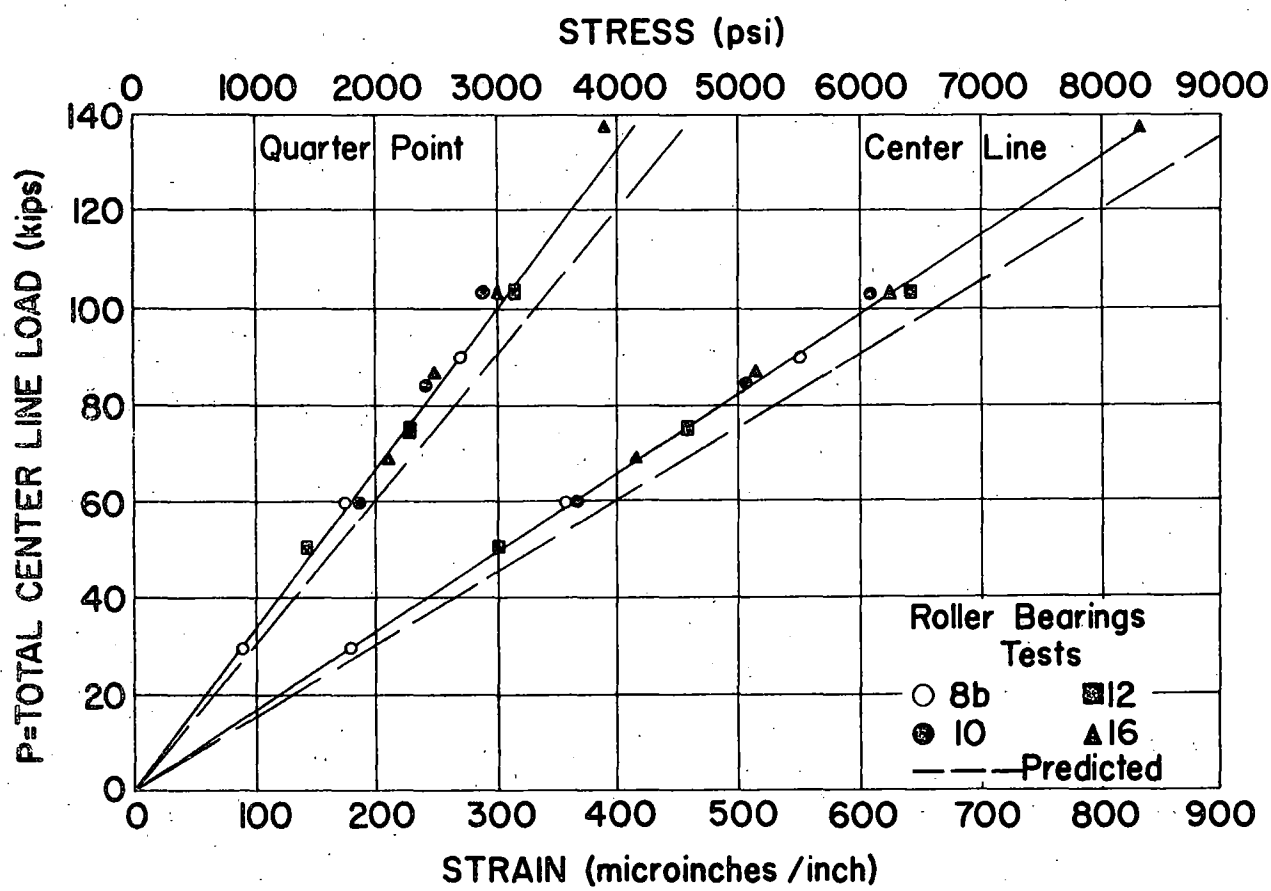

FIG. 35 CONCENTRIC LOAD-STRAIN CURVE FOR LONGITUDINAL MEMBER A

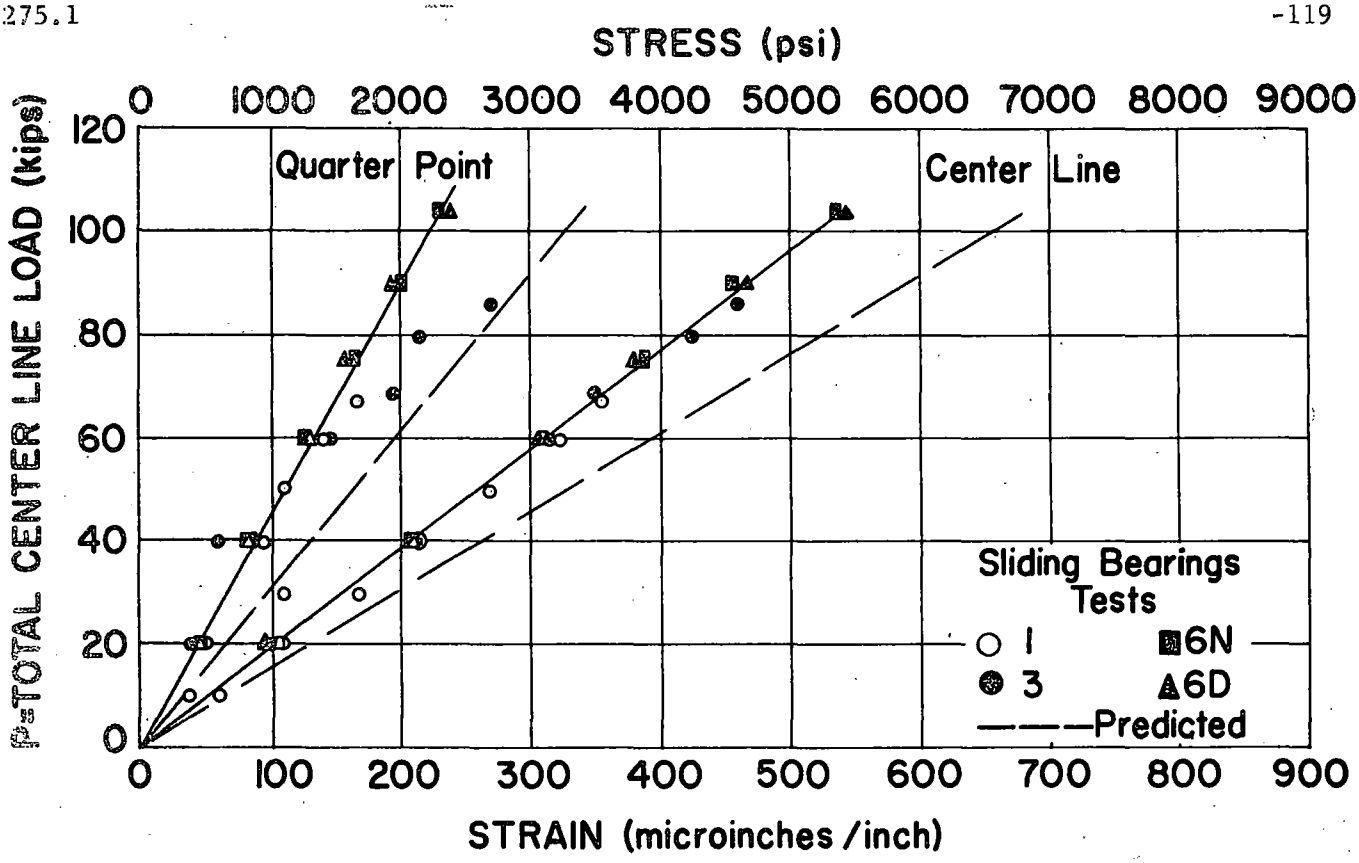

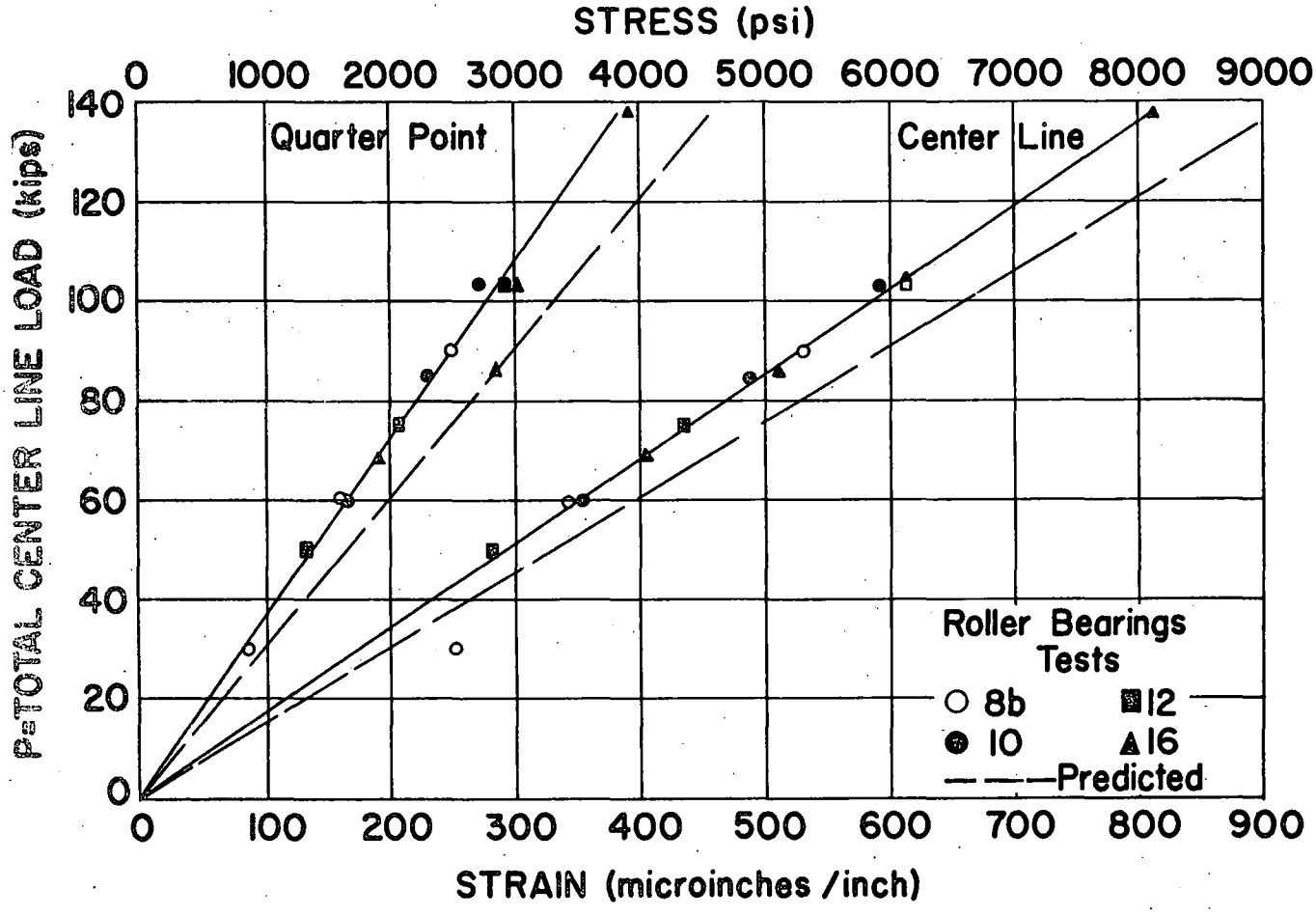

FIG. 36 CONCENTRIC LOAD-STRAIN CURVE FOR LONGITUDINAL MEMBER G

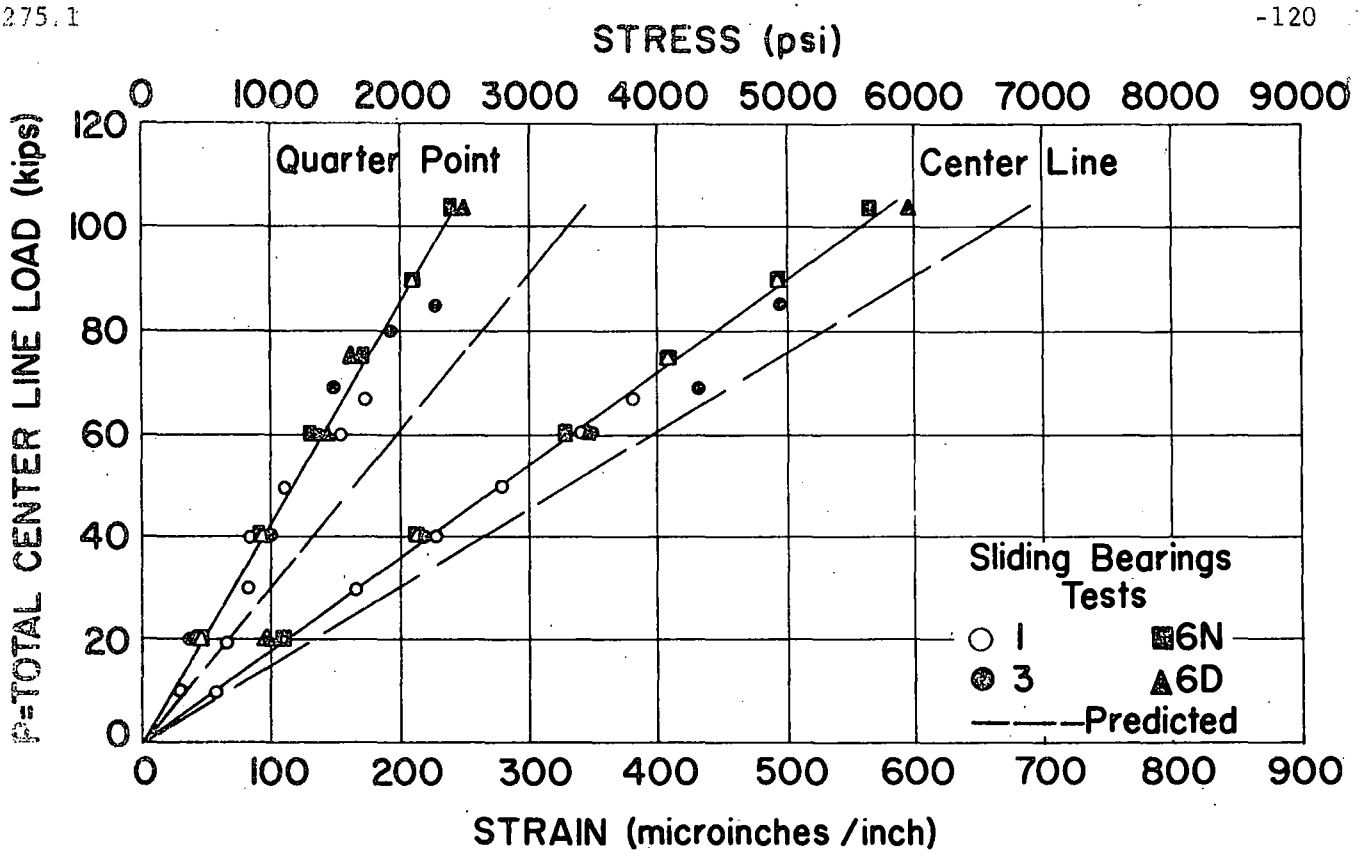

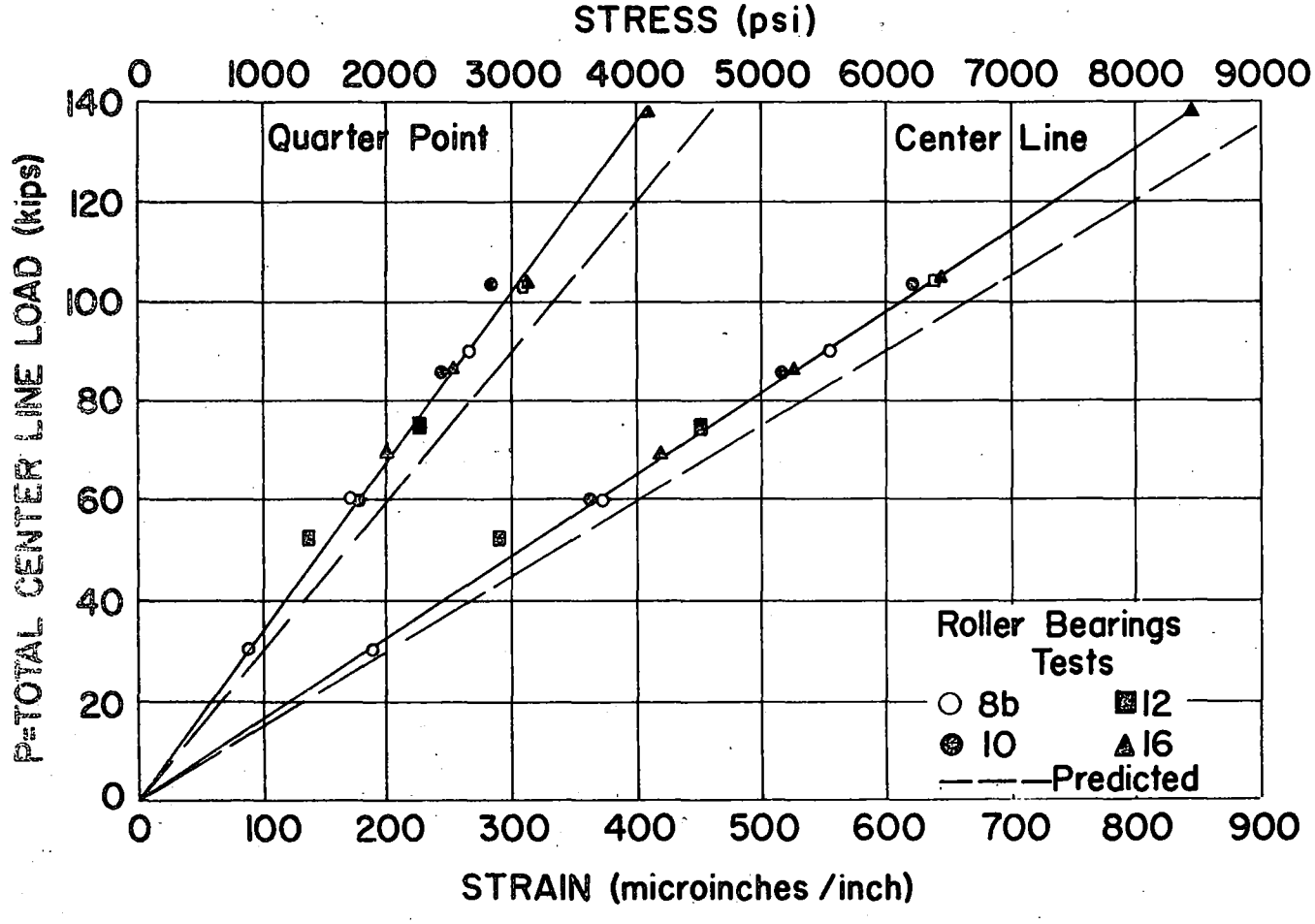

FIG. 37 CONCENTRIC LOAD-STRAIN CURVE FOR LONGITUDINAL MEMBER F

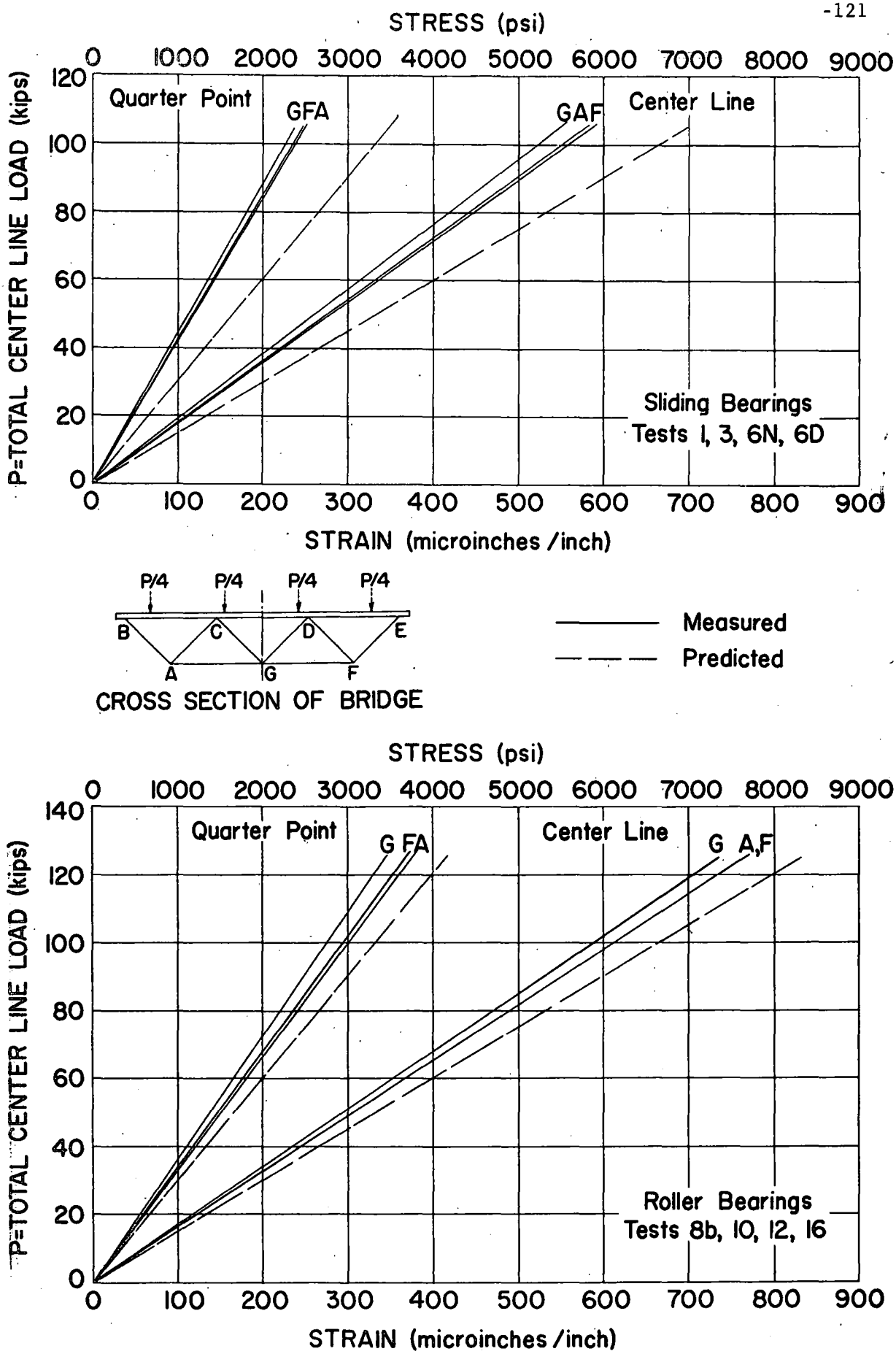

FIG. 38 COMPARISON OF STRAINS IN BOTTOM LONGITUDINAL MEMBERS UNDER CONCENTRIC LOADING

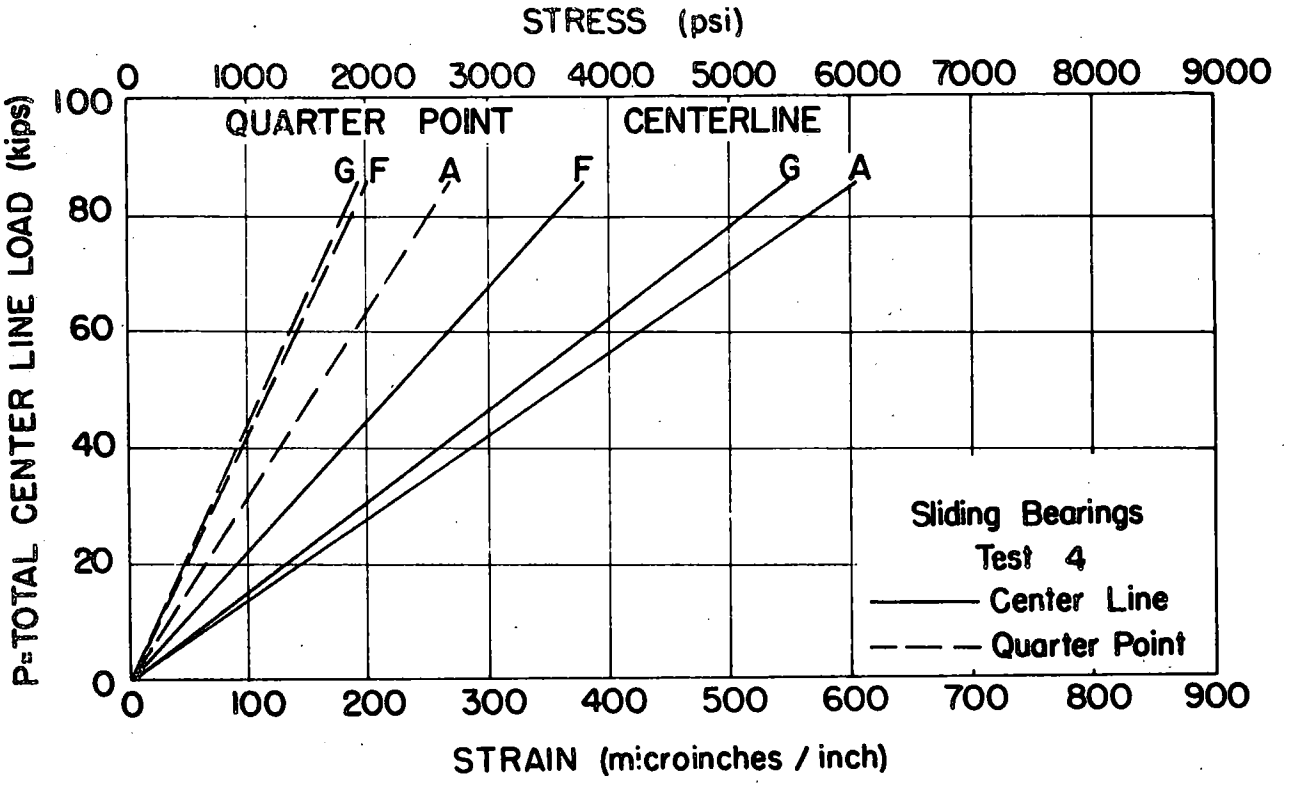

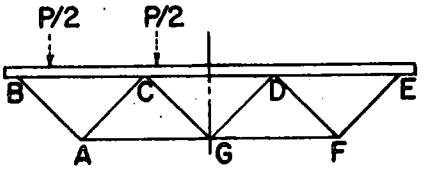

CROSS SECTION

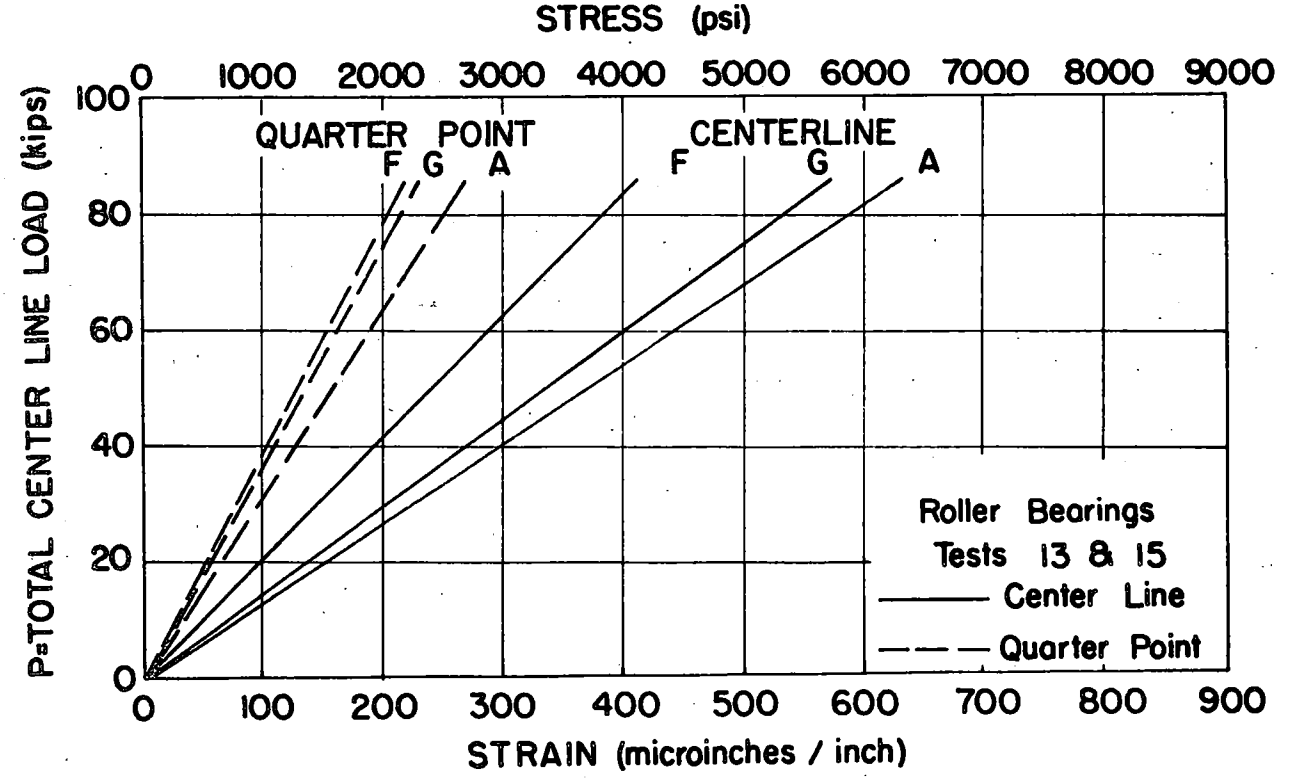

FIG. 39 COMPARISON OF STRAINS IN BOTTOM LONGITUDINAL MEMBERS UNDER ECCENTRIC LOADING

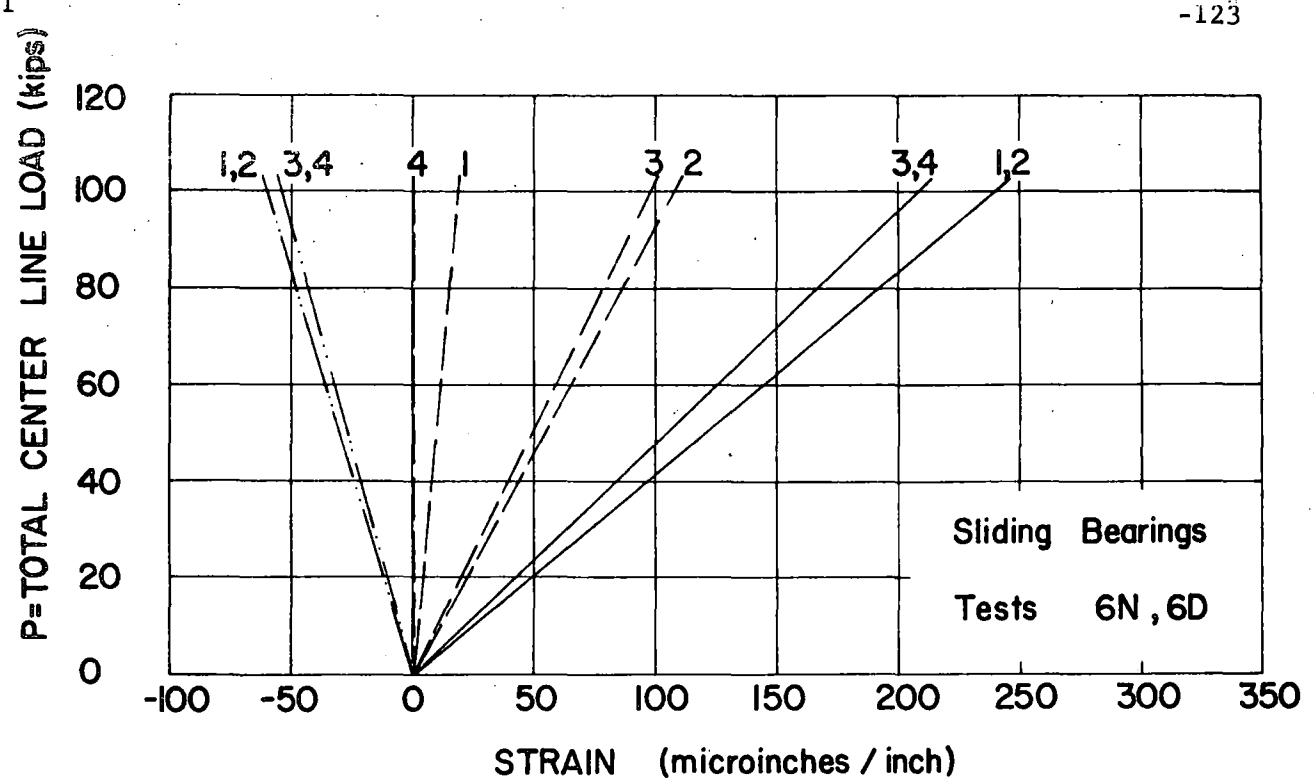

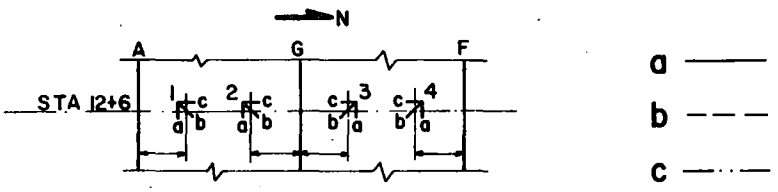

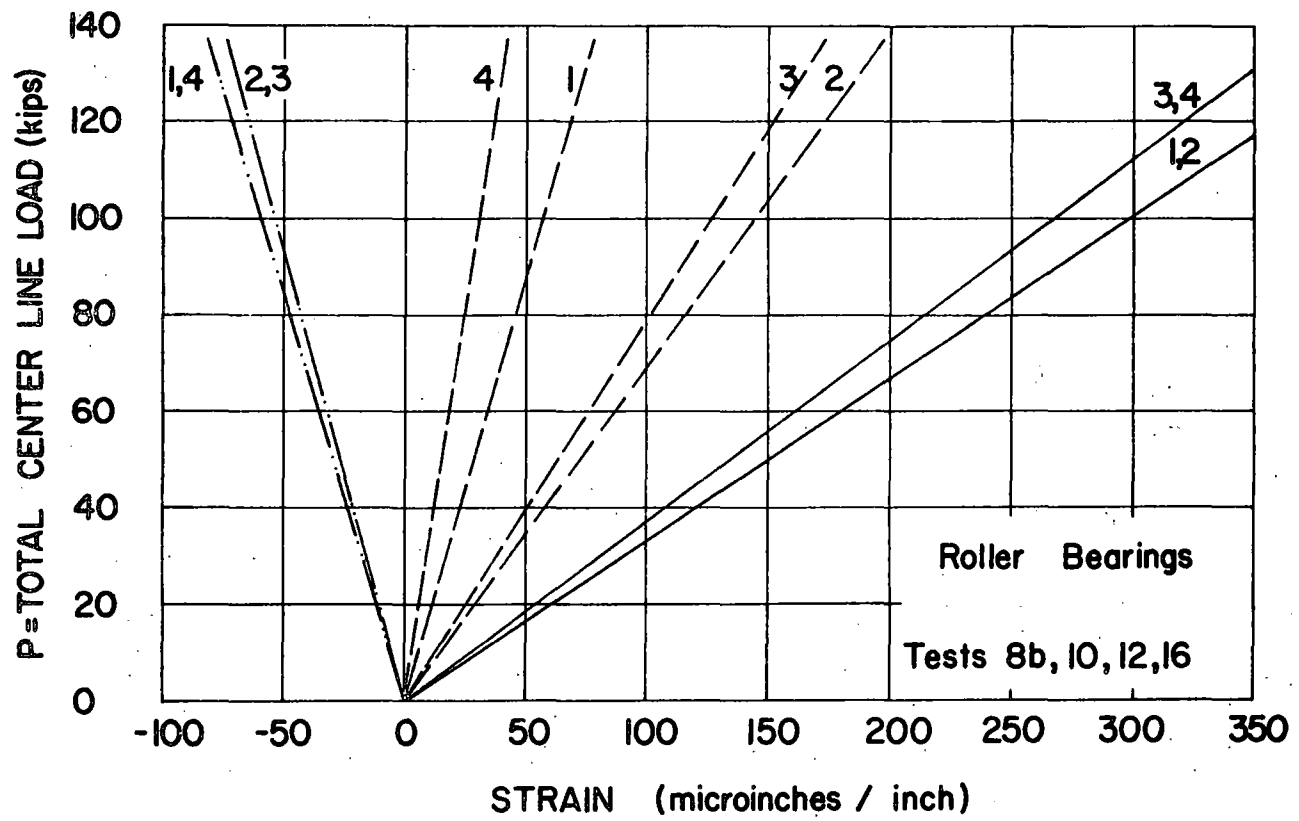

FIG.40 CONCENTRIC LOAD-STRAIN CURVES FOR INDIVIDUAL GAGES OF BOTTOM SHEET ROSETTES

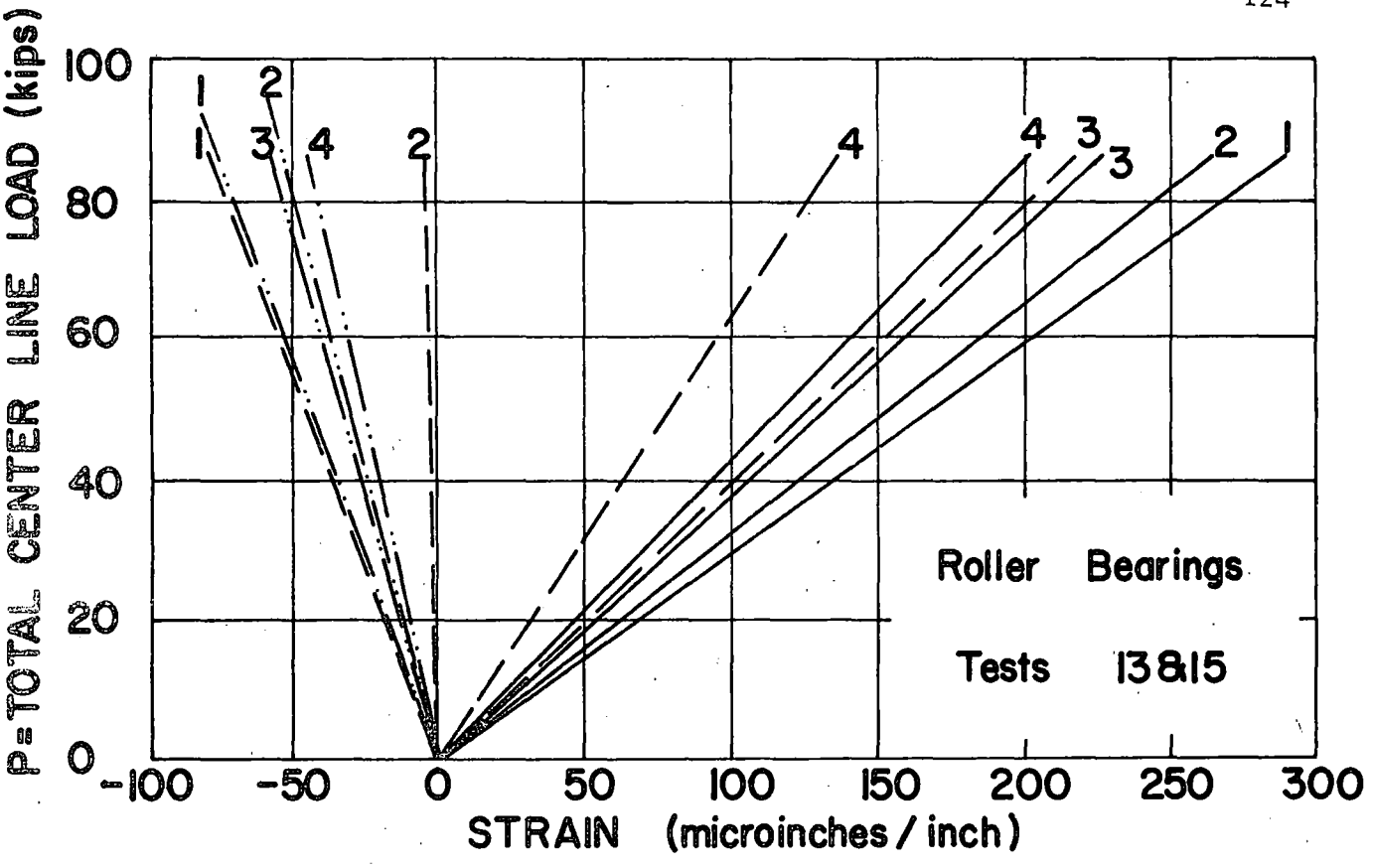

Note: Strain gage readings for test 4 were scattered. Results are not shown.

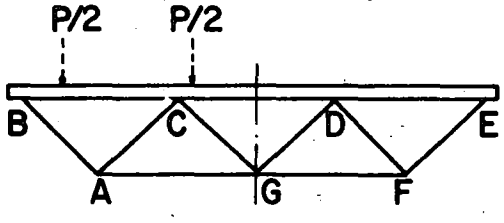

CROSS SECTION

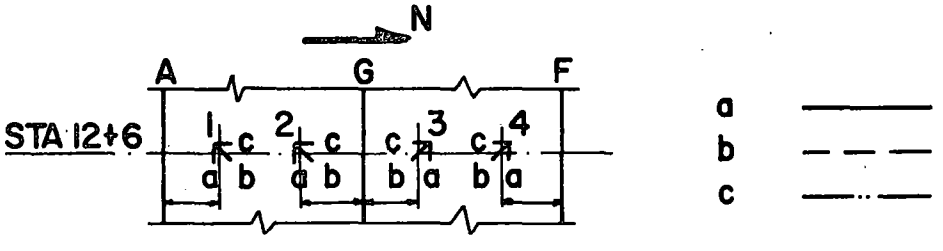

BOTTOM FLANGE SECTION

FIG. 41 ECCENTRIC LOAD-STRAIN CURVES FOR INDIVIDUAL GAGES OF BOTTOM SHEET ROSETTES

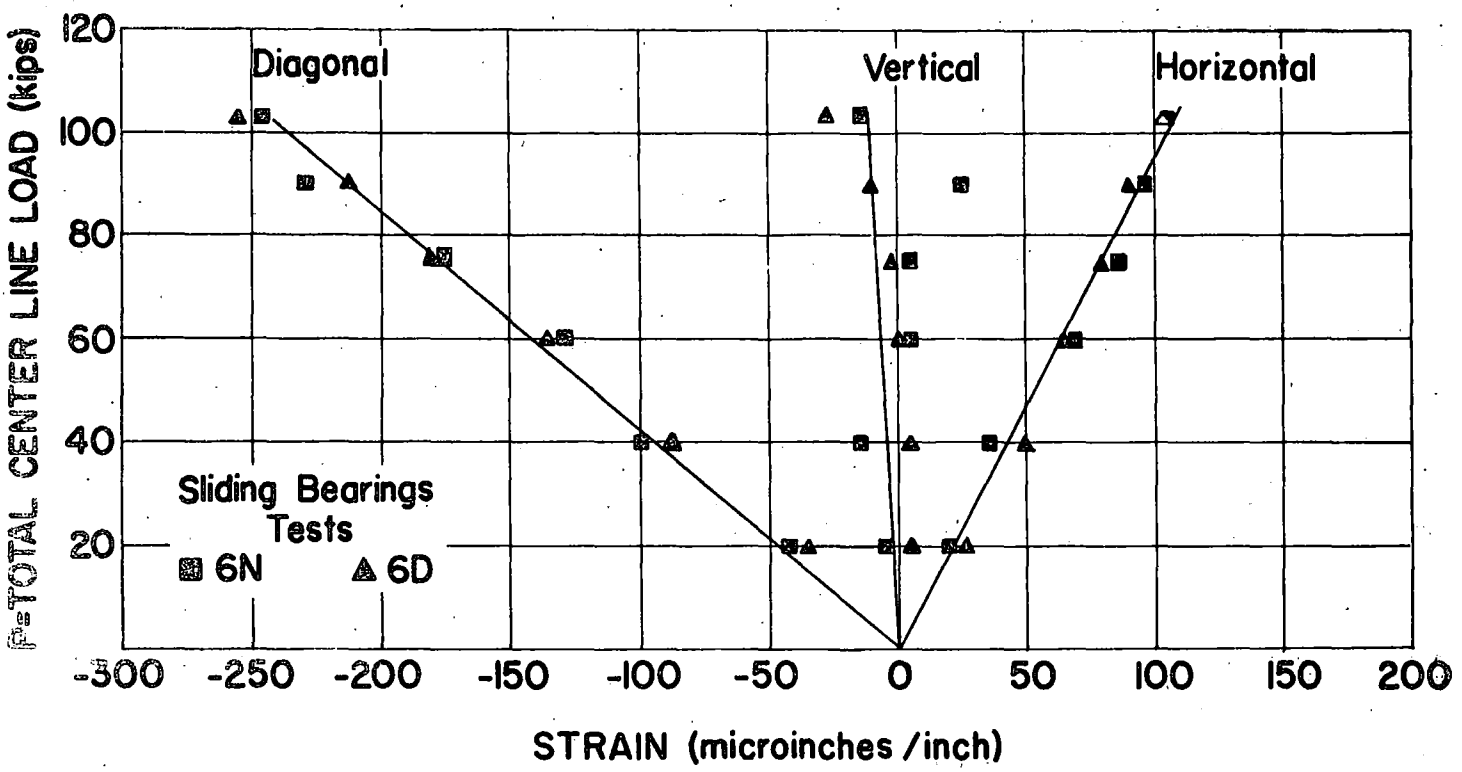

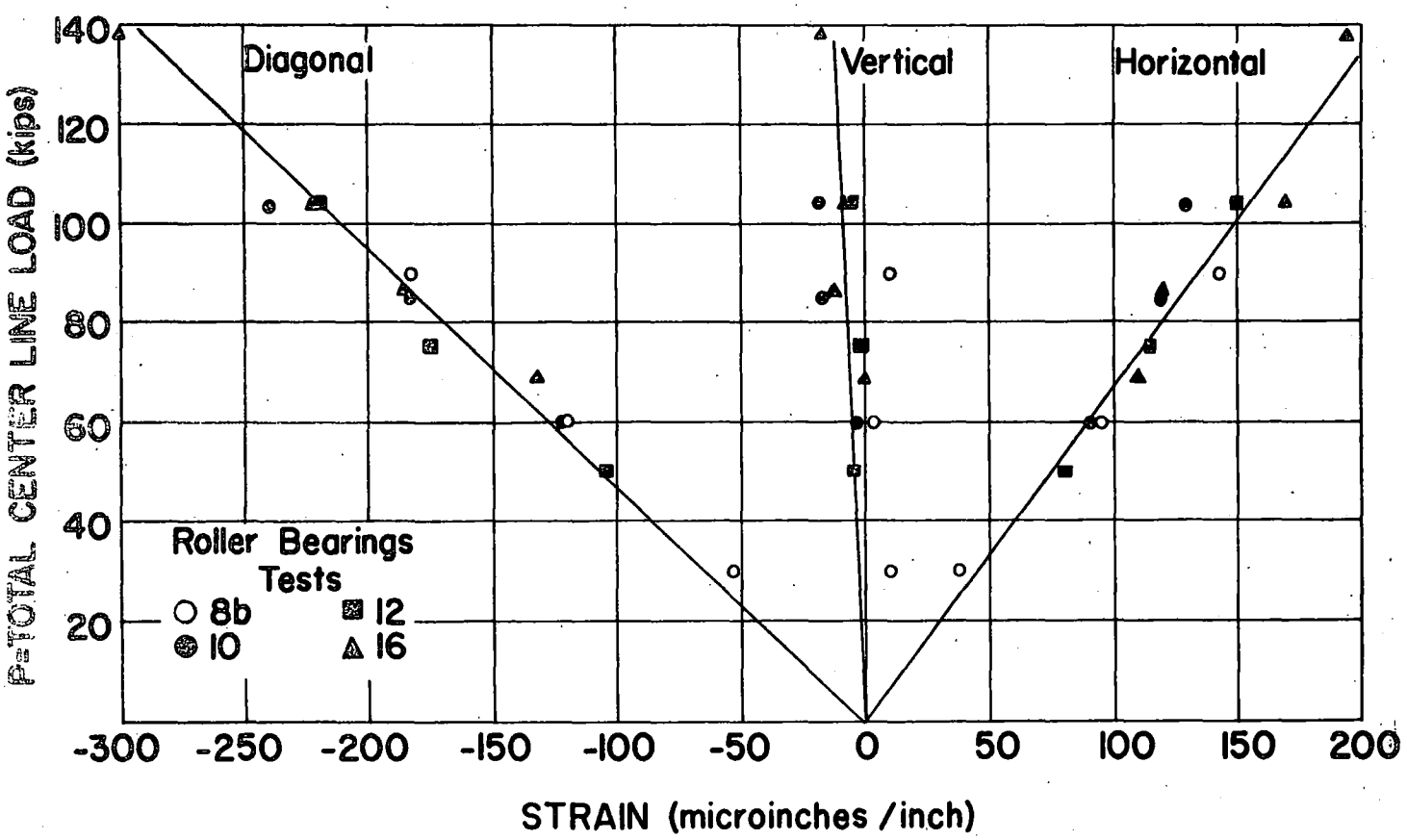

FIG. 42 CONCENTRIC LOAD-STRAIN CURVE FOR INDIVIDUAL GAGES OF ROSETTE ON WEB AB

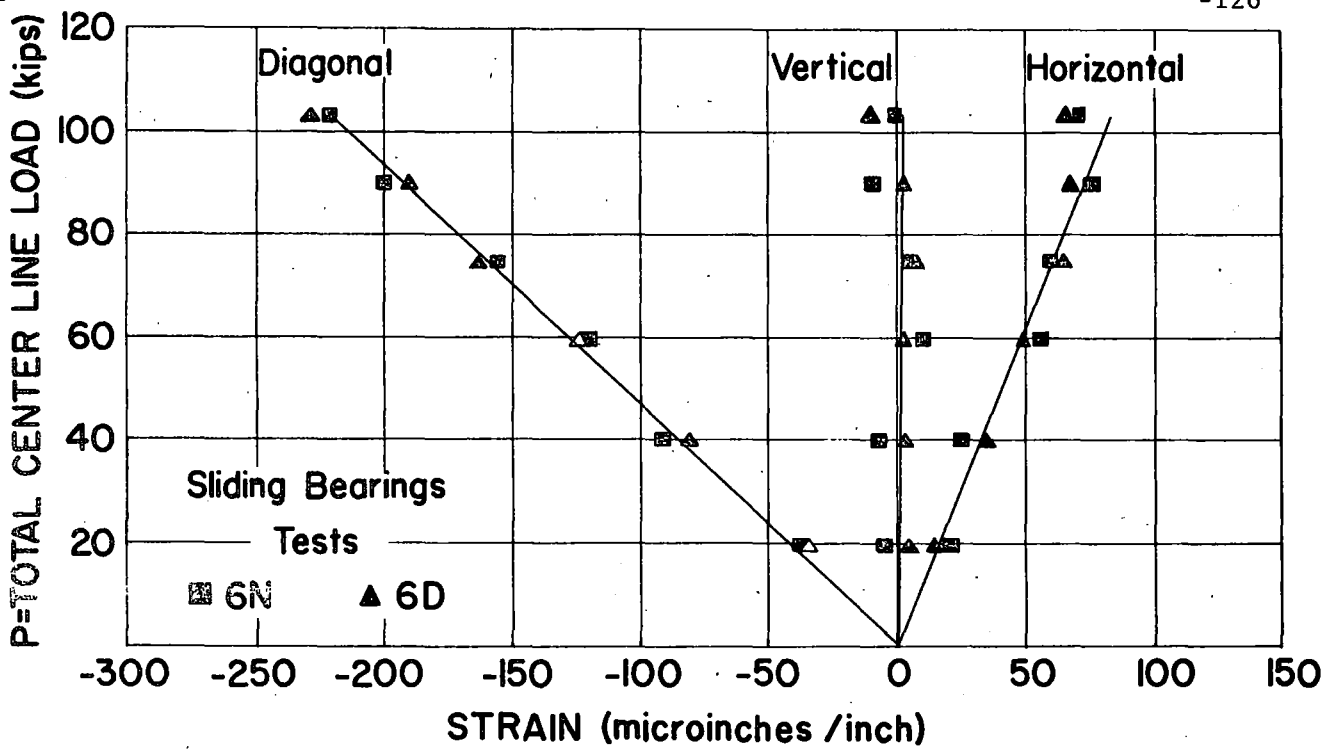

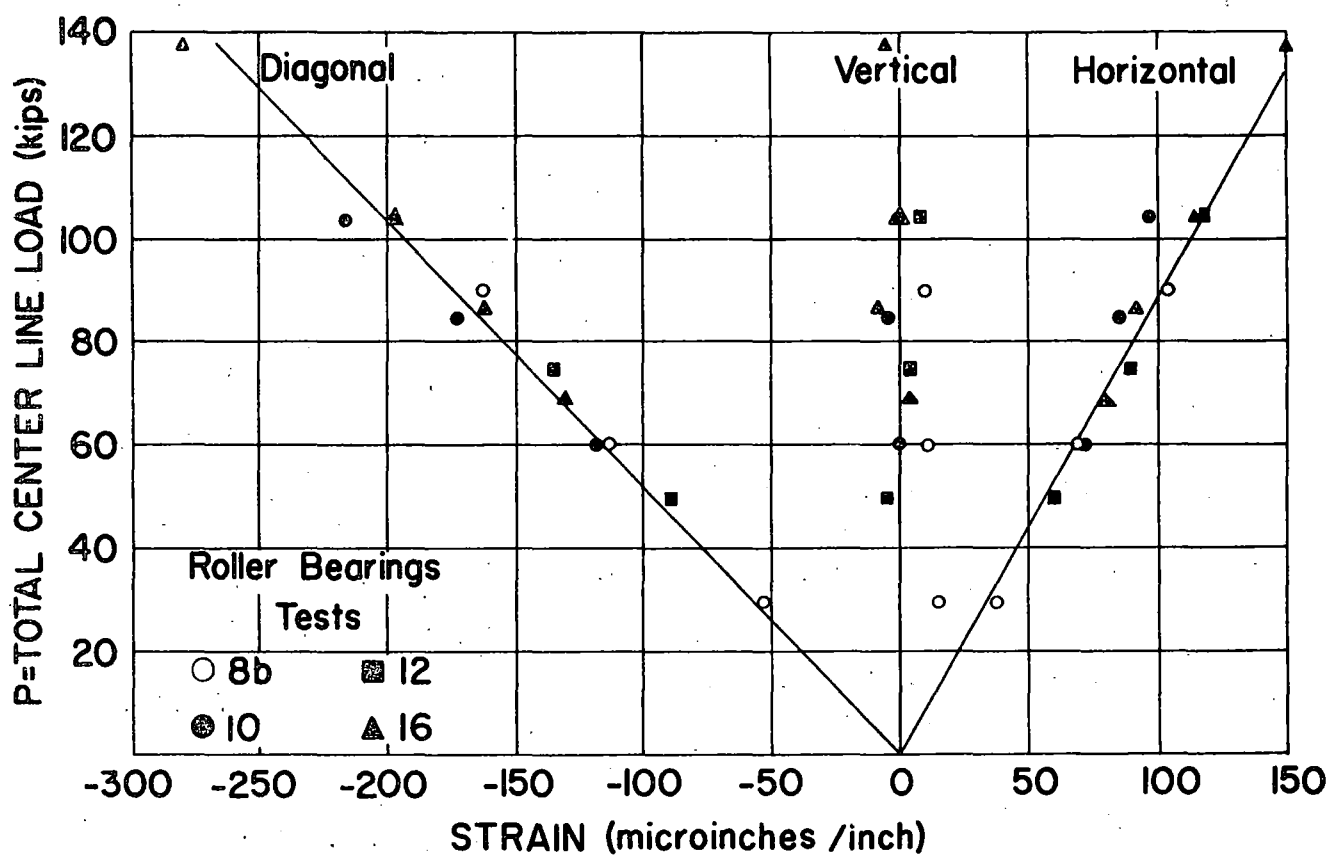

FIG. 43 CONCENTRIC LOAD-STRAIN CURVE FOR INDIVIDUAL GAGES OF ROSETTE ON WEB AC

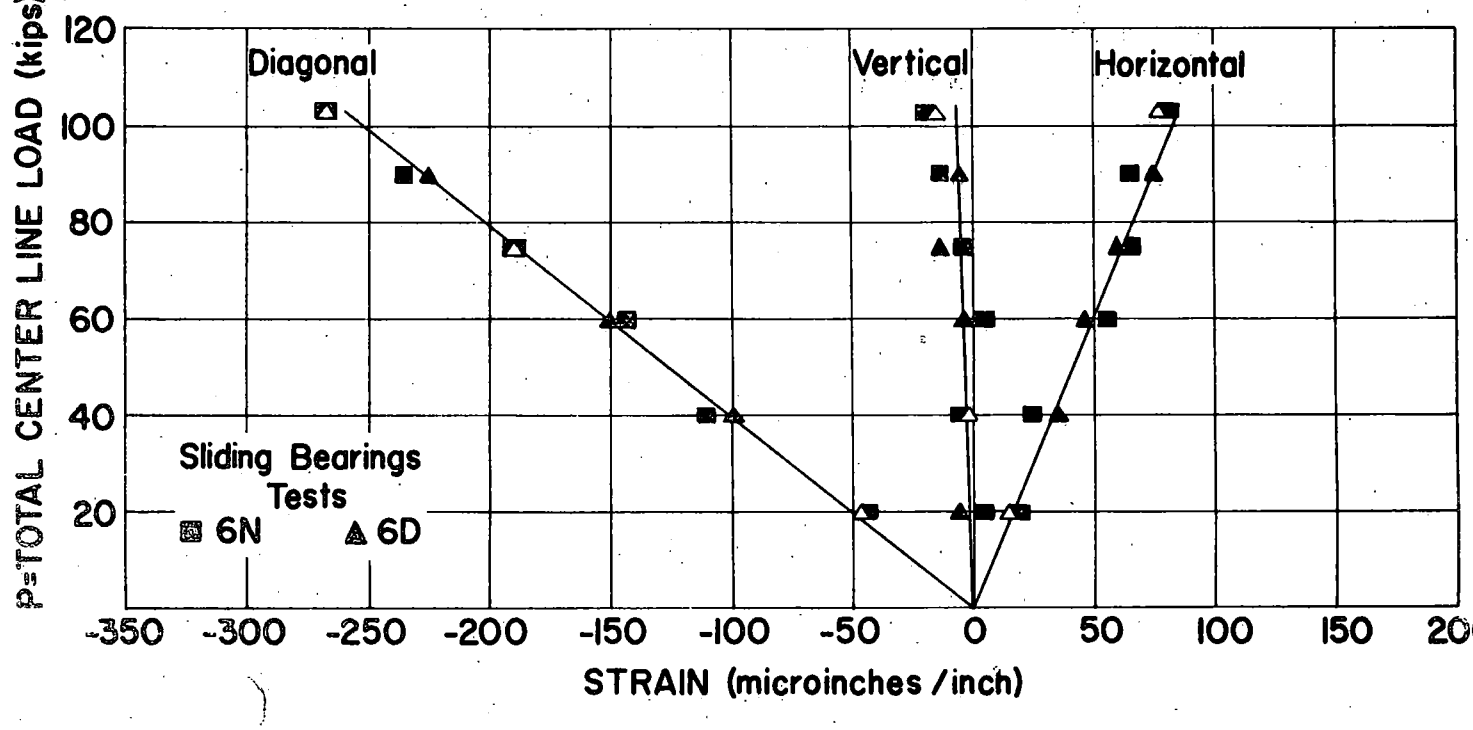

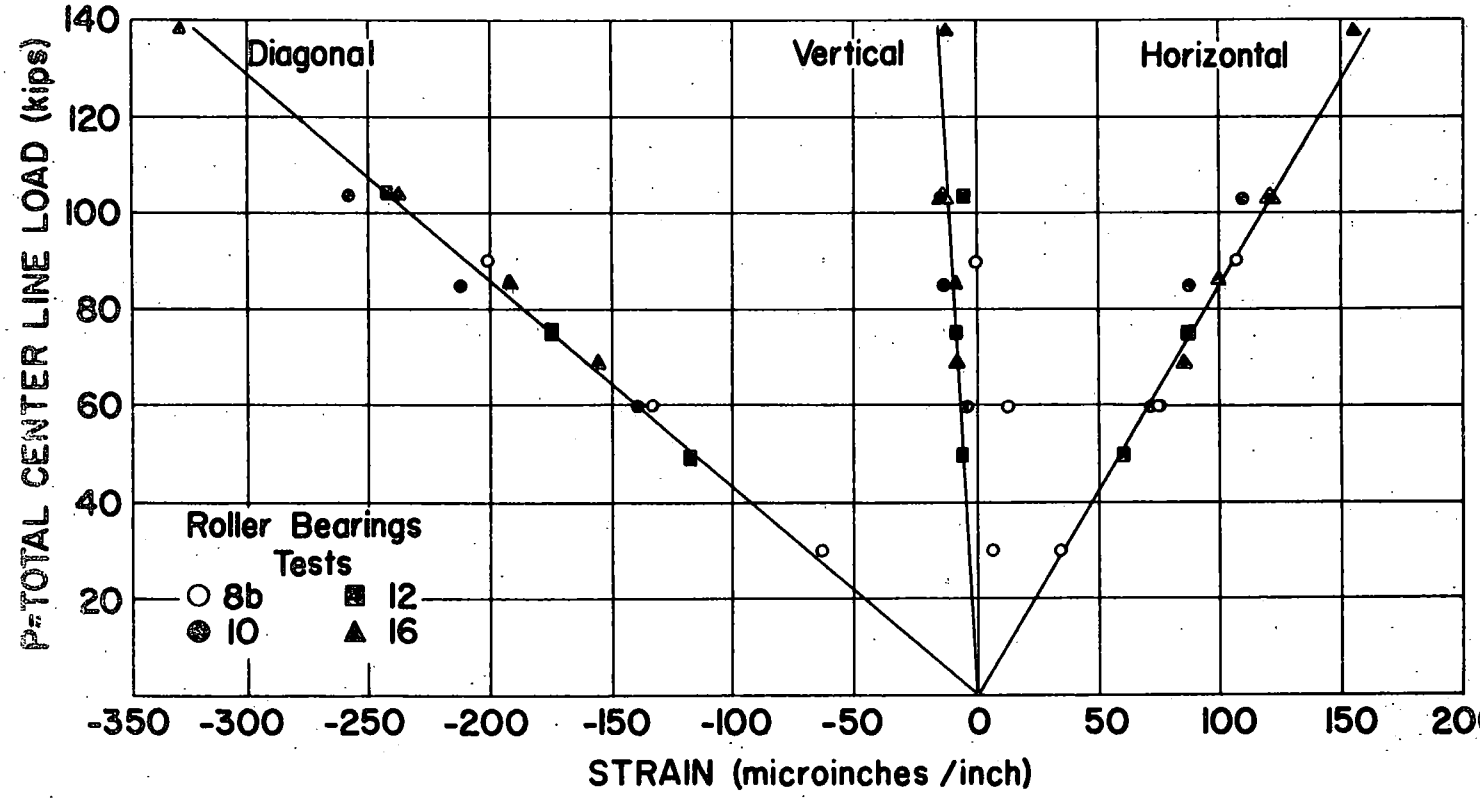

FIG. 44 CONCENTRIC LOAD-STRAIN CURVE FOR INDIVIDUAL GAGES OF ROSETTE ON WEB GC

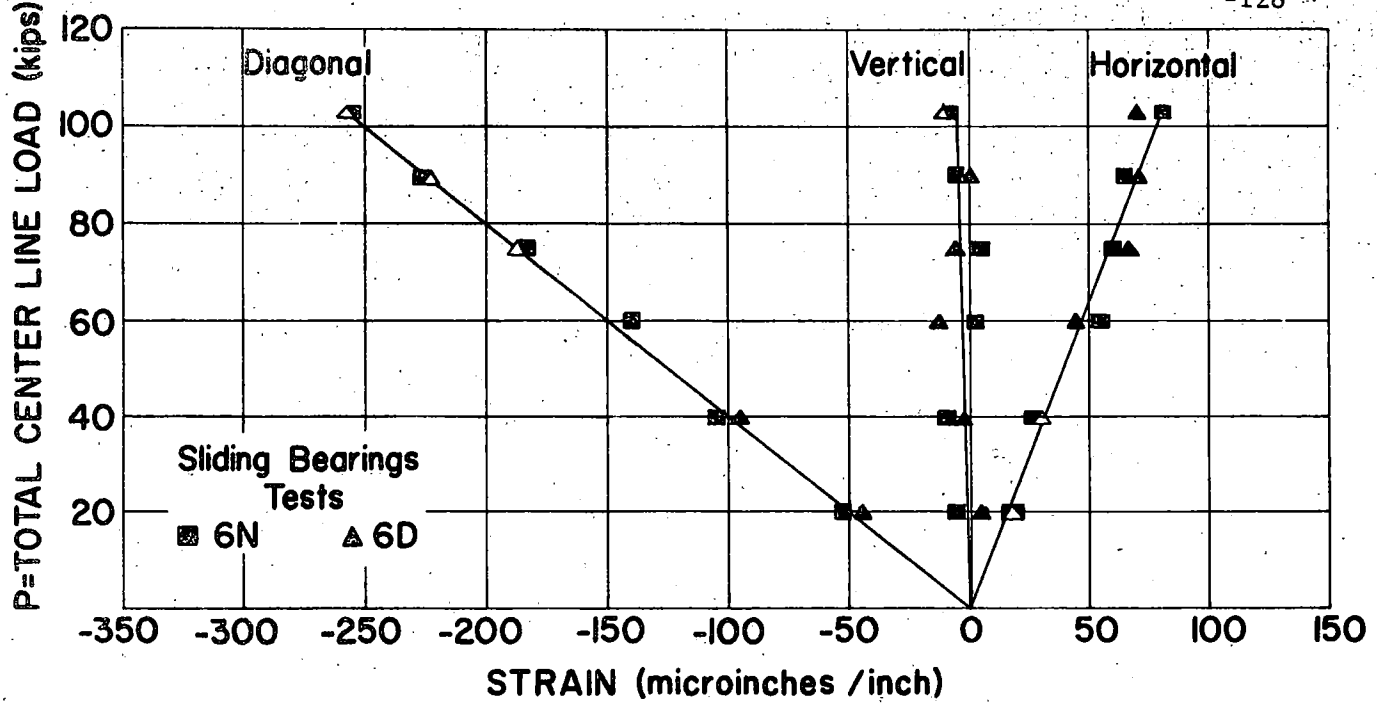

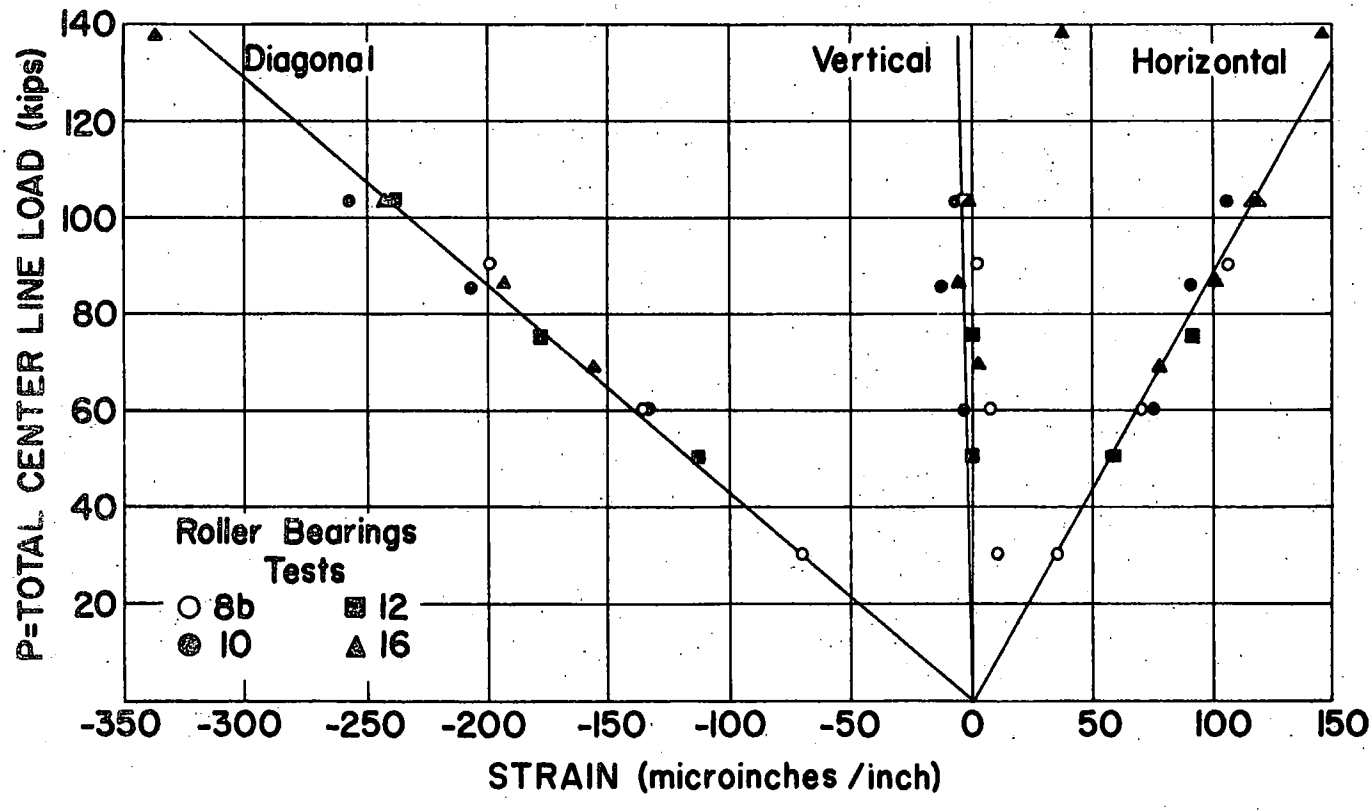

FIG. 45 CONCENTRIC LOAD-STRAIN CURVE FOR INDIVIDUAL GAGES OF ROSETTE ON WEB GD

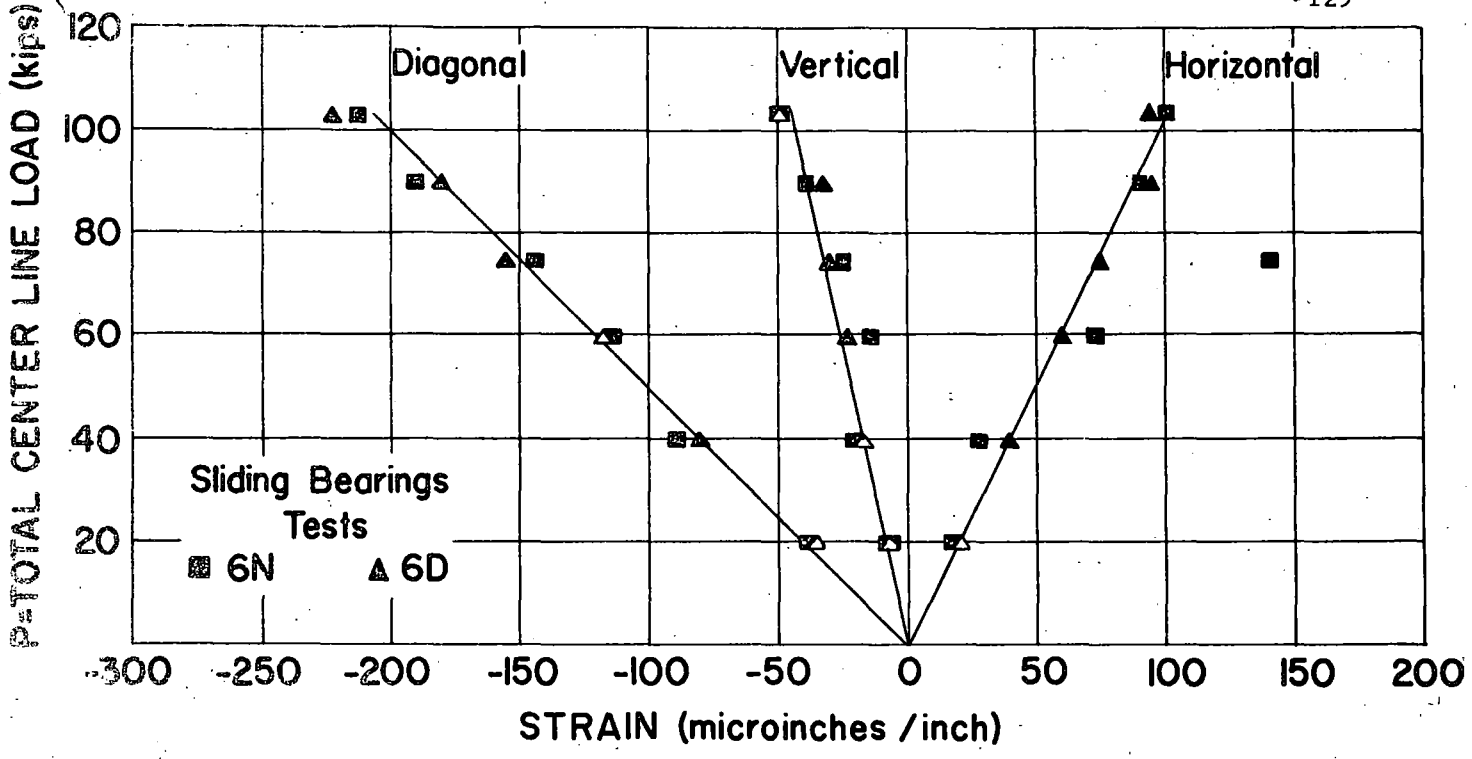

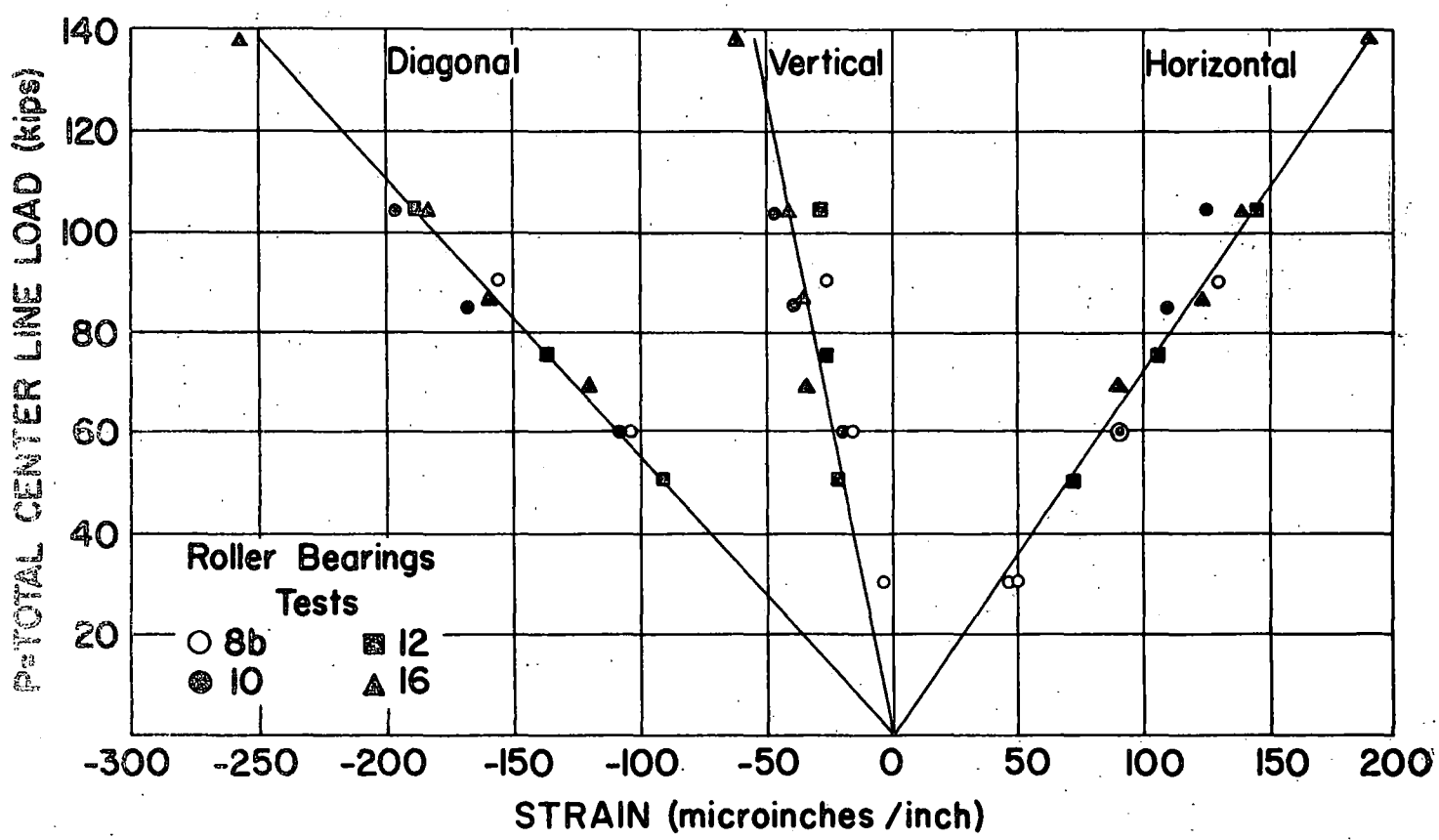

FIG. 46 CONCENTRIC LOAD-STRAIN CURVE FOR INDIVIDUAL GAGES OF ROSETTE ON WEB FD

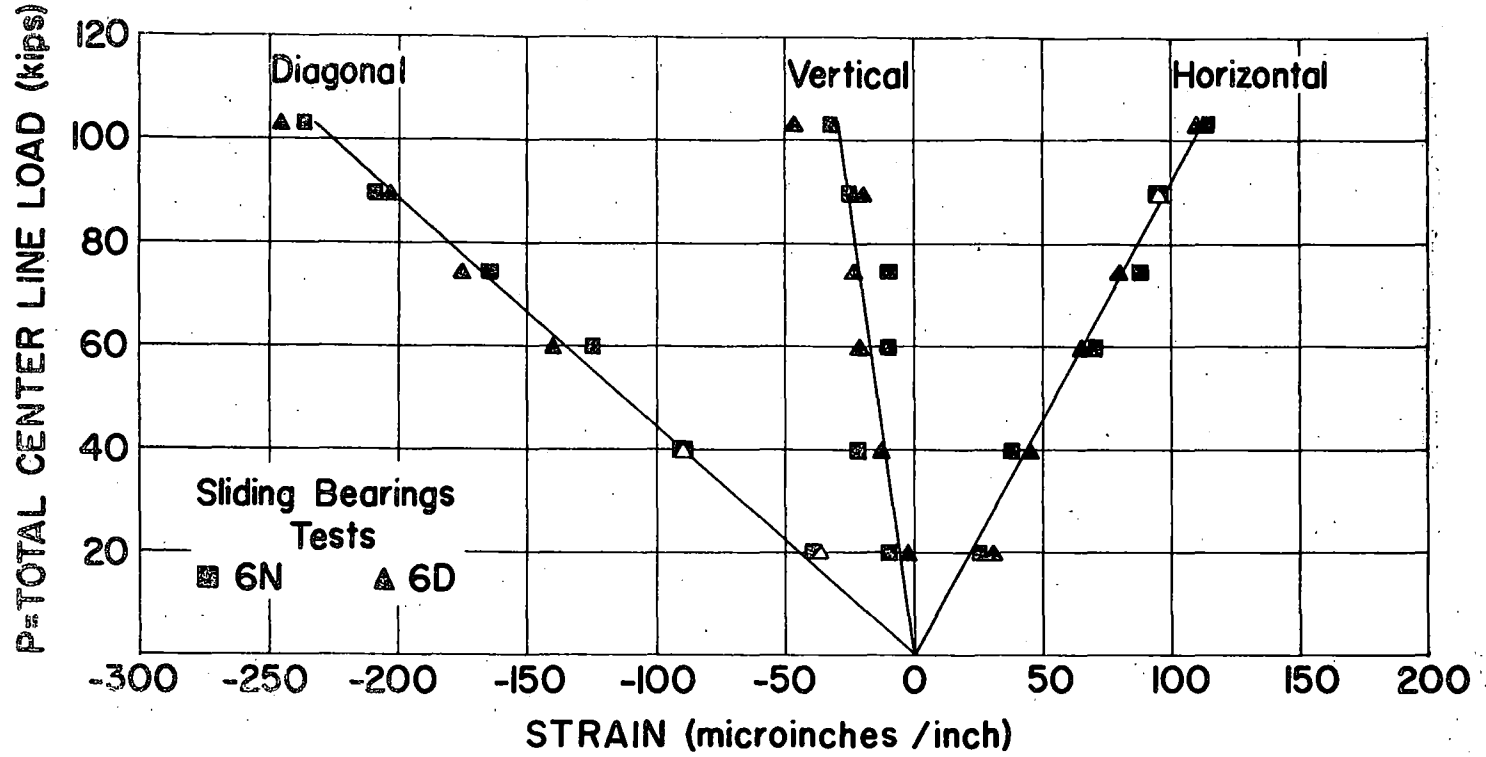

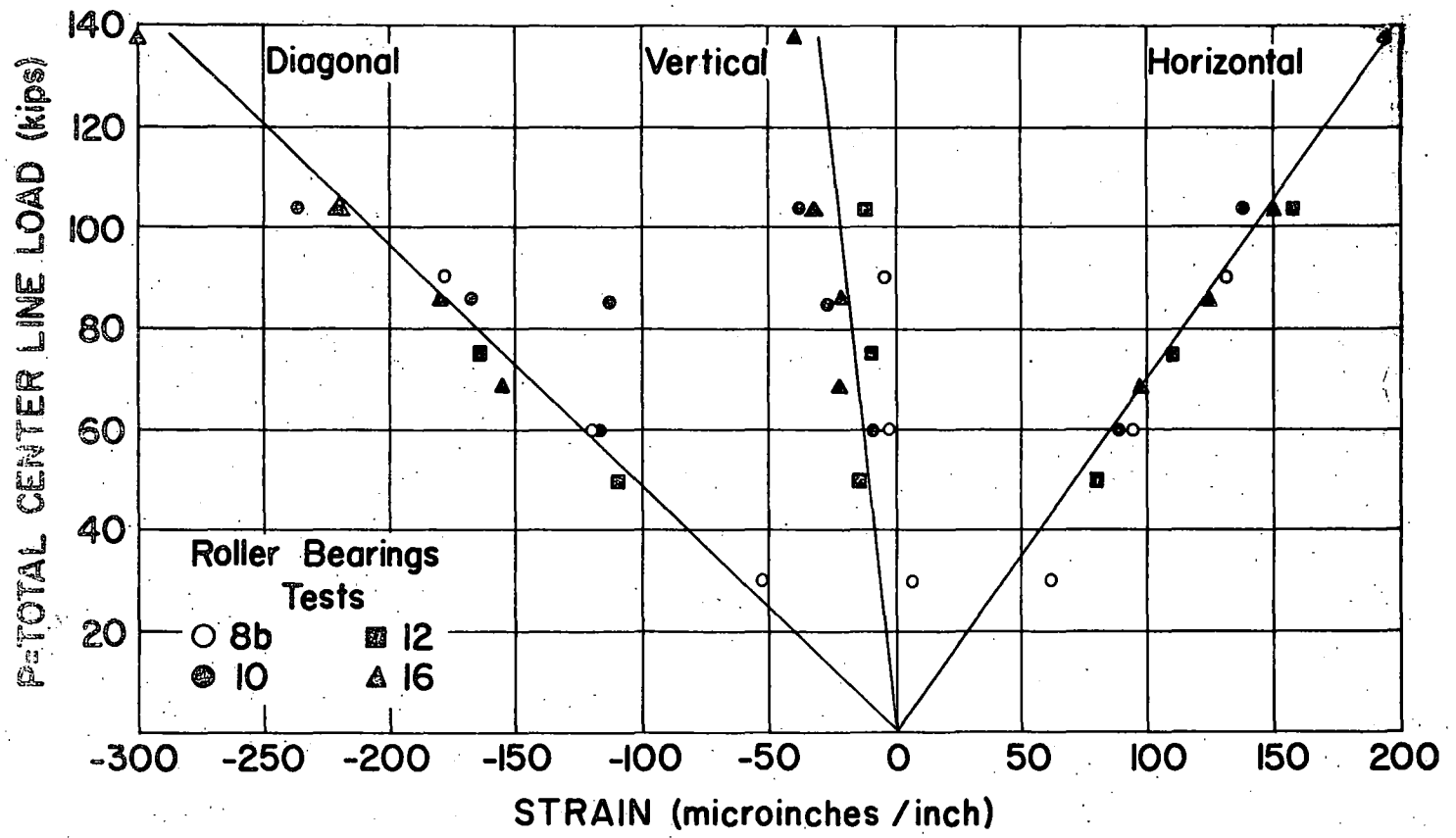

FIG. 47 CONCENTRIC LOAD-STRAIN CURVE FOR INDIVIDUAL GAGES OF ROSETTE ON WEB FE

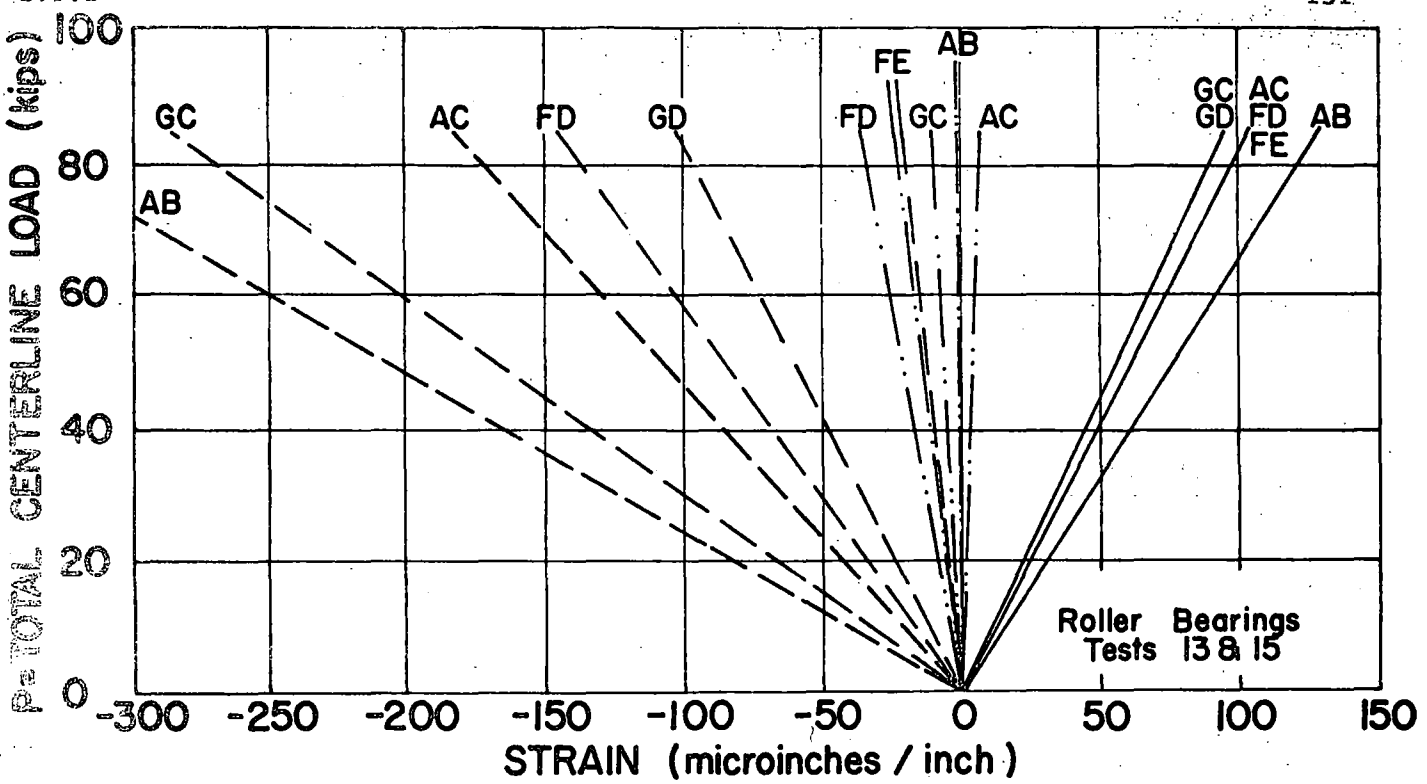

Note: Strain gage readings for test 4 were scattered. Results are not shown.

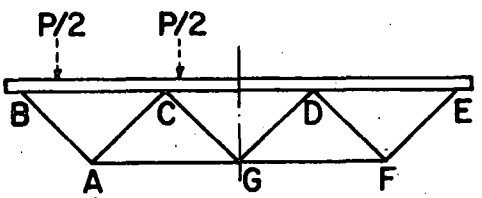

BRIDGE CROSS SECTION

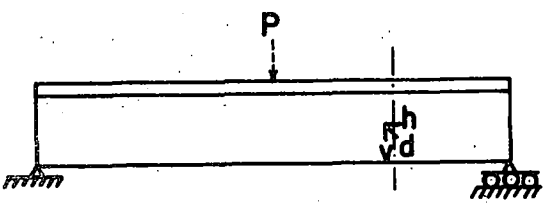

h = HORIZONTAL
d = DIAGONAL
v = VERTICAL

GAGE ORIENTATION

FIG. 48 ECCENTRIC LOAD-STRAIN CURVES FOR INDIVIDUAL GAGES OF WEB ROSETTES

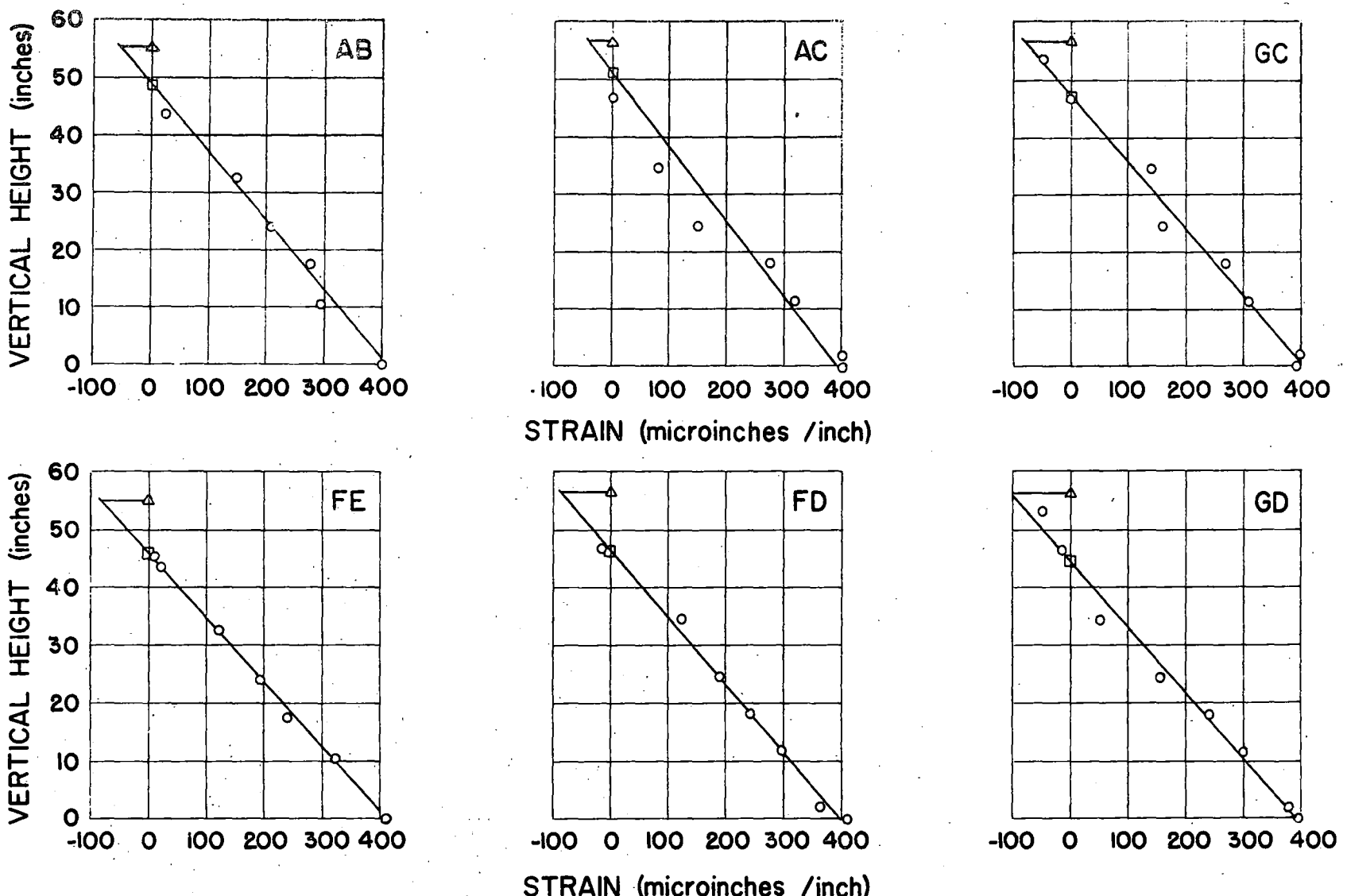

Gage at "0" height located on bottom longitudinal member

Loads: Moment=10,300,000 inch-pounds
Shear =69,000 pounds

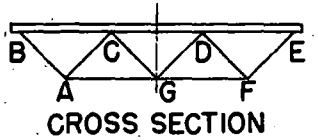

CROSS SECTION

○ Test Points
□ Neutral axis location for section through web
△ Deck Surface

FIG. 49 VERTICAL STRAIN DISTRIBUTION AT QUARTER POINT CROSS SECTION

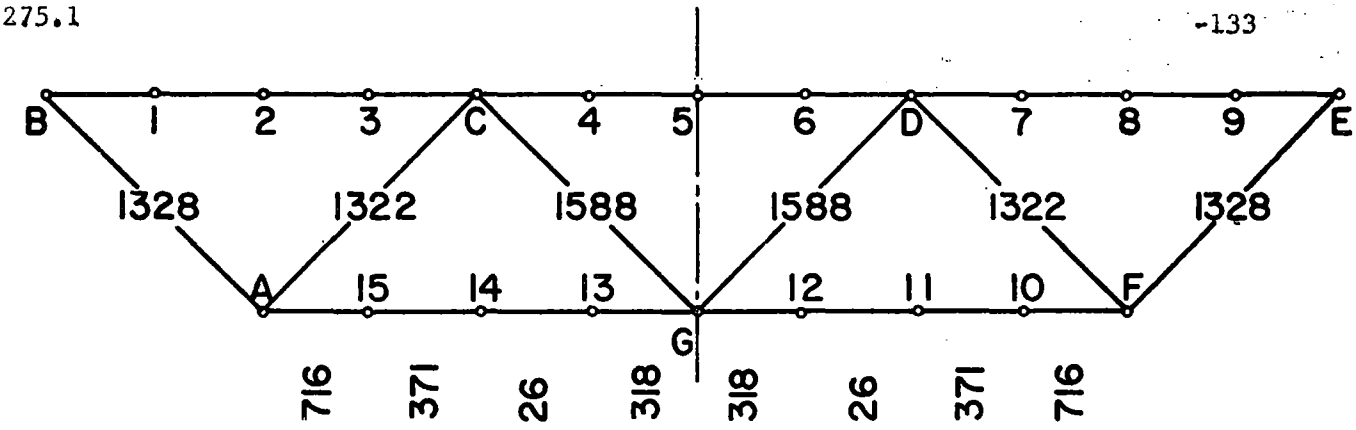

PREDICTED SHEAR STRESSES (psi) V_z = 34,500 lbs.

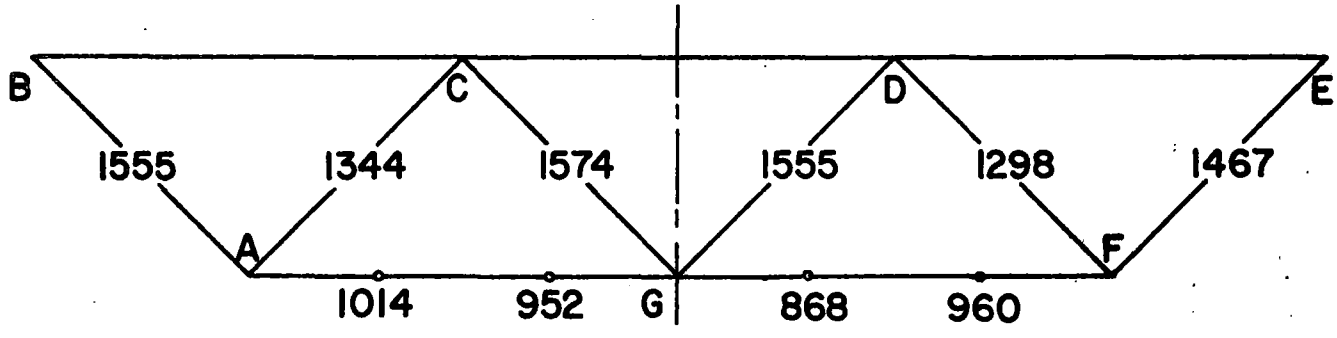

MEASURED SHEAR STRESSES (psi) G = 3.84 x 10^6 psi

(Scale 1/40)

FIG. 50 COMPARISON OF PREDICTED AND MEASURED SHEAR STRESSES FOR CONCENTRIC TEST LOADING

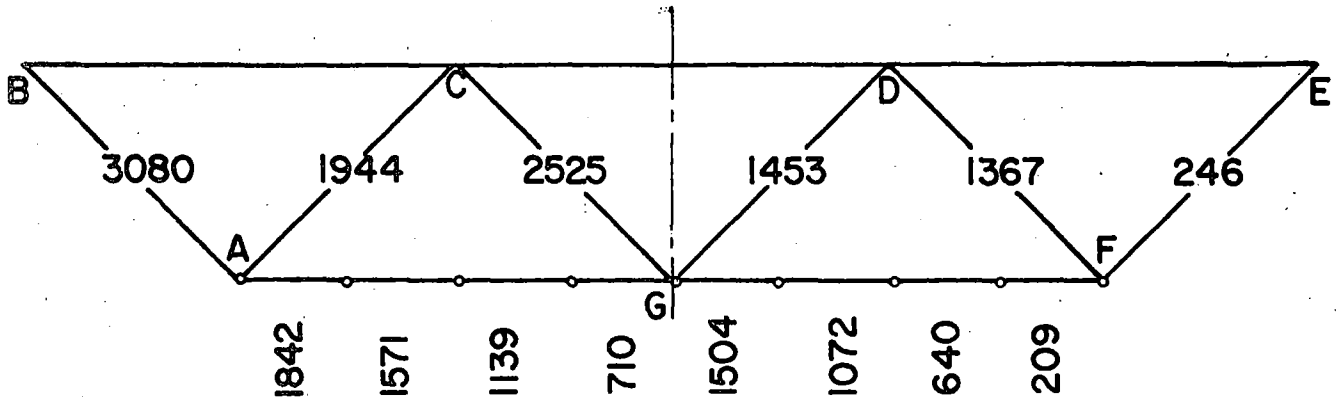

PREDICTED SHEAR STRESSES (psi)

(V_z = 43,200 and T = 3.11 x 10^6 in-lb)

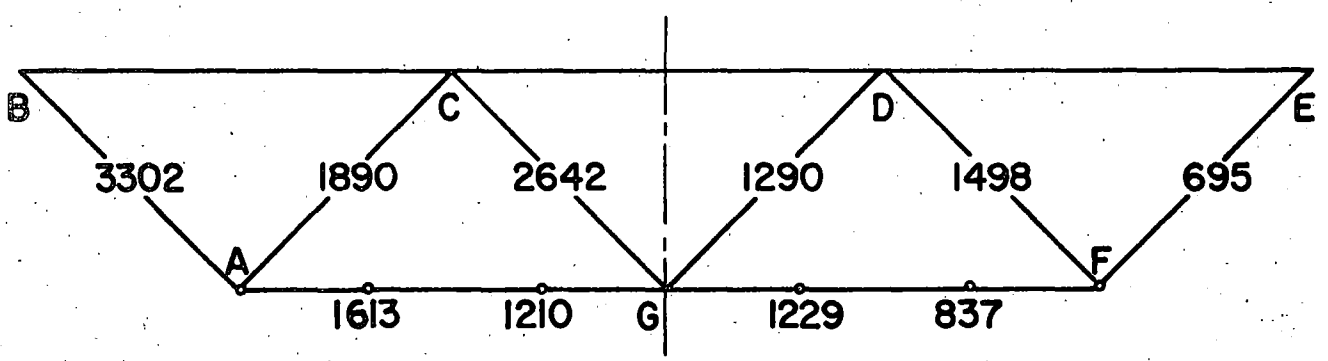

MEASURED SHEAR STRESSES (psi)

(Scale 1/40) (G= 3.84 x 10^6 psi)

FIG. 51 COMPARISON OF PREDICTED AND MEASURED SHEAR STRESSES FOR MAXIMUM ECCENTRIC LOADING

CONCENTRIC LOADING

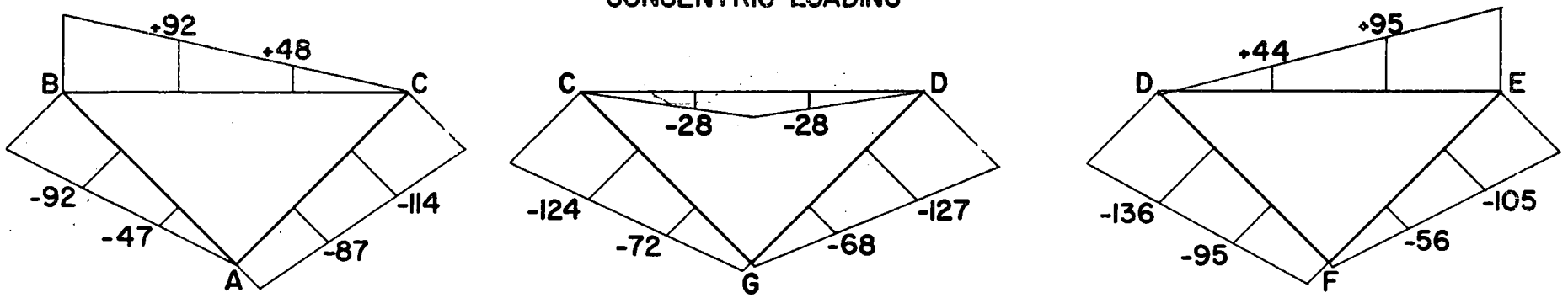

ECCENTRIC LOADING

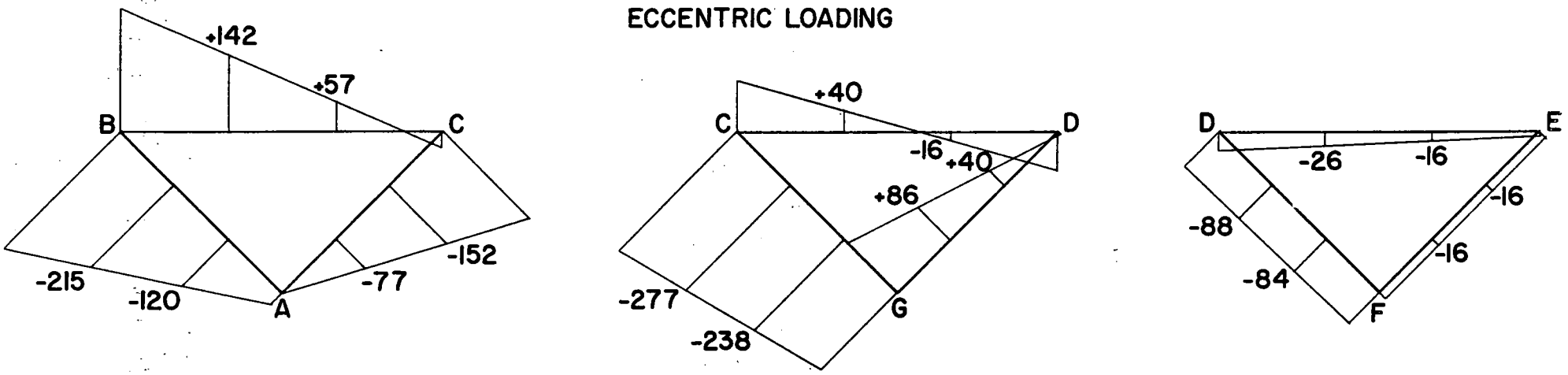

Applied Load=69 Kips at Center Line

Scales: 1 unit=200 microinches / inch for strains

1 inch=30 inches for lengths

0 units 1

(+) Tension

(-) Compression

FIG. 52 STRAIN DISTRIBUTION IN CENTER LINE FRAME

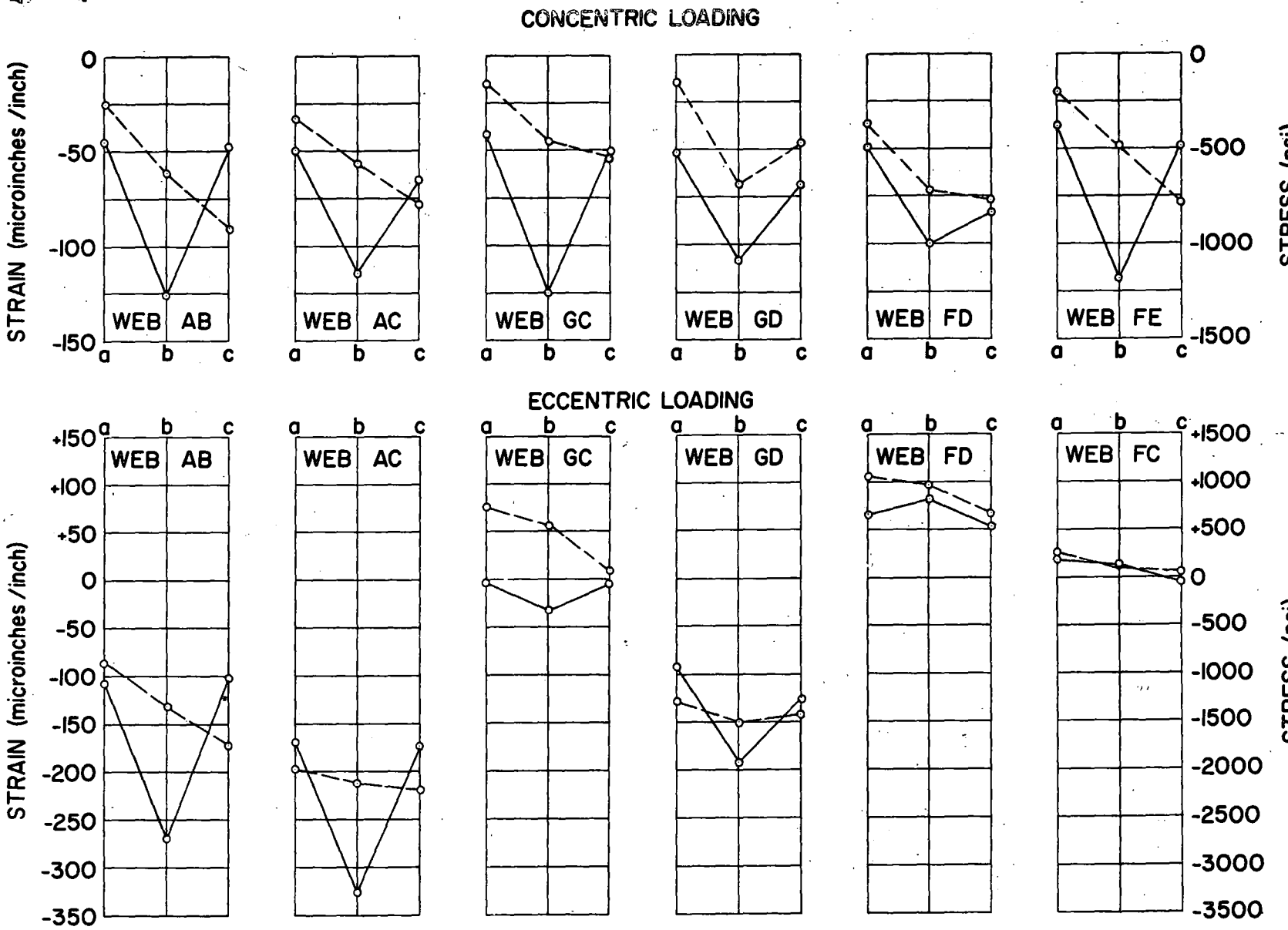

FIG. 53 STRAIN DISTRIBUTION IN DIAGONAL MEMBERS OF END FRAME

Predicted Natural Frequency=400 cycles per minute

Chart Speed=25 millimeters per second

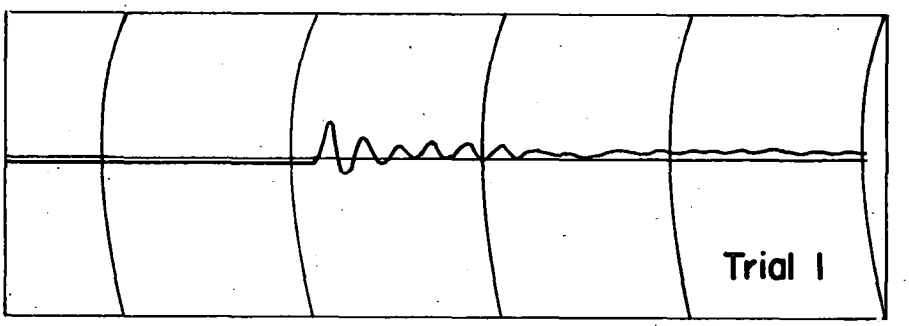

Natural Frequency=329 cycles per minute

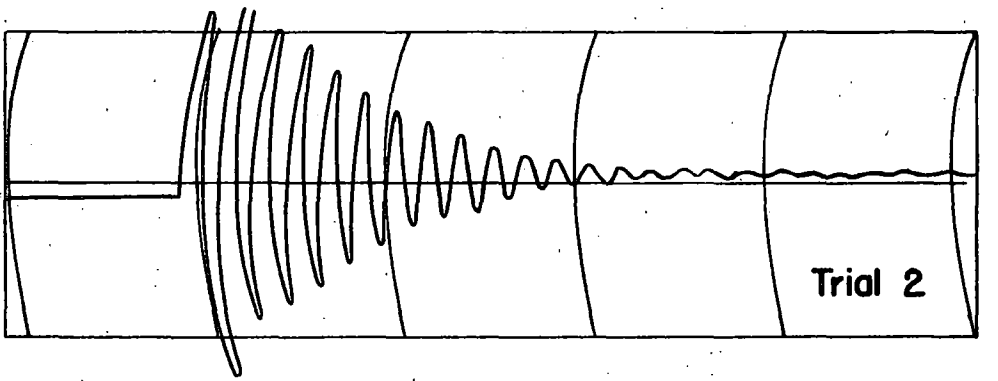

Natural Frequency=329 cycles per minute

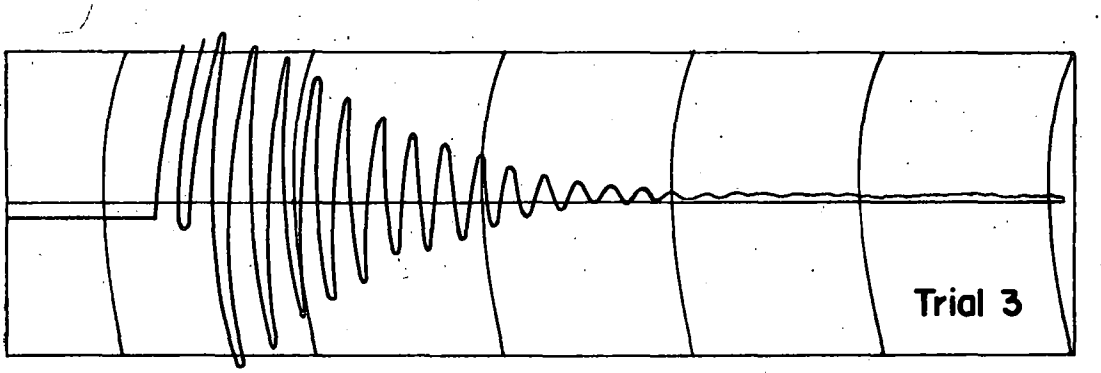

Natural Frequency=336 cycles per minute

FIG. 54 RECORDINGS OF FREQUENCY RESPONSE

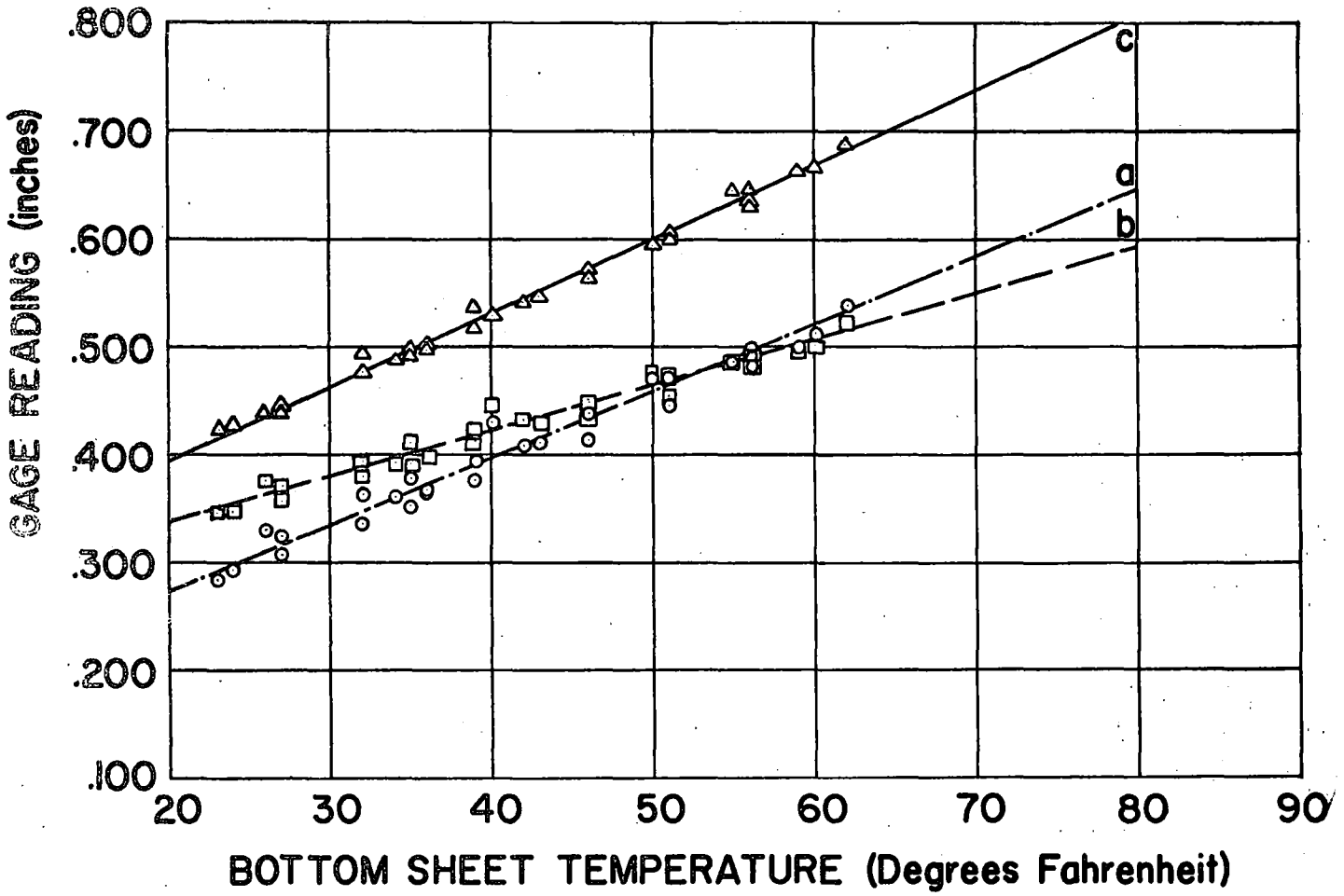

GAGE LOCATIONS

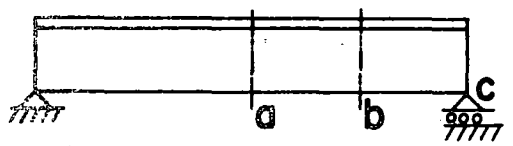

a. Center Line Deflection ○

b. Quarter Point Deflection □

c. End Movement △

SLOPES

(inches /degree Fahrenheit)

a.	.0062
b.	.0042
c.	.0068

FIG. 55 TEMPERATURE-DEFLECTION OBSERVATIONS OF UNLOADED SPAN

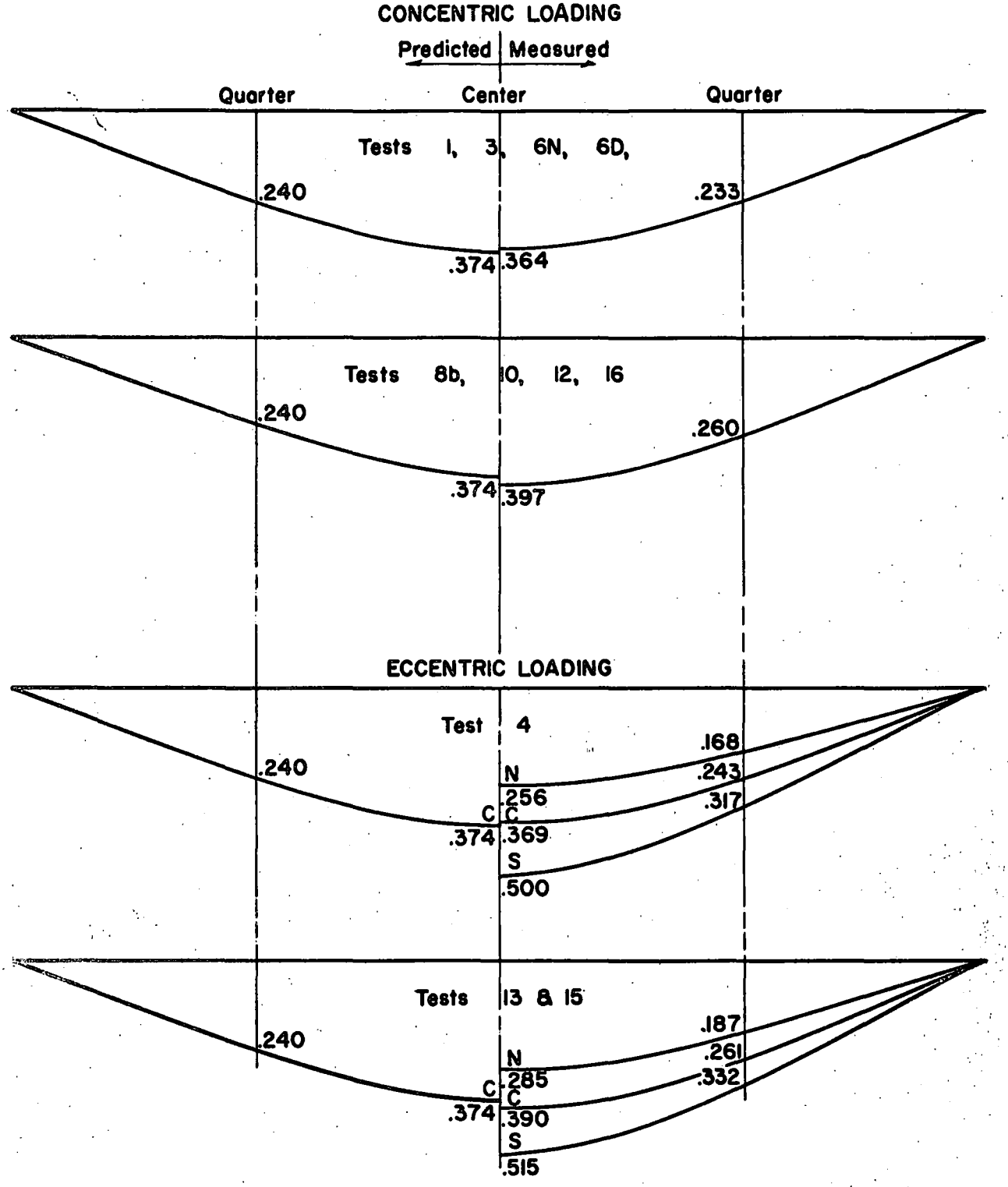

FIG. 56 COMPARISON OF MEASURED AND PREDICTED DEFLECTIONS FOR AN APPLIED CENTER LINE LOAD OF 69,000 LBS.

FIG. 57 OVERALL VIEW OF SPAN AFTER FAILURE

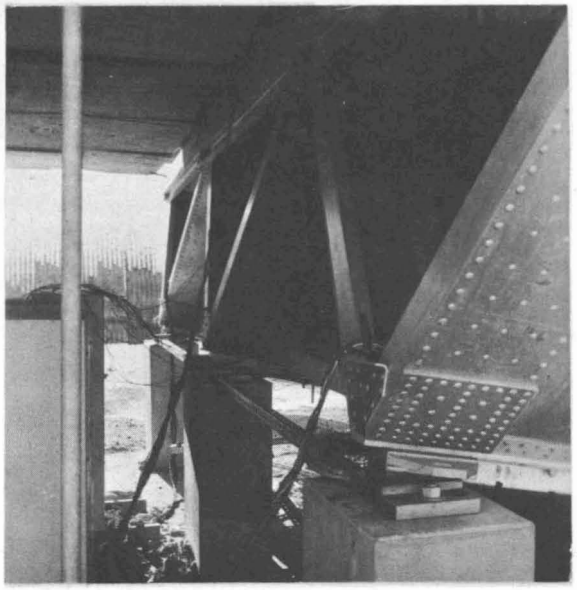

FIG. 58
FREE END OF BRIDGE AFTER FAILURE

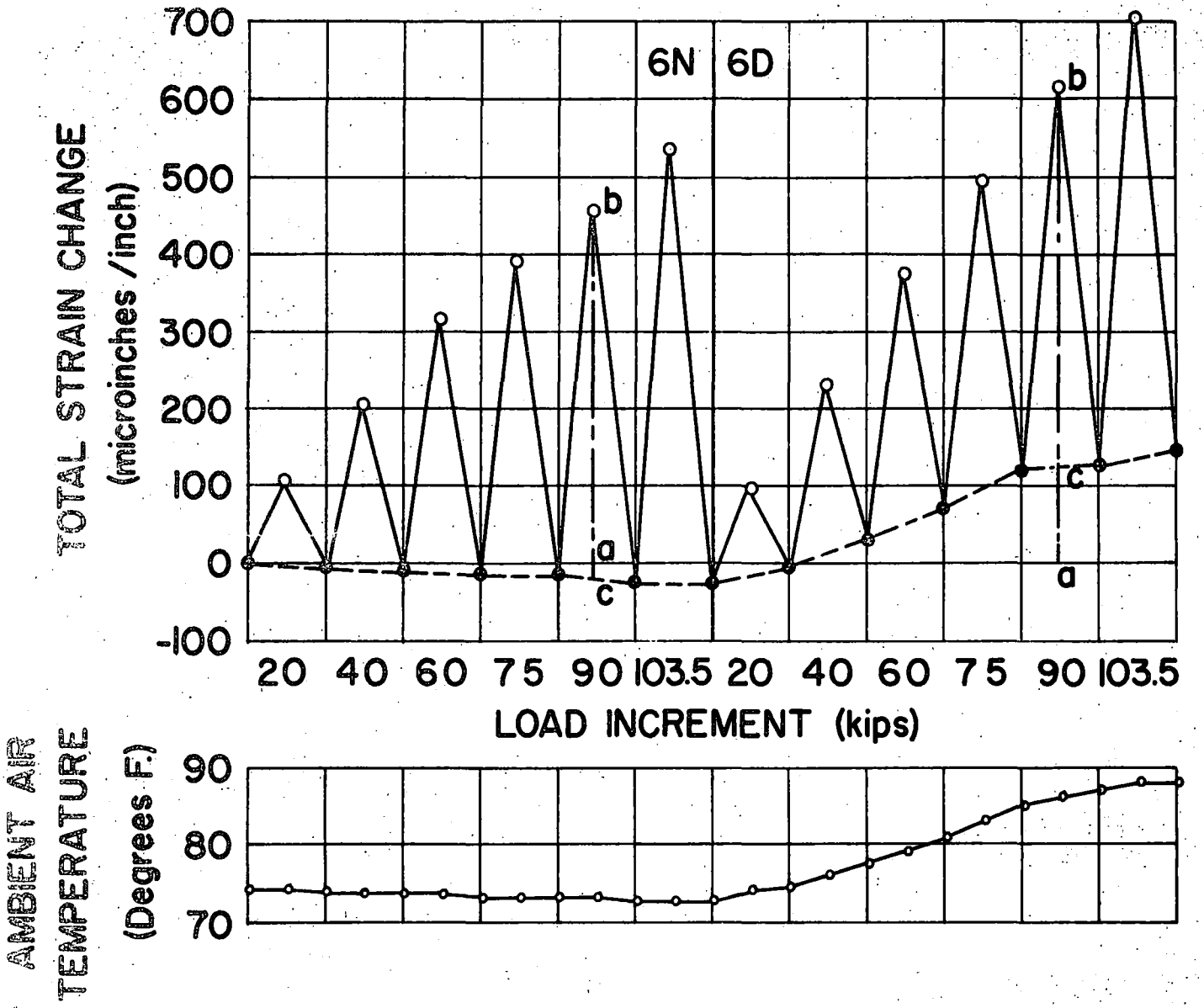

Note:
- Load and Unload Sequence
- Zero Change (Temperature Only)
- a-b Total Strain Increment
- a-c Average Zero Change

FIG. 59 TEMPERATURE EFFECTS ON MEMBER A AT CENTER LINE DURING TESTS 6N AND 6D

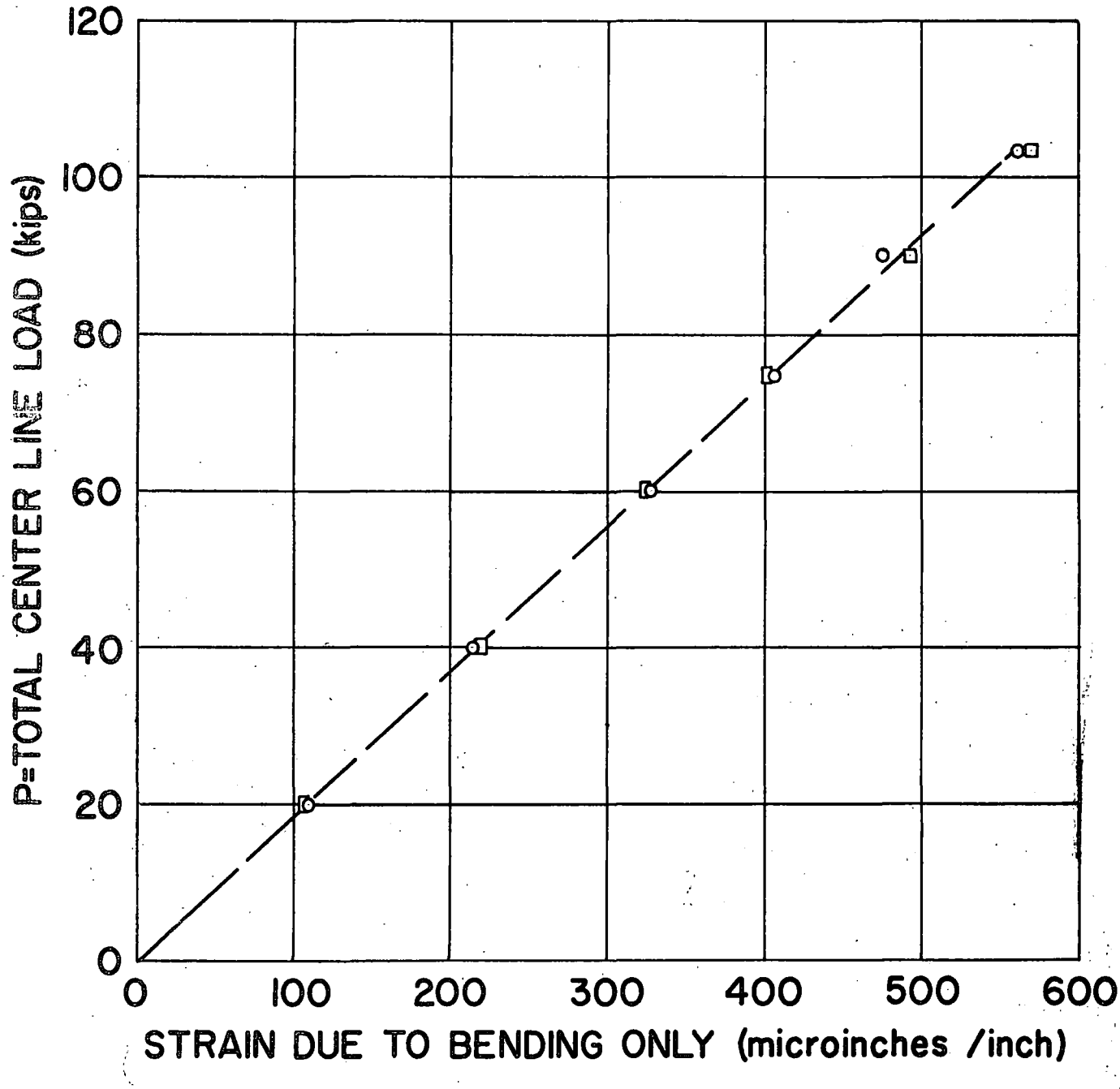

FIG. 60 TEMPERATURE CORRECTED STRAINS FOR MEMBER A, TESTS 6N AND 6D

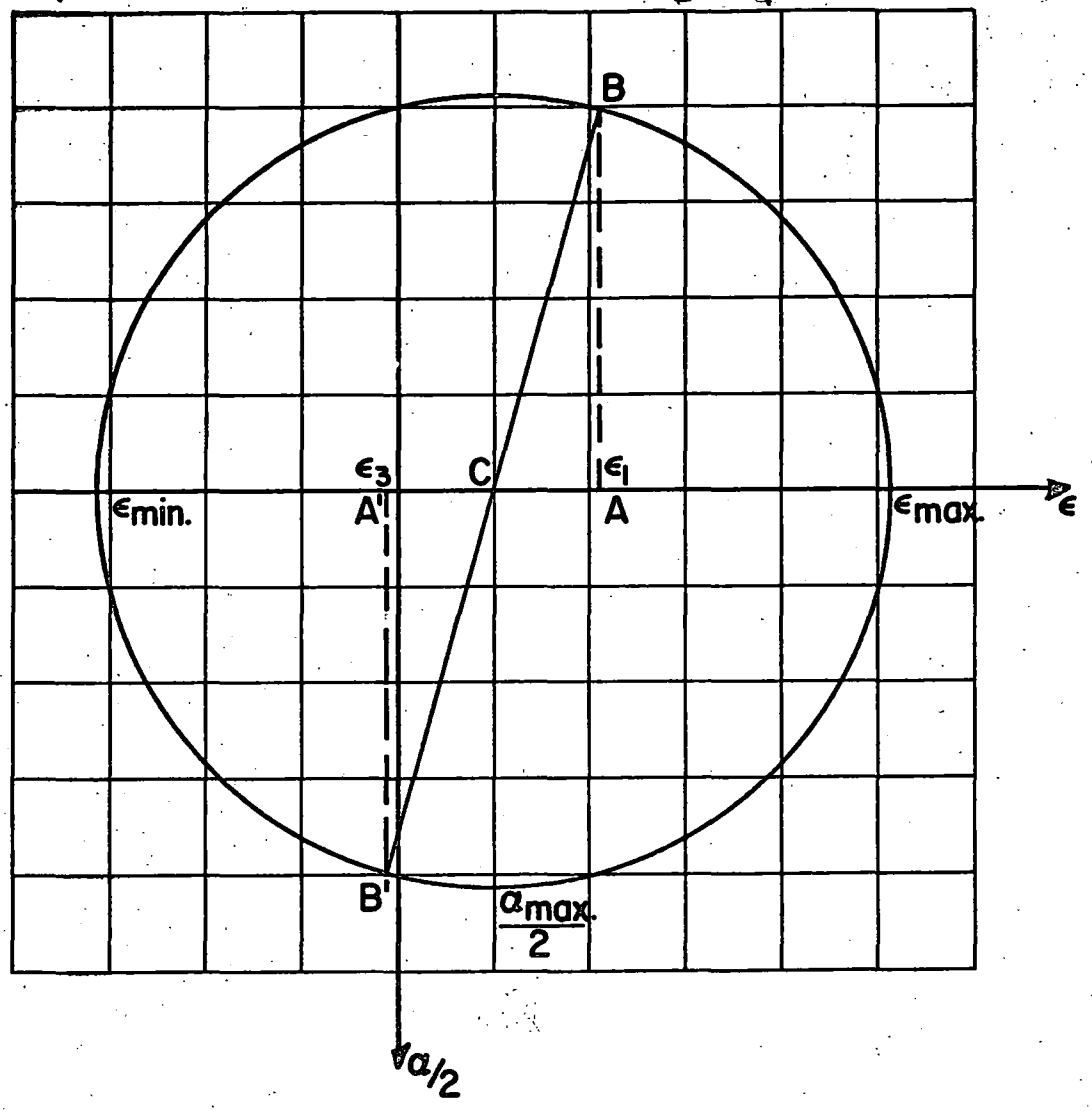

Scale: 1 unit = 50 microinches/inch

ϵ = Strain

α = Shear Strain

Gage Orientation

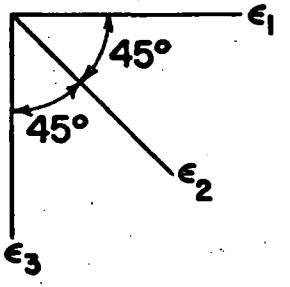

Example:

Gage on Web AB at Design Load. (P=69 K)

ϵ_1 = 103 microinches/inch

ϵ_2 = -148

ϵ_3 = -6

Center of Circle, C,

$$\epsilon = \frac{\epsilon_1 + \epsilon_3}{2} = 48.5$$

$$= \epsilon_2 - \frac{\epsilon_1 + \epsilon_3}{2} = -196.5$$

FIG. 61 SAMPLE MOHR'S CIRCLE SOLUTION FOR RECTANGULAR (45°) STRAIN ROSETTE DATA